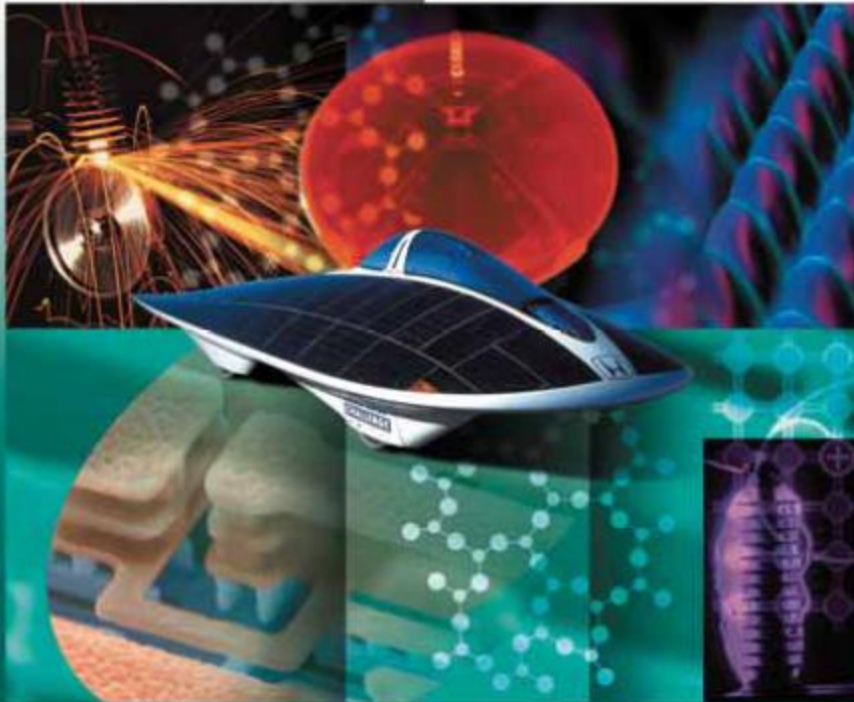


Principles of **Electronic Materials and Devices**

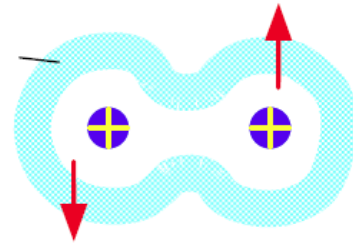
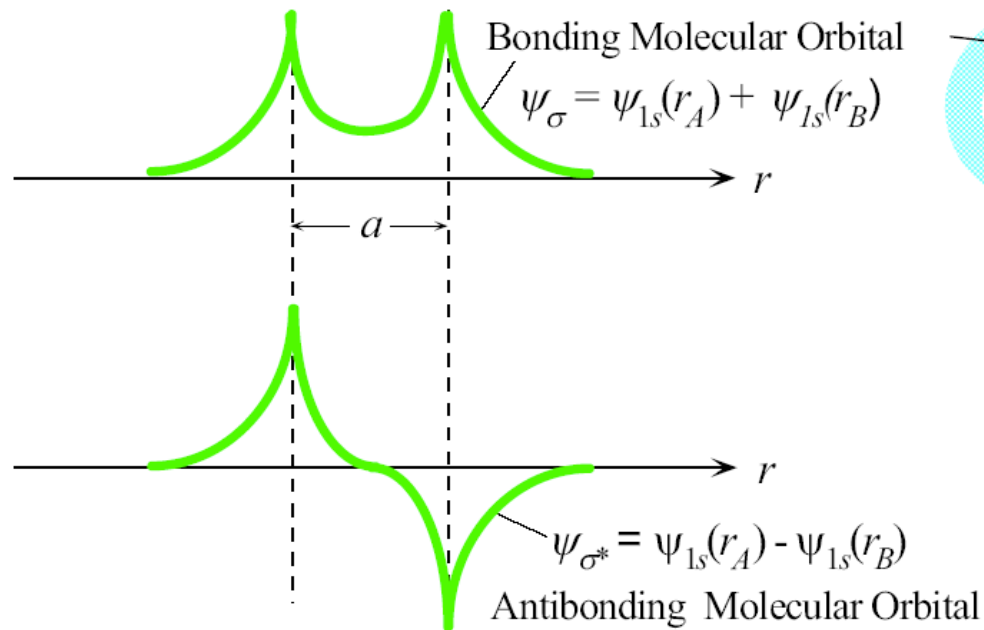
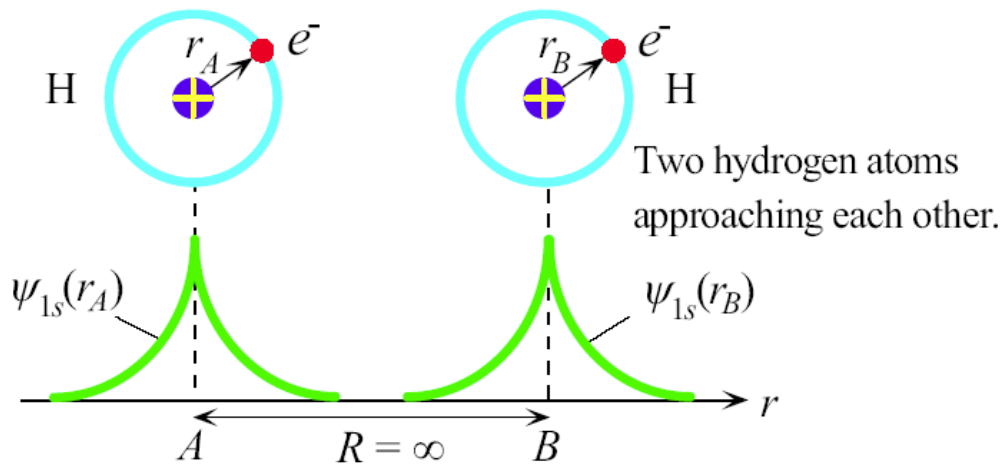
Third Edition



S. O. Kasap

These PowerPoint color diagrams can only be used by instructors if the 3rd Edition has been adopted for his/her course. Permission is given to individuals who have purchased a copy of the third edition with CD-ROM **Electronic Materials and Devices** to use these slides in seminar, symposium and conference presentations provided that the book title, author and © McGraw-Hill are displayed under each diagram.

**Mc
Graw
Hill**



Formation of molecular orbitals, bonding, and antibonding (ψ_{σ} and ψ_{σ^*}) when two H atoms approach each other. The two electrons pair their spins and occupy the bonding orbital ψ_{σ}

Fig 4.1

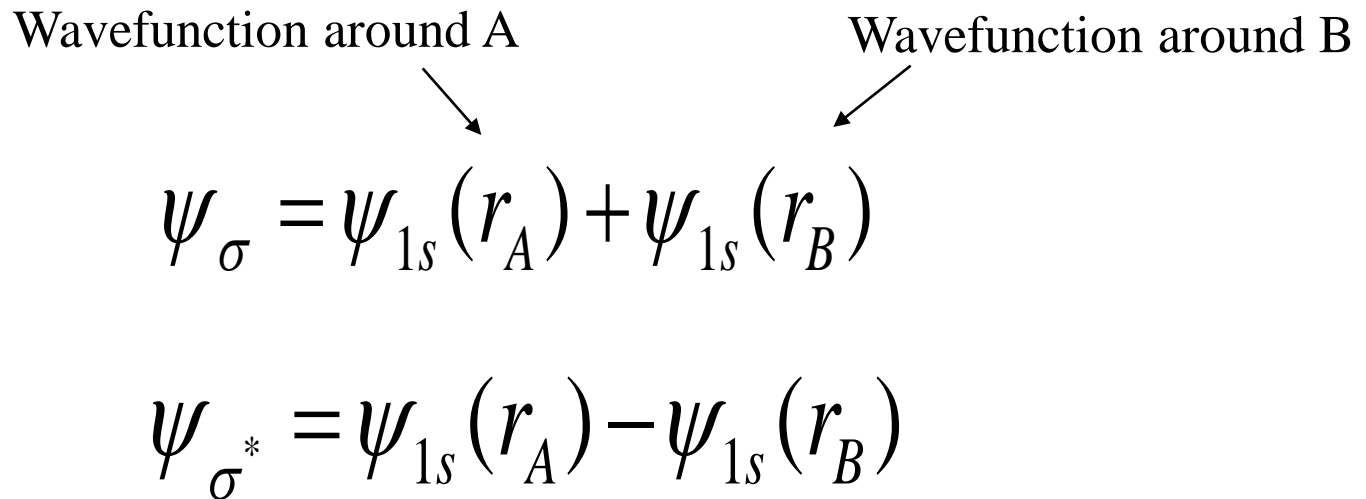
Linear Combination of Atomic Orbitals

Two identical atomic orbitals ψ_{1s} on atoms A and B can be combined linearly in two different ways to generate two separate molecular orbitals ψ_{σ} and ψ_{σ^*}

ψ_{σ} and ψ_{σ^*} generated from a
linear combination of atomic orbitals (LCAO)

Wavefunction around A

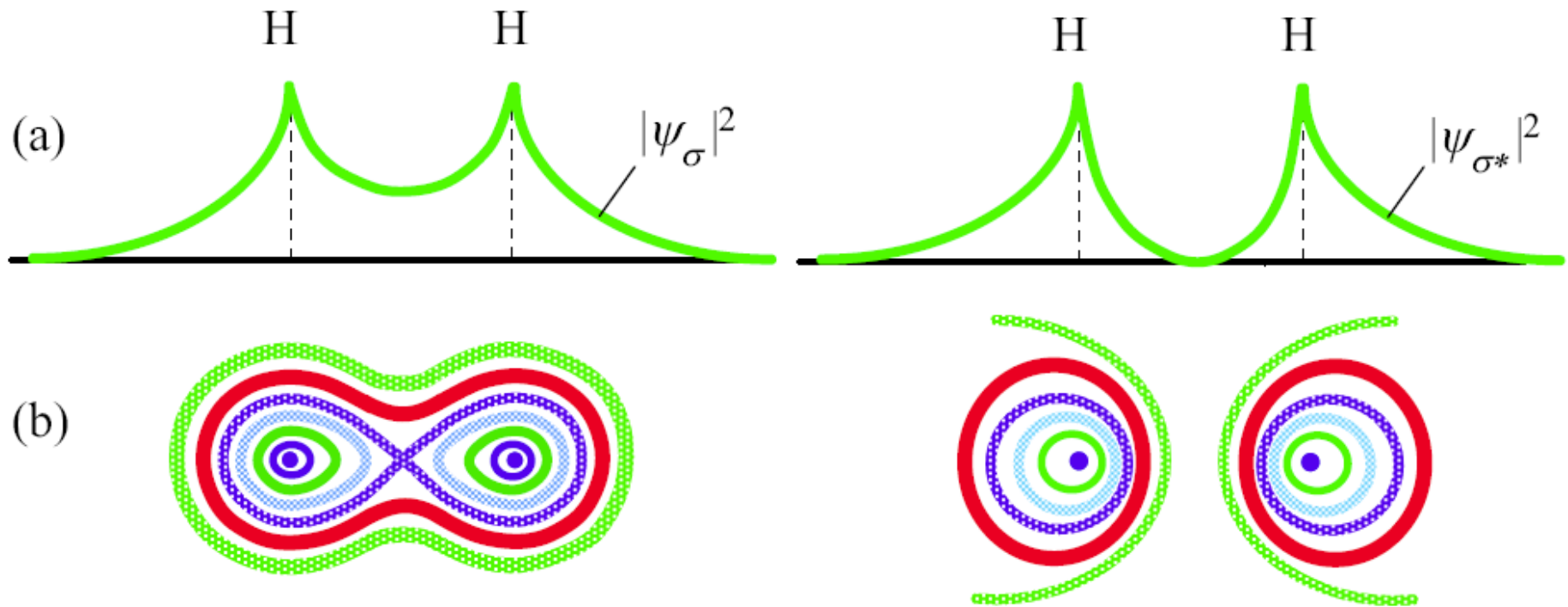
Wavefunction around B



The diagram illustrates the Linear Combination of Atomic Orbitals (LCAO) method. At the top, two labels 'Wavefunction around A' and 'Wavefunction around B' have arrows pointing down towards the equations for the bonding and antibonding molecular orbitals. The first equation shows the bonding orbital as the sum of the two atomic orbitals, and the second equation shows the antibonding orbital as the difference between them.

$$\psi_{\sigma} = \psi_{1s}(r_A) + \psi_{1s}(r_B)$$

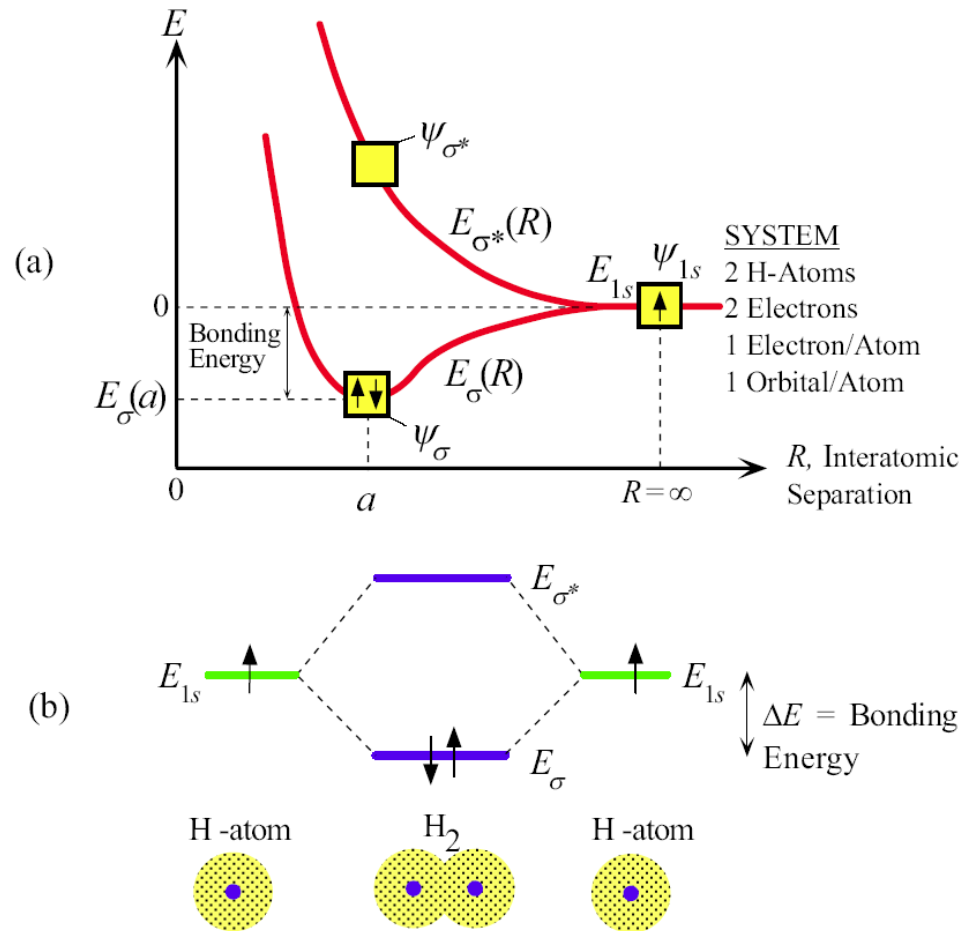
$$\psi_{\sigma^*} = \psi_{1s}(r_A) - \psi_{1s}(r_B)$$



(a) Electron probability distributions for bonding and antibonding orbitals, ψ_σ and

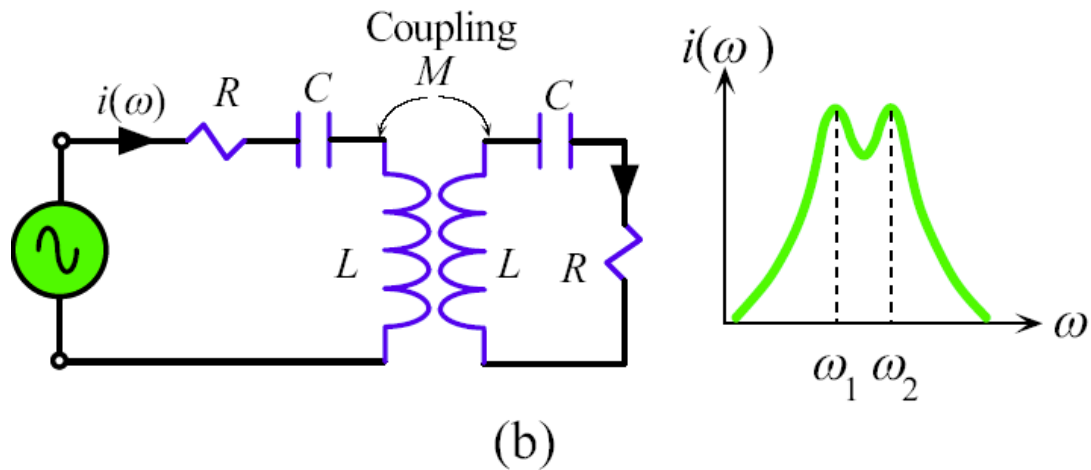
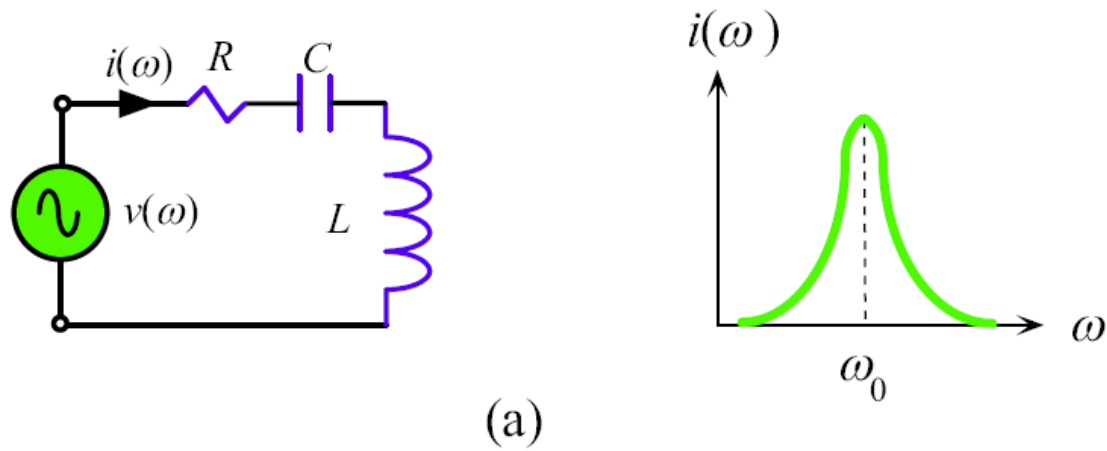
ψ_{σ^*} .
 (b) Lines representing contours of constant probability (darker lines represent greater relative probability).

Fig 4.2



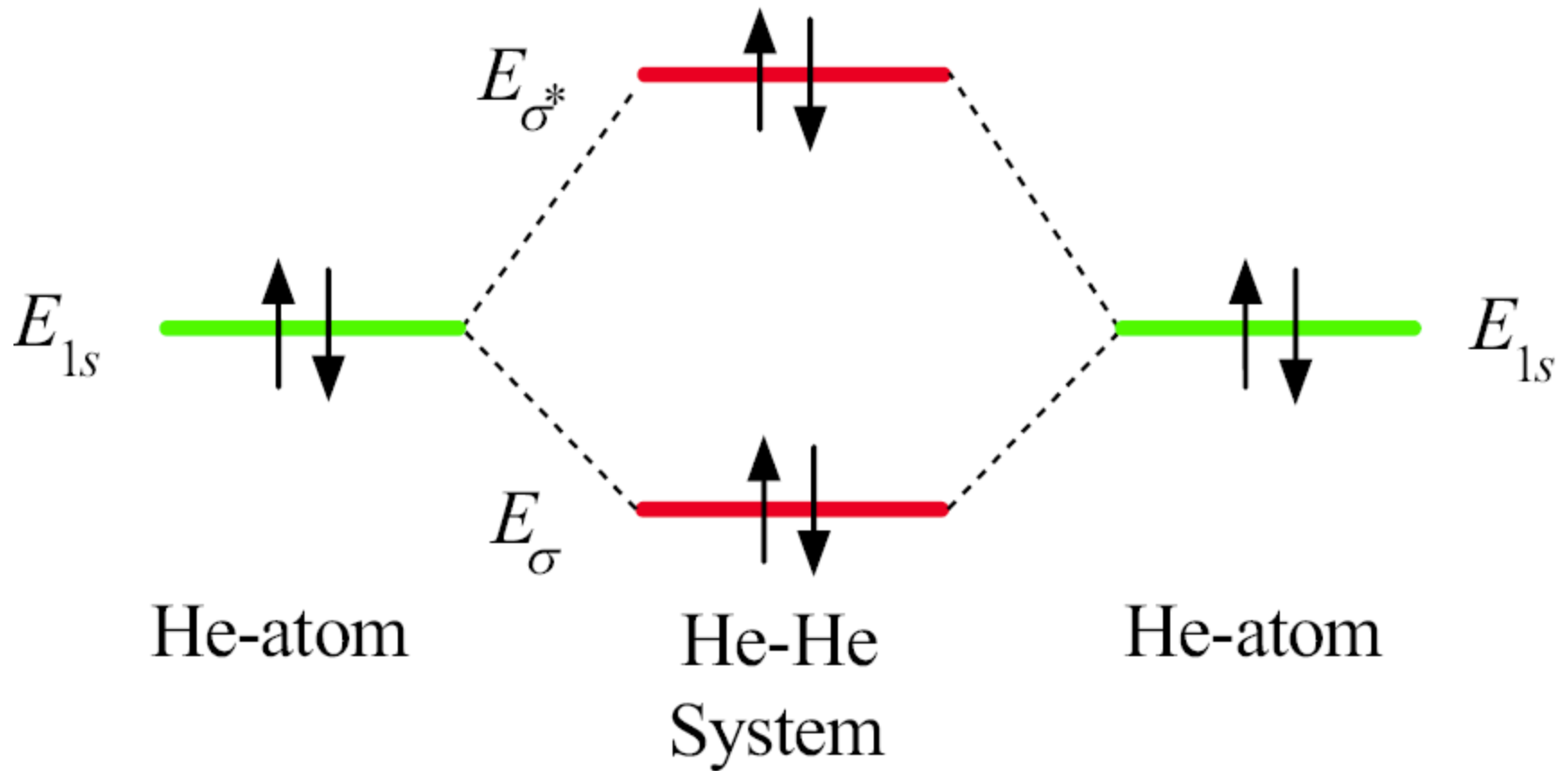
- (a) Energy of ψ_σ and ψ_{σ^*} vs. the interatomic separation R .
- (b) Schematic diagram showing the changes in the electron energy as two isolated H atoms, far left and far right, come together to form a hydrogen molecule.

Fig 4.3



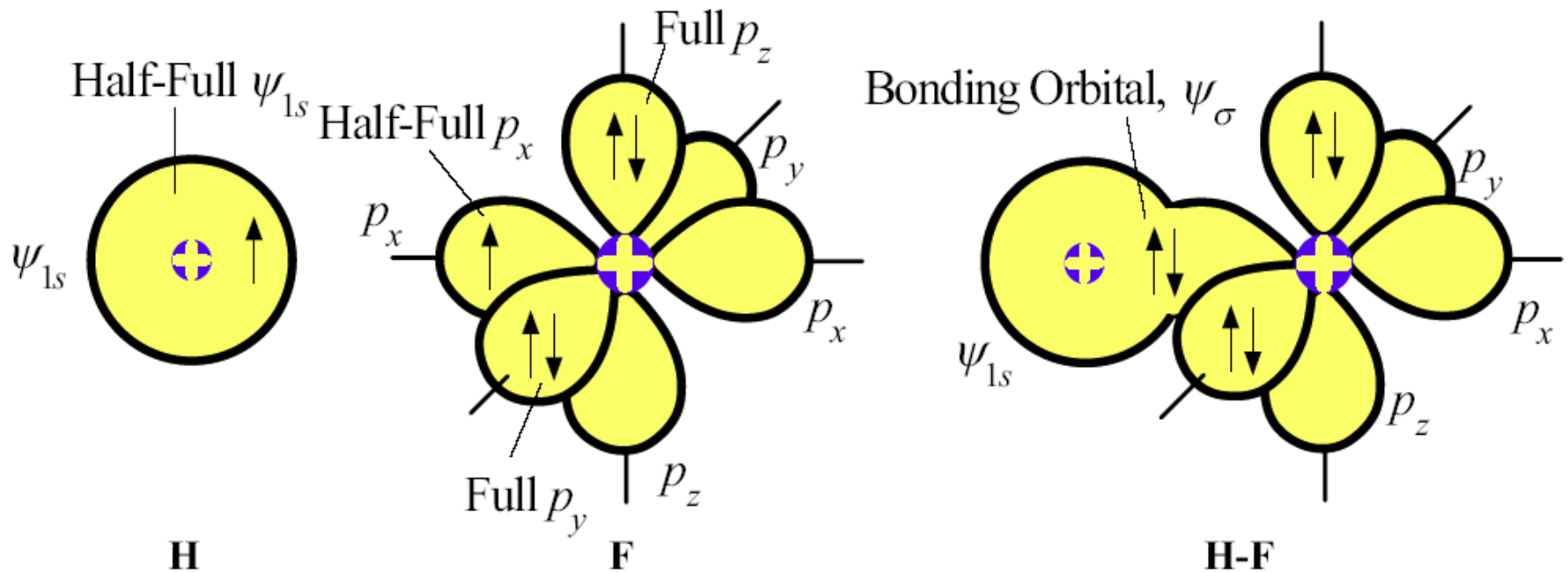
- (a) There is one resonant frequency, ω_0 in an isolated RLC circuit.
- (b) There are two resonant frequencies in two coupled RLC circuits: one below and the other above ω_0

Fig 4.4



Two He atoms have four electrons. When He atoms come together, two of the electrons enter the E_{σ} level and two the E_{σ^*} level, so the overall energy is greater than two isolated He atoms.

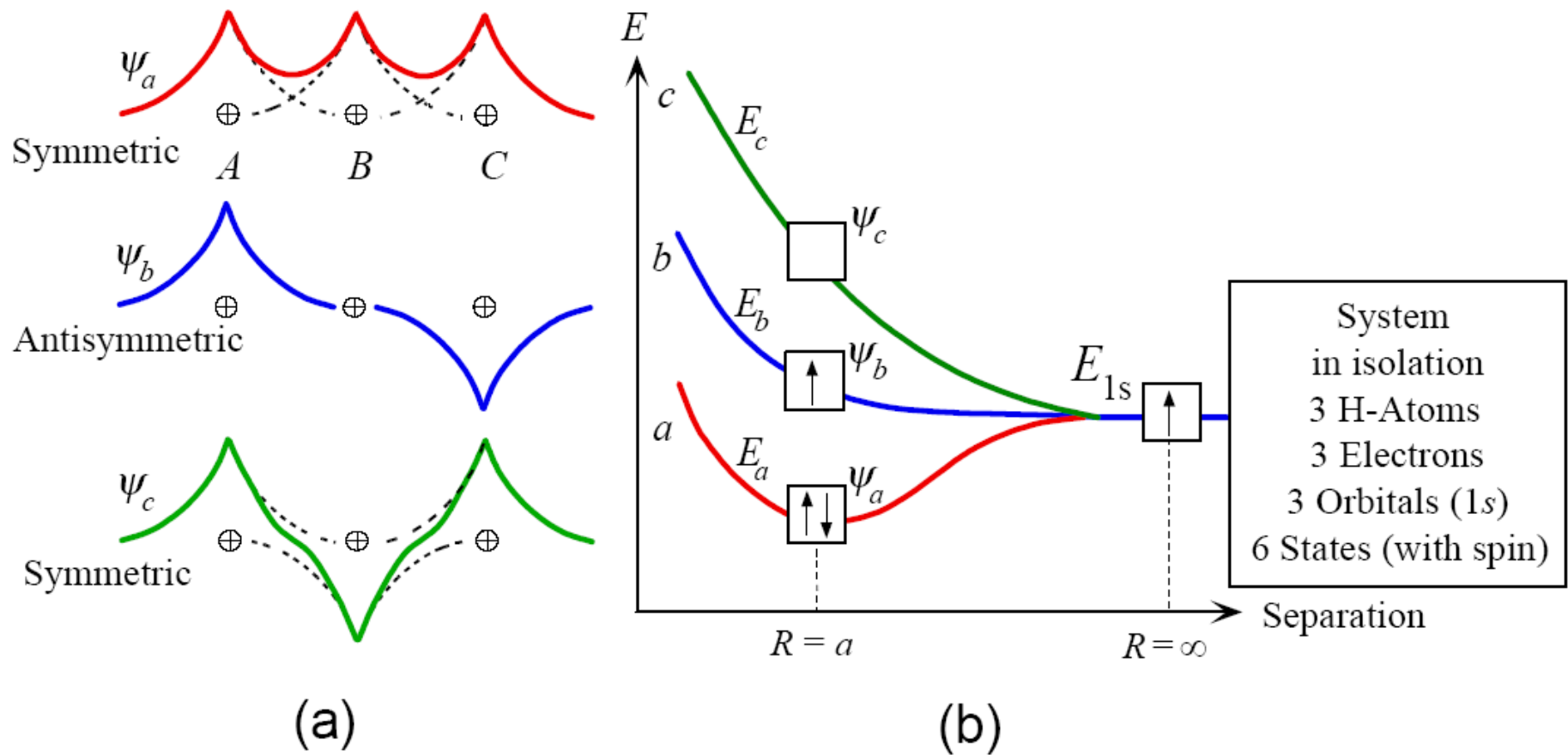
Fig 4.5



H has one half-empty ψ_{1s} orbital.

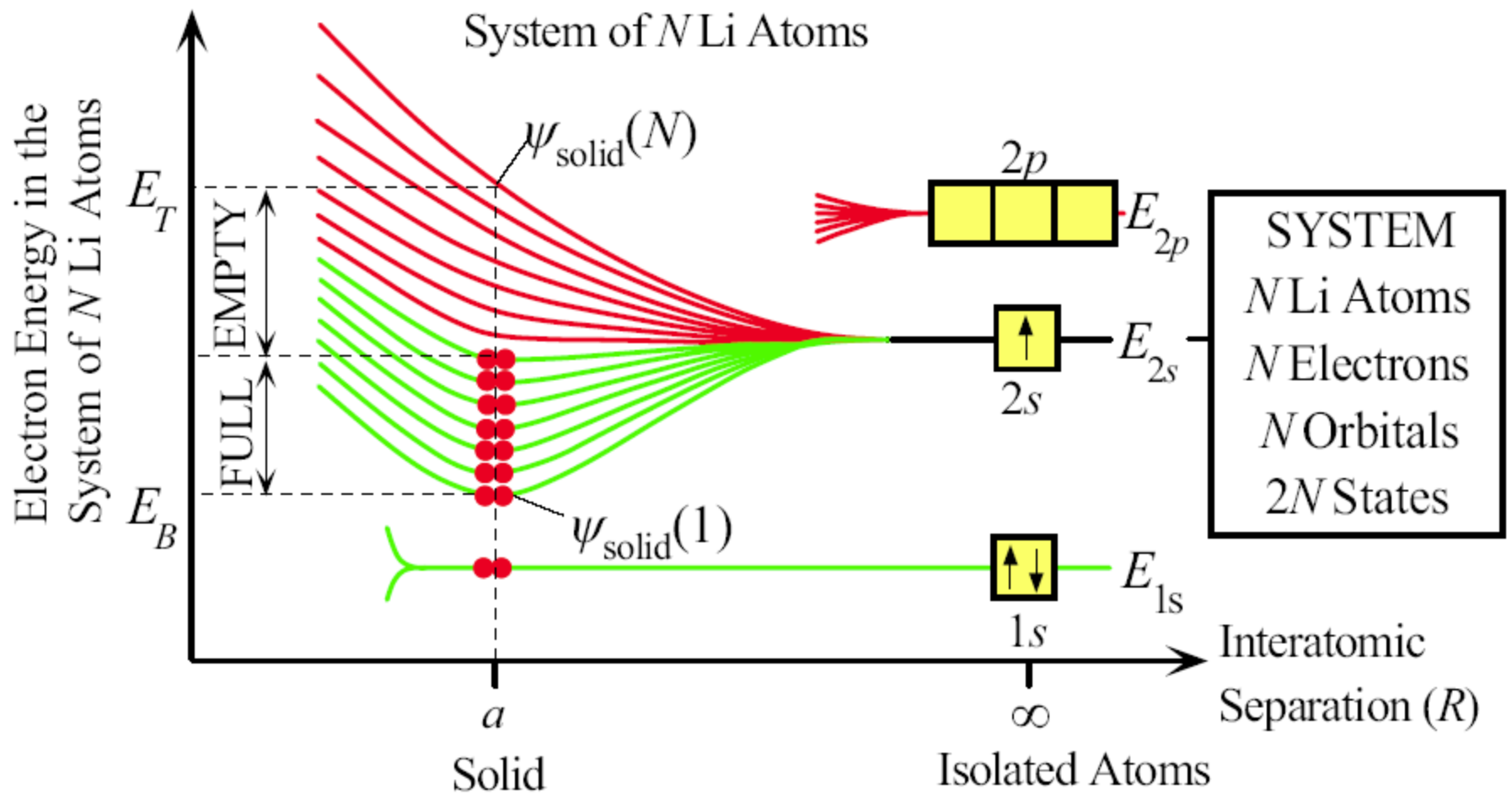
F has one half-empty p_x orbital but full p_y and p_z orbitals. The overlap between ψ_{1s} and p_x produces a bonding orbital and an antibonding orbital. The two electrons fill the bonding orbital and thereby form a covalent bond between H and F.

Fig 4.6



- (a) Three molecular orbitals from three ψ_{1s} atomic orbitals overlapping in three different ways.
- (b) The energies of the three molecular orbitals, labeled a, b, and c, in a system with three H atoms.

Fig 4.7

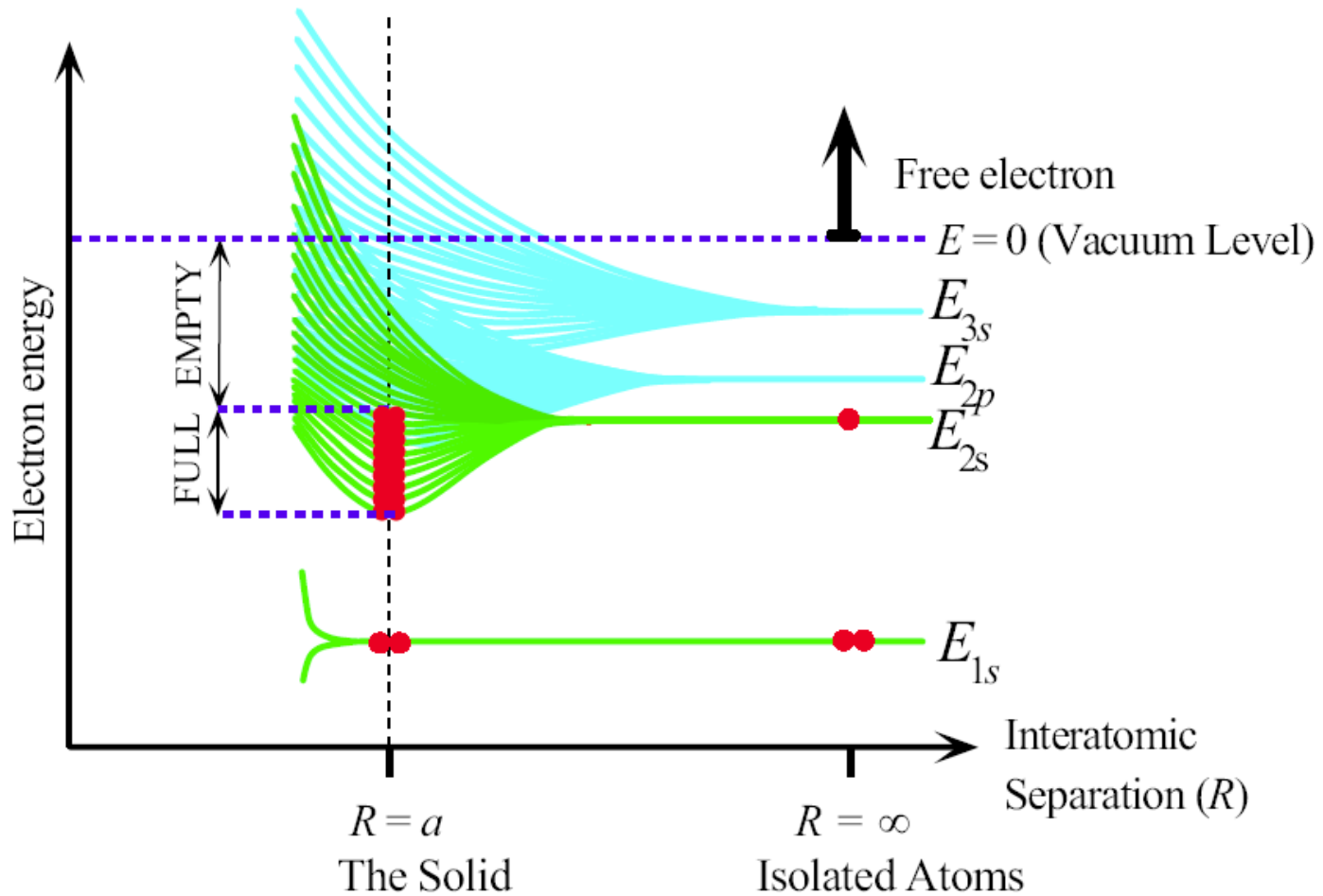


The formation of $2s$ energy band from the $2s$ orbitals when N Li atoms come together to form the Li solid.

There are N $2s$ electrons, but $2N$ states in the band. The $2s$ band is therefore only half full.

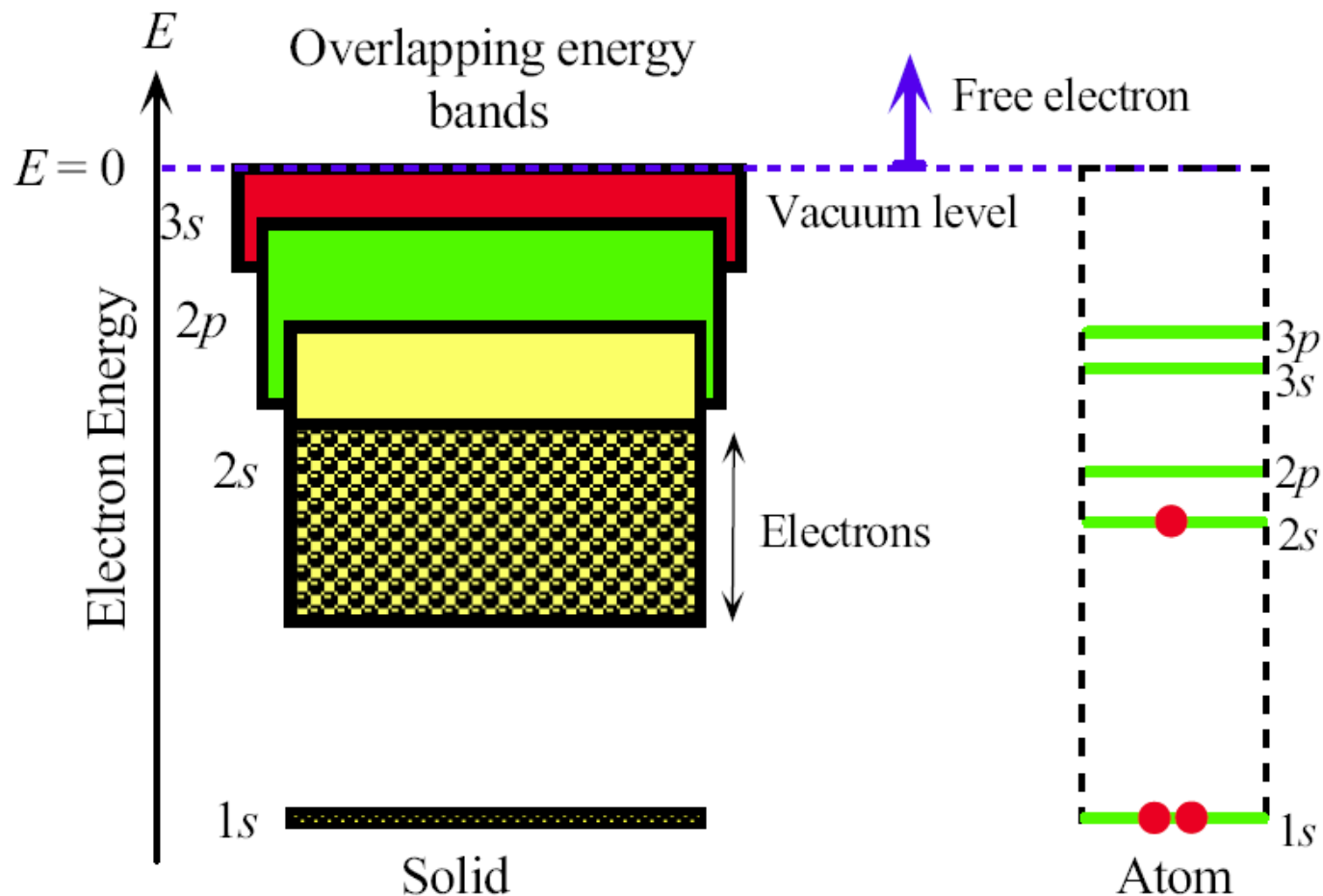
The atomic $1s$ orbital is close to the Li nucleus and remains undisturbed in the solid. Thus, each Li atom has a closed K shell (full $1s$ orbital).

Fig 4.8



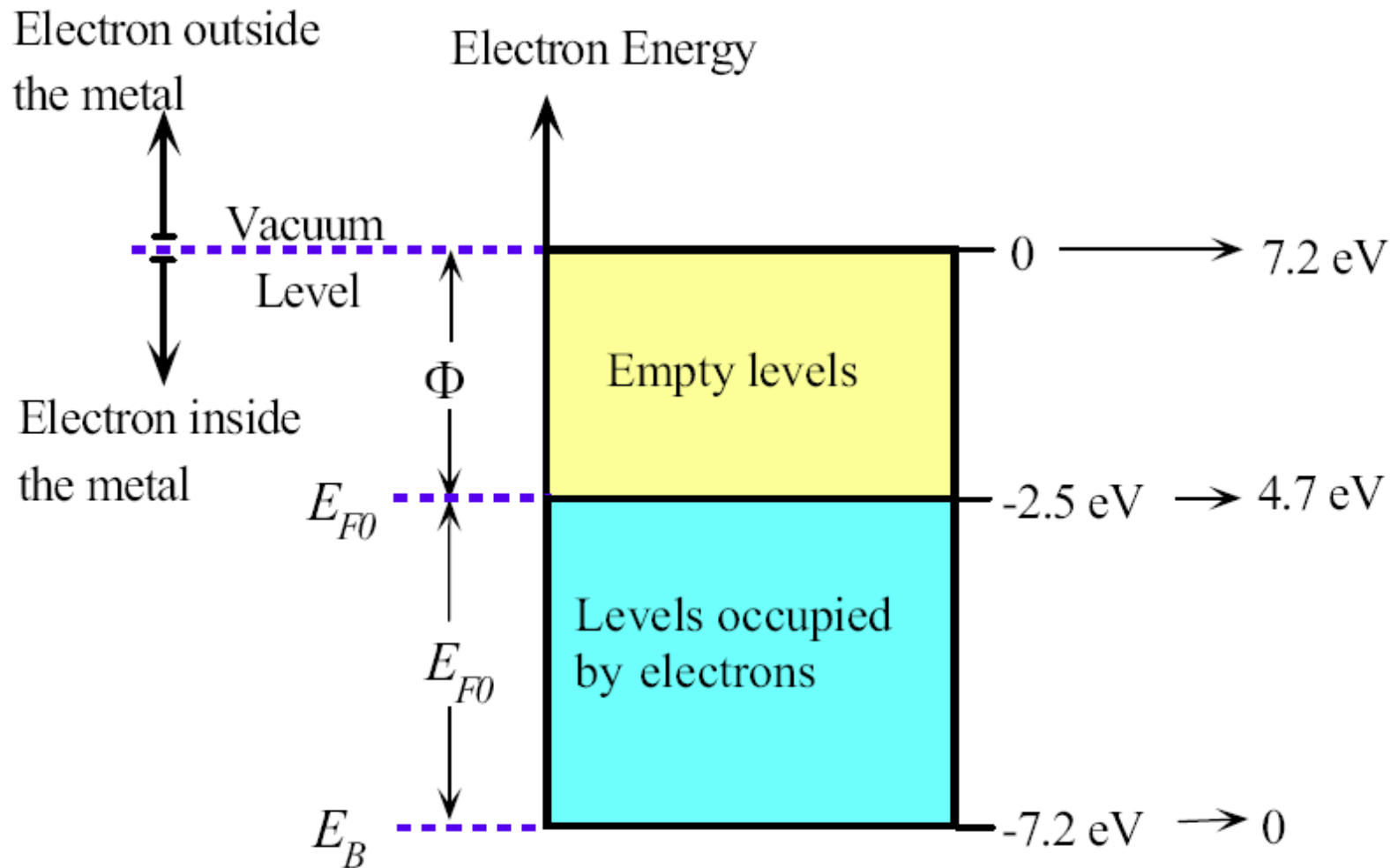
As Li atoms are brought together from infinity, the atomic orbitals overlap and give rise to bands. Outer orbitals overlap first. The 3s orbitals give rise to the 3s band, 2p orbitals to the 2p band, and so on. The various bands overlap to produce a single band in which the energy is nearly continuous.

Fig 4.9



In a metal, the various energy bands overlap to give a single energy band that is only partially full of electrons. There are states with energies up to the vacuum level, where the electron is free.

Fig 4.10



Typical electron energy band diagram for a metal.

All the valence electrons are in an energy band, which they only partially fill. The top of the band is the vacuum level, where the electron is free from the solid ($PE = 0$).

Fig 4.11

Work function Φ

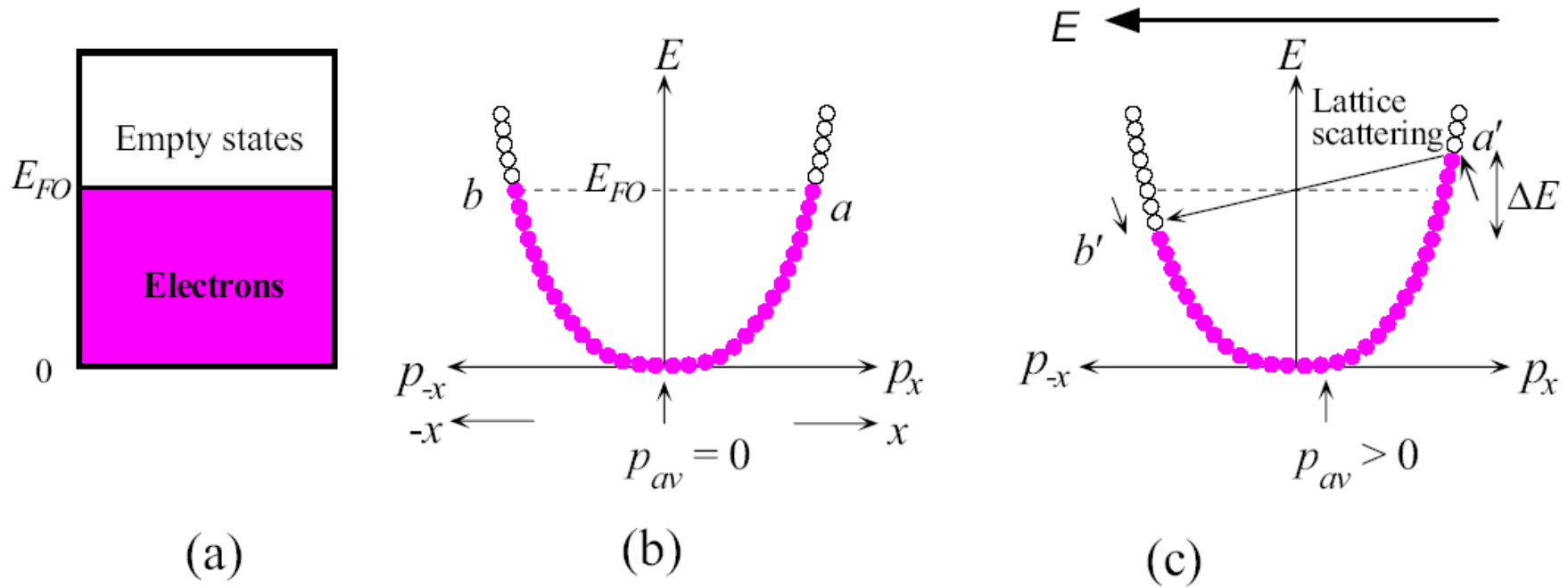
The energy required to excite an electron from the Fermi level to the vacuum level, that is, to liberate the electron from the metal, is called the **work function** Φ of the metal.

Electron gas in a metal

The electrons in the energy band of a metal are loosely bound valence electrons, which become free in the crystal and thereby form a kind of **electron gas** within the crystal. It is this electron gas that holds the metal ions together in the crystal structure and constitutes the metallic bond.

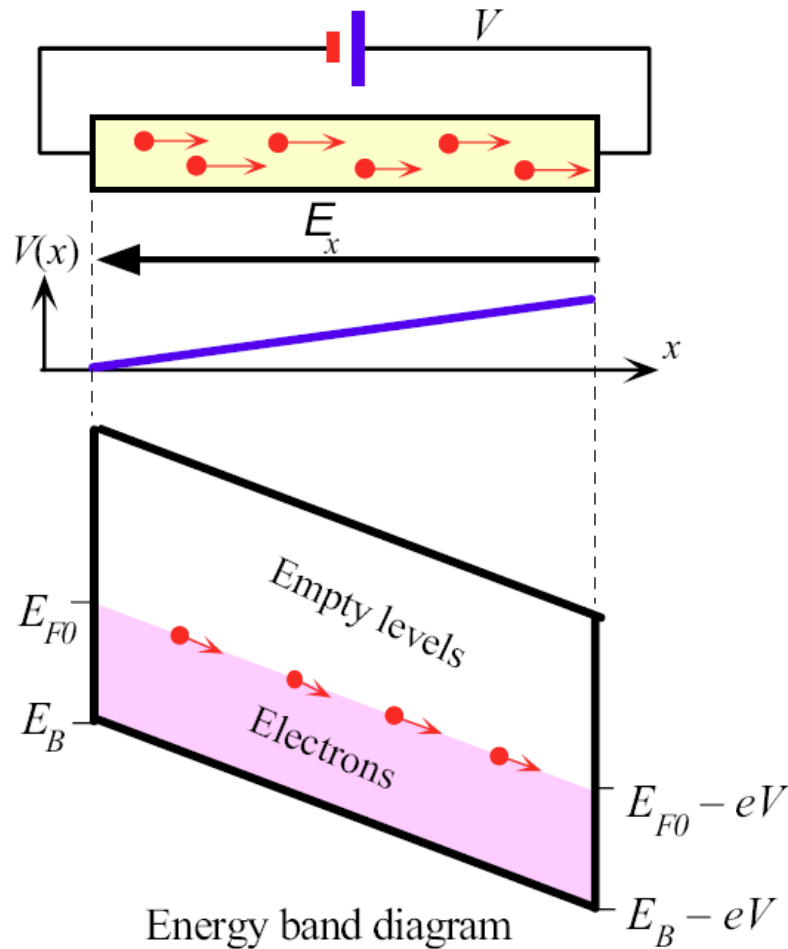
Table 4.1 Fermi energy and work function of selected metals

	Metal							
	Ag	Al	Au	Cs	Cu	Li	Mg	Na
Φ (eV)	4.5	4.28	5.0	2.14	4.65	2.3	3.7	2.75
E_{FO} (eV)	5.5	11.7	5.5	1.58	7.0	4.7	7.1	3.2



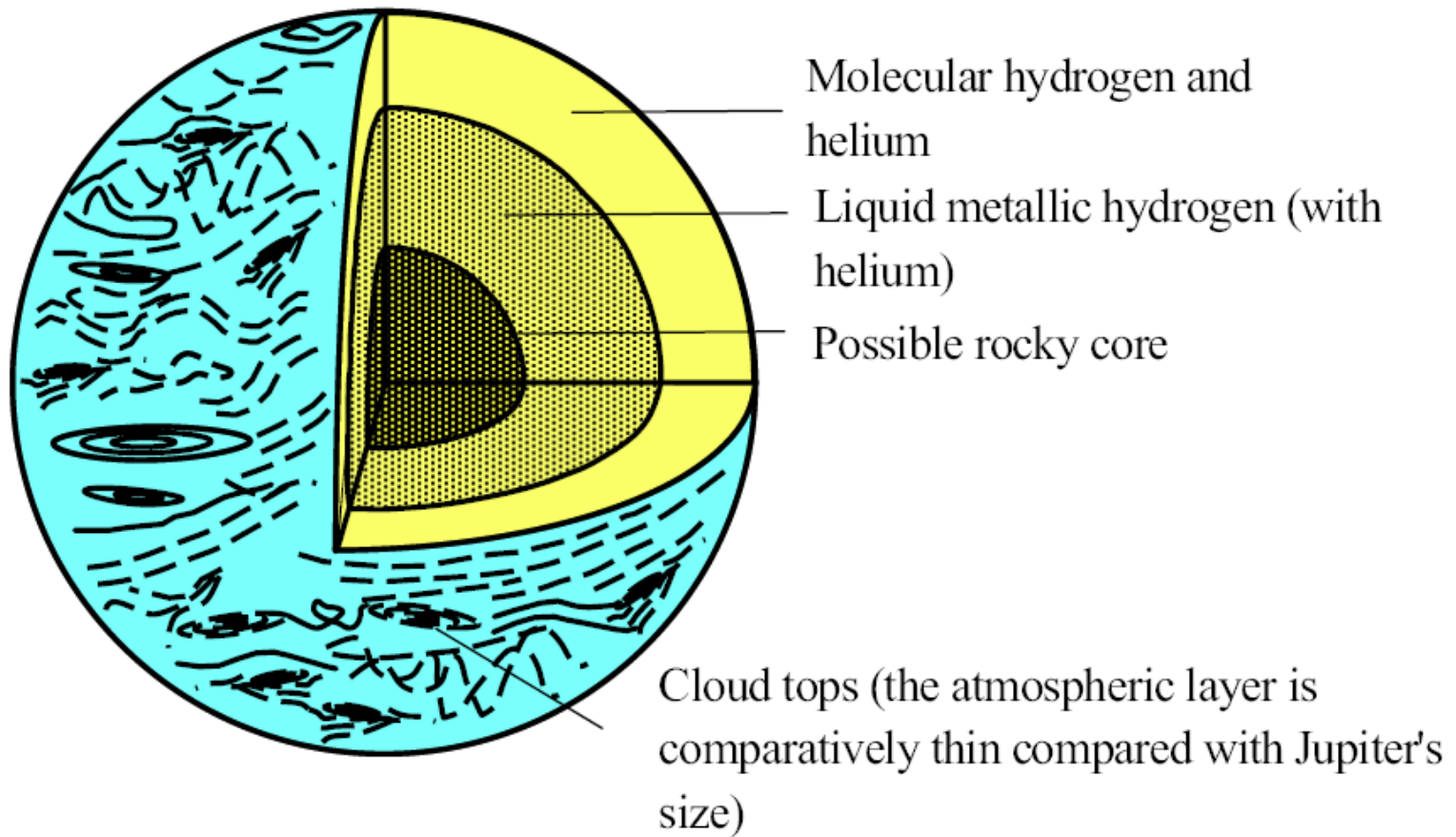
(a) Energy band diagram of a metal. (b) In the absence of a field, there are as many electrons moving right as there are moving left. The motions of two electrons at each energy cancel each other as for a and b. (c) In the presence of a field in the $-x$ direction, the electron a accelerates and gains energy to a' where it is scattered to an empty state near E_{FO} but moving in the $-x$ direction. The average of all momenta values is along the $+x$ direction and results in a net electrical current.

Fig 4.12



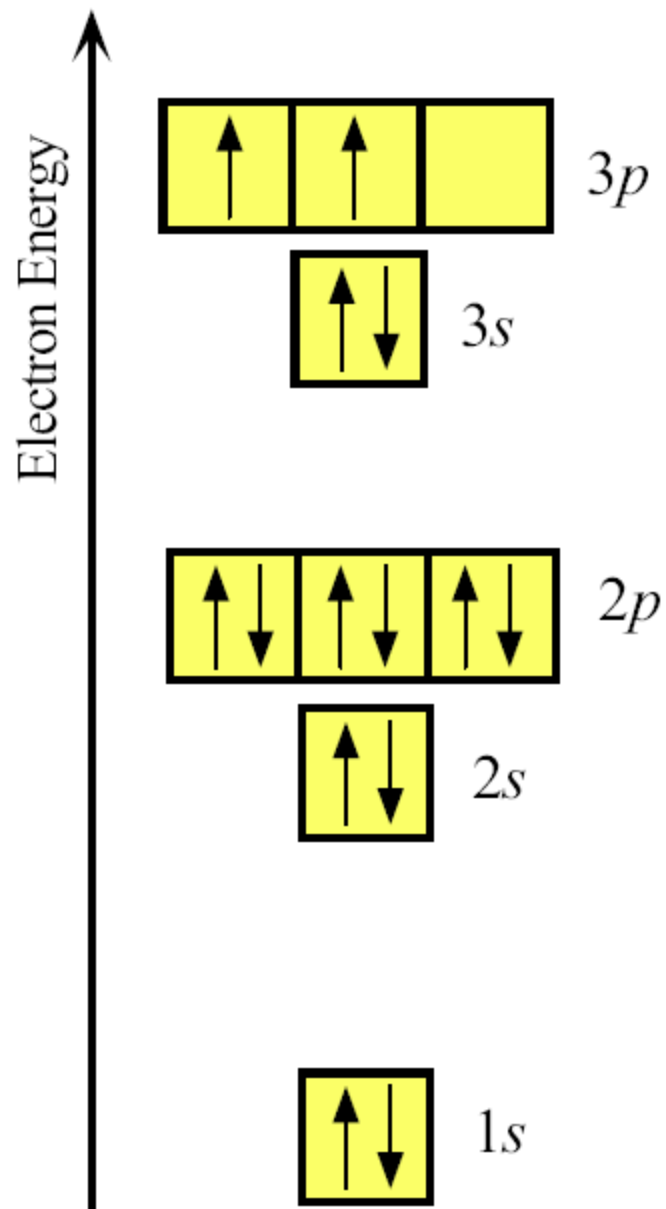
Conduction in a metal is due to the drift of electrons around the Fermi level. When a voltage is applied, the energy band is bent to be lower at the positive terminal so that the electron's potential energy decreases as it moves toward the positive terminal.

Fig 4.13



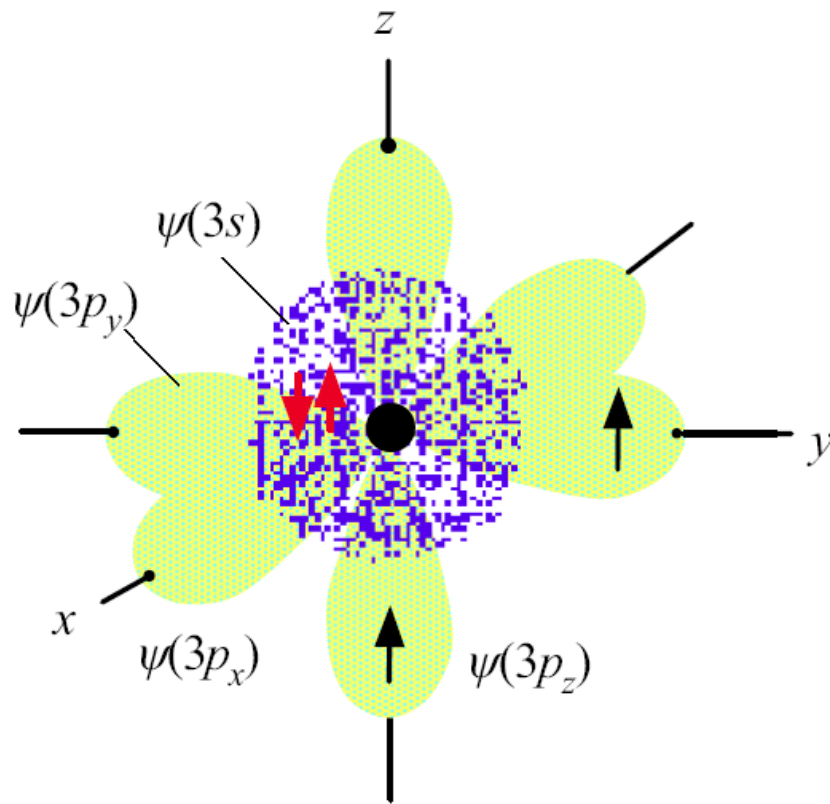
The interior of Jupiter is believed to contain liquid hydrogen, which is metallic.
SOURCE: Drawing adapted from T. Hey and P. Walters, *The Quantum Universe*, Cambridge, MA: Cambridge University Press, 1988, p. 96, figure 7.1.

Fig 4.14

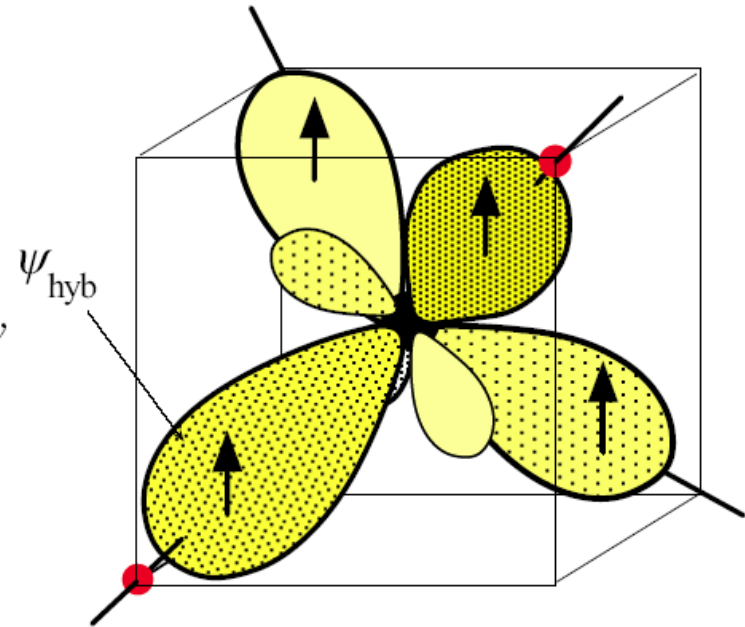


The electronic structure of Si

Fig 4.15



(a) Isolated Si



(b) Si preparing to bond

(a) Si is in Group IV in the Periodic Table. An isolated Si atom has two electrons in the 3s and two electrons in the 3p orbitals.

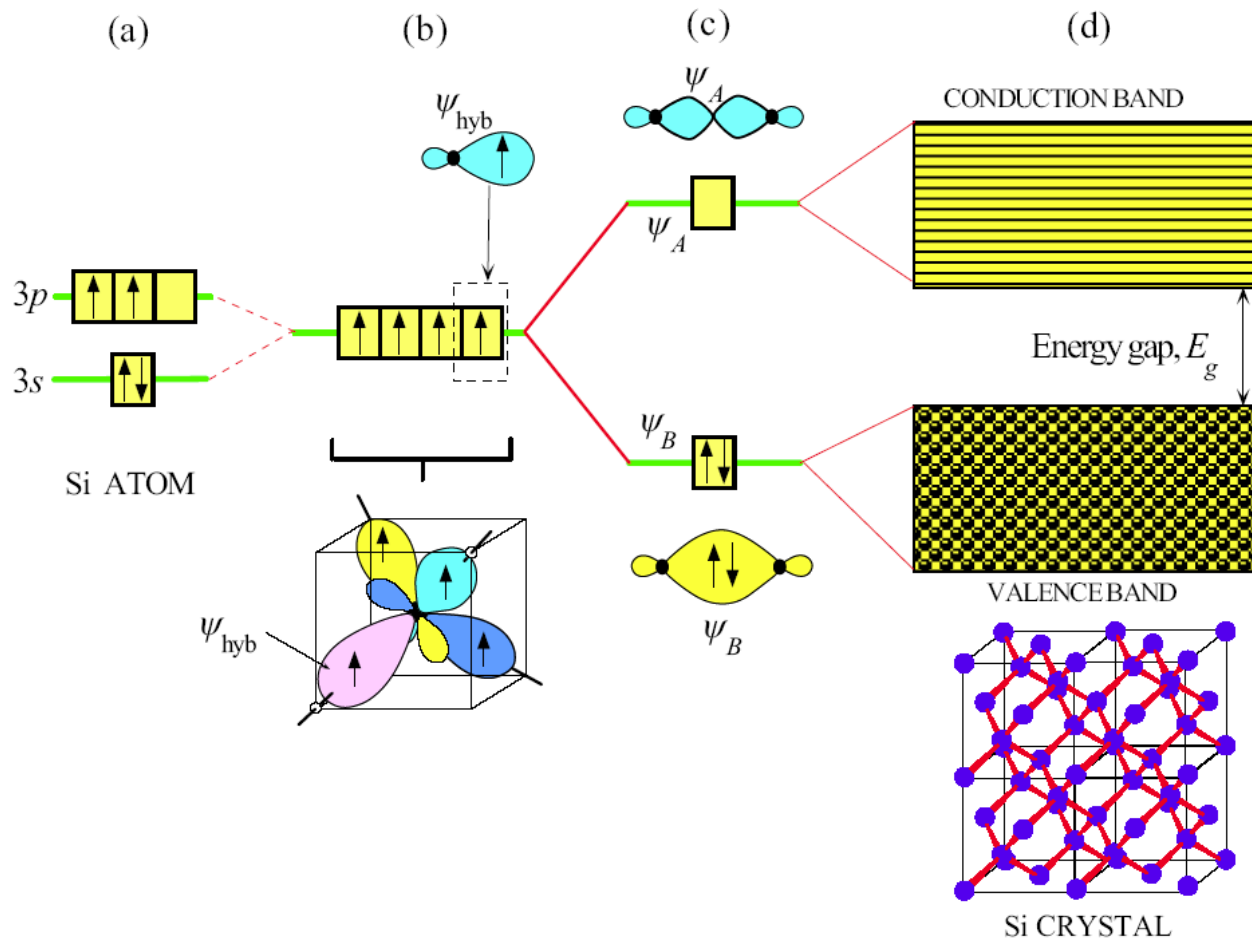
(b) When Si is about to bond, the one 3s orbital and the three 3p orbitals become perturbed and mixed to form four hybridized orbitals, ψ_{hyb} , called sp^3 orbitals, which are directed toward the corners of a tetrahedron. The ψ_{hyb} orbital has a large major lobe and a small back lobe. Each ψ_{hyb} orbital takes one of the four valence electrons.

Fig 4.16

Hybridization

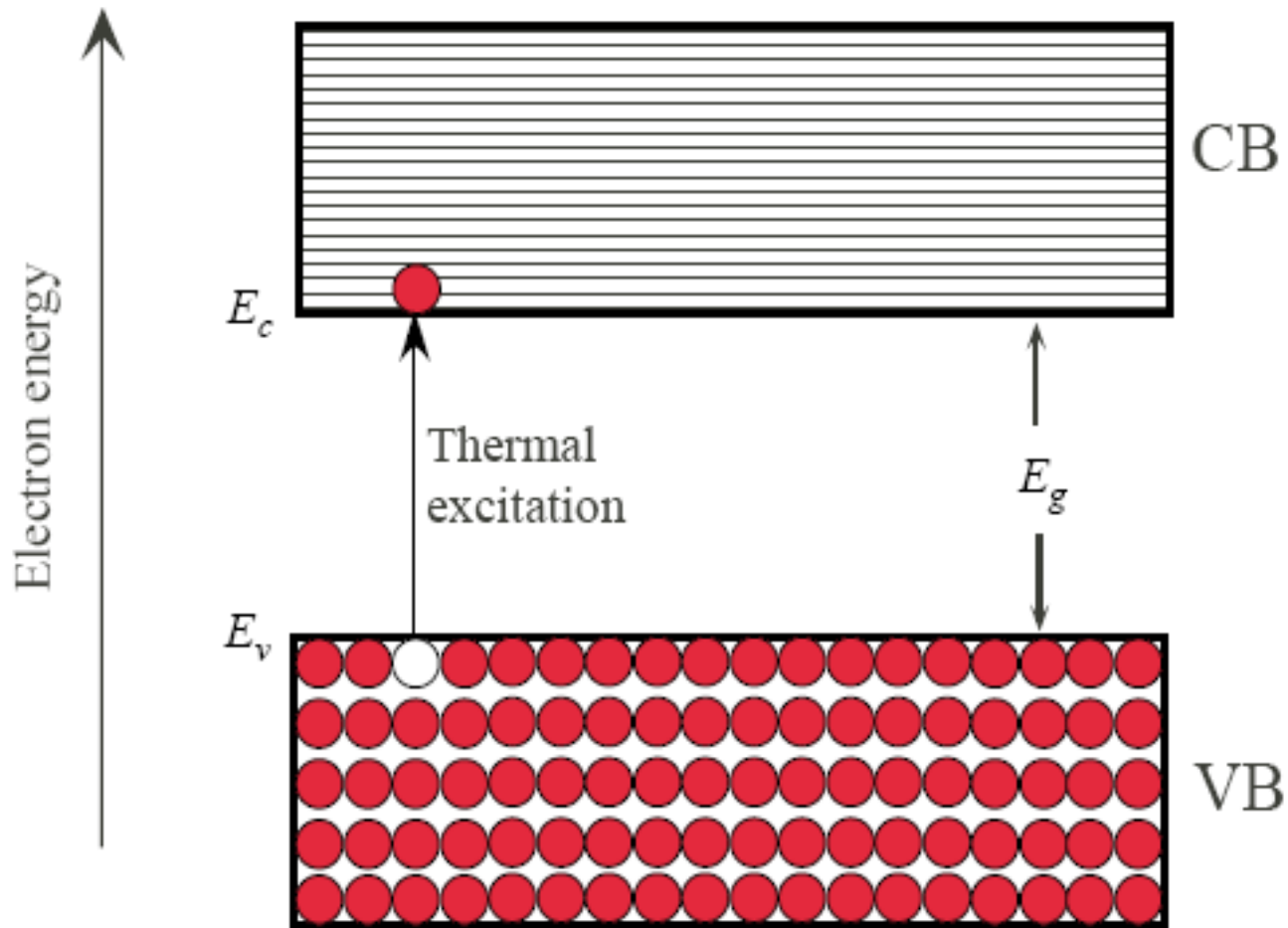
sp^3 hybridization

The $3s$ and $3p$ energy levels are quite close, and when five Si atoms approach each other, the interaction results in the four orbitals $\psi(3s)$, $\psi(3p_x)$, $\psi(3p_y)$ and $\psi(3p_z)$ mixing together to form four new hybrid orbitals, which are directed in tetrahedral directions; that is, each one is aimed as far away from the others as possible.



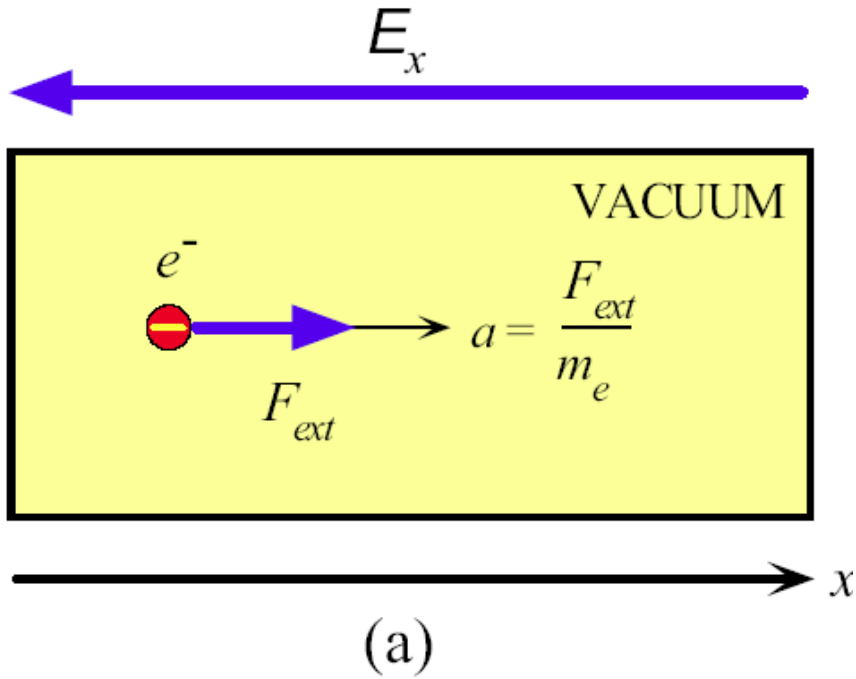
(a) Formation of energy bands in the Si crystal first involves hybridization of 3s and 3p orbitals to four identical ψ_{hyb} orbitals which make 109.5° with each other as shown in (b). (c) ψ_{hyb} orbitals on two neighboring Si atoms can overlap to form ψ_B or ψ_A . The first is a bonding orbital (full) and the second is an antibonding orbital (empty). In the crystal yB overlap to give the valence band (full) and ψ_A overlap to give the conduction band (empty).

Fig 4.17

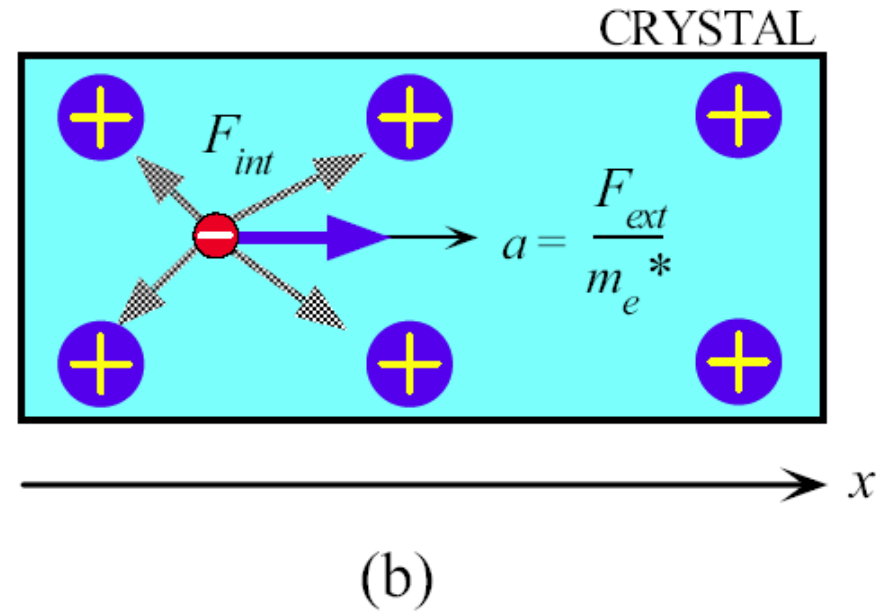


Energy band diagram of a semiconductor. CB is the conduction band and VB is the valence band. AT 0 K, the VB is full with all the valence electrons.

Fig 4.18



(a) An external force F_{ext} applied to an Electron in a vacuum results in an acceleration $a_{vac} = F_{ext} / m_e$.

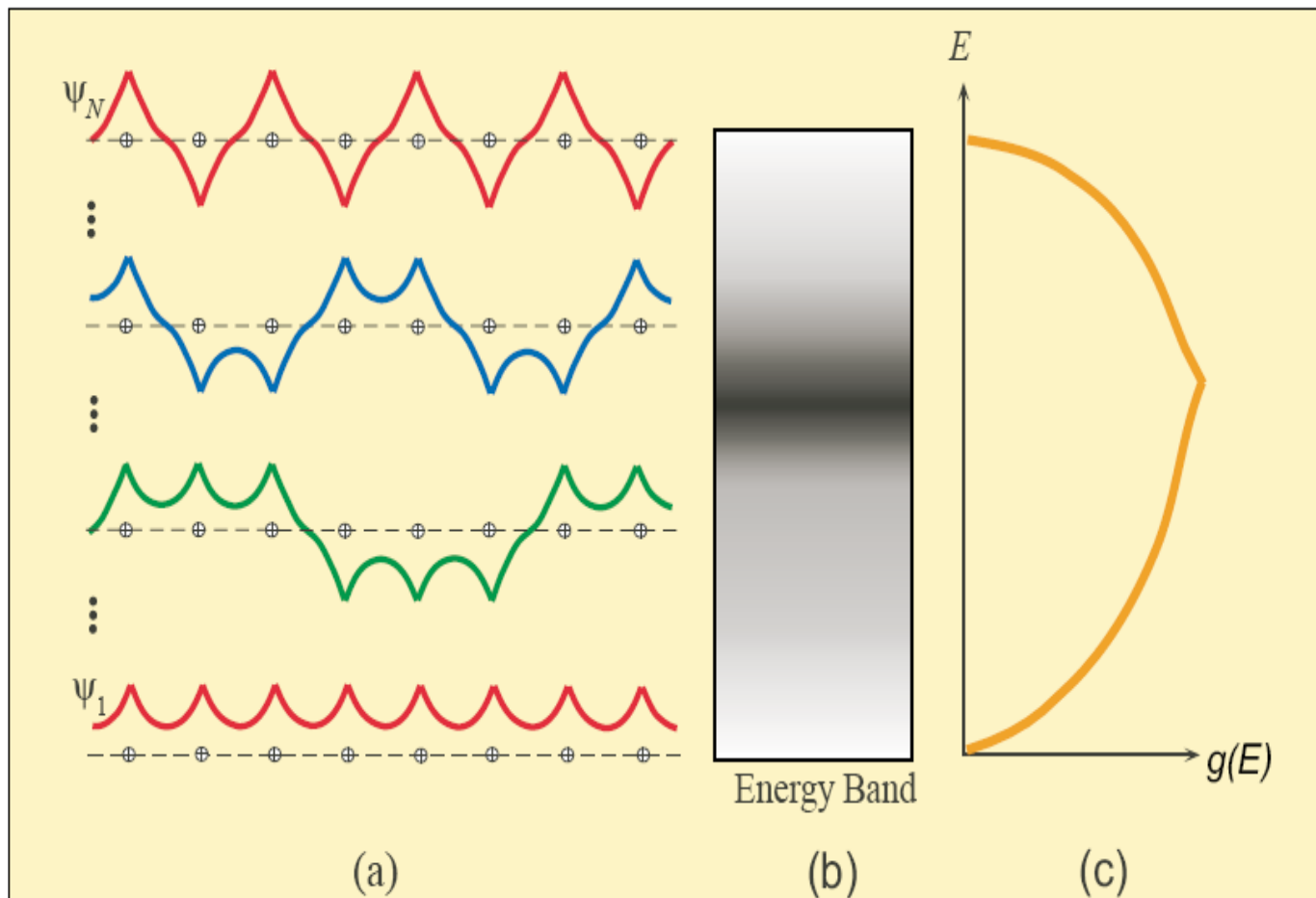


(b) An external force F_{ext} applied to an electron in a crystal results in an acceleration $a_{cryst} = F_{cryst} / m_{e^*}$.

Fig 4.19

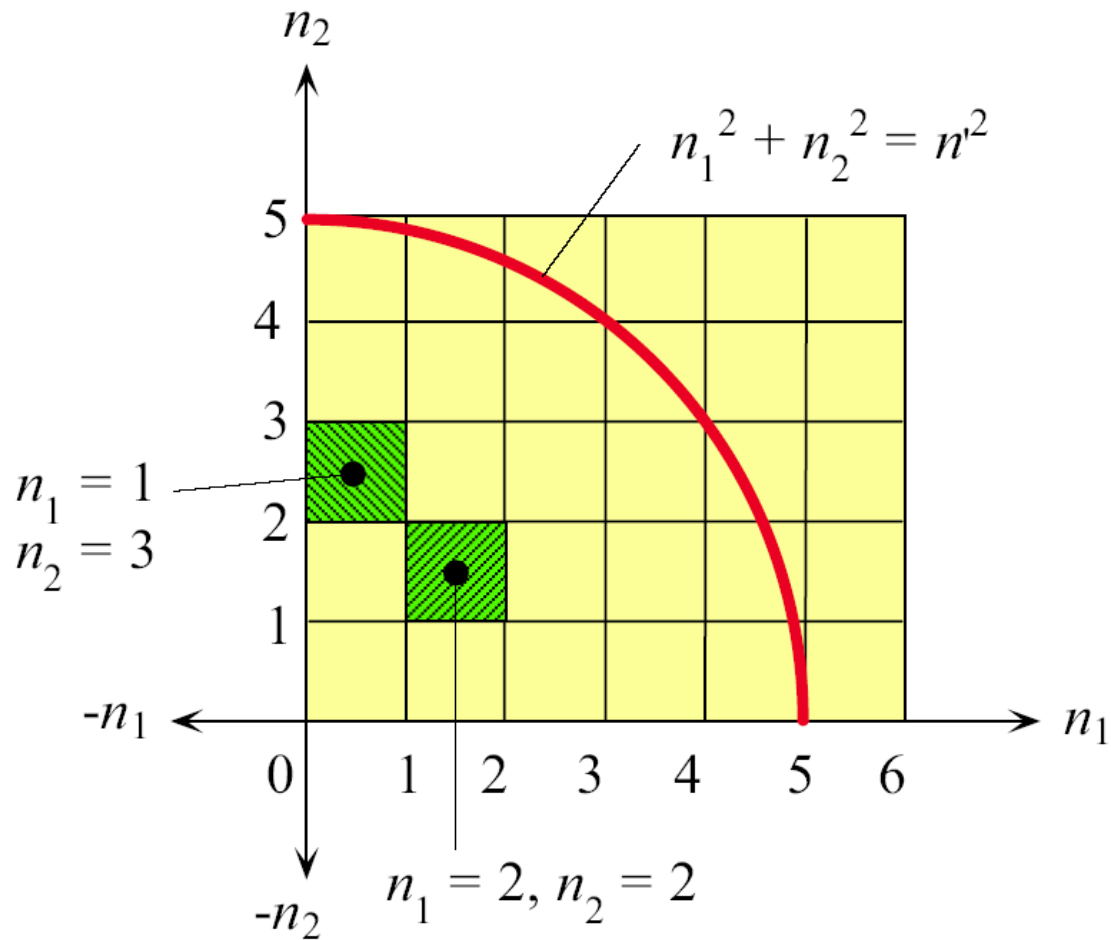
Table 4.2 Effective mass m_e^* of electrons in some metals

Metal	Ag	Au	Bi	Cu	K	Li	Na	Ni	Pt	Zn
$\frac{m_e^*}{m_e}$	0.99	1.10	0.047	1.01	1.12	1.28	1.2	28	13	0.85



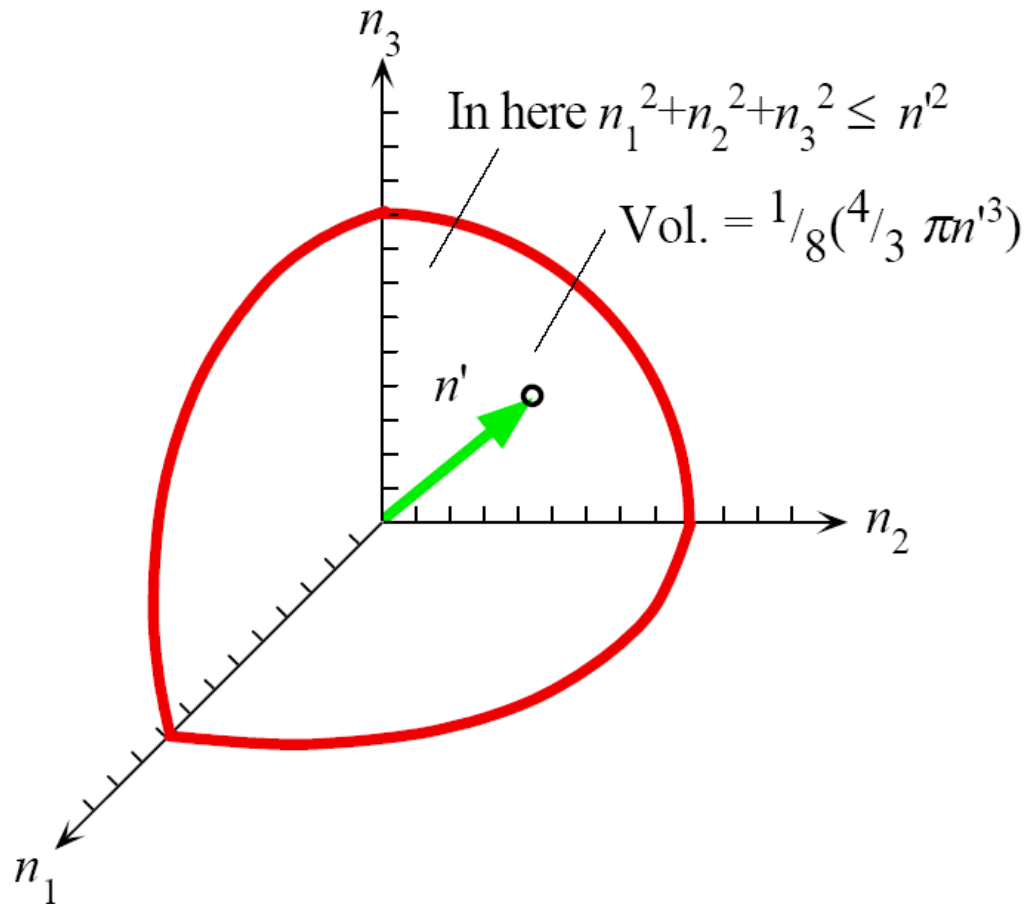
- (a) In the solid there are N atoms and N extended electron wavefunctions from ψ_1 all the way to ψ_N . There are many wavefunctions, states, that have energies that fall in the central regions of the energy band.
- (b) The distribution of states in the energy band; darker regions have a higher number of states.
- (c) Schematic representation of the density of states $g(E)$ versus energy E .

Fig 4.20



Each state, or electron wavefunctions in the crystal, can be represented by a box at n_1, n_2 .

Fig 4.21



In three dimensions, the volume defined by a sphere of radius n' and the positive axes n_1 , n_2 , and n_3 , contains all the possible combinations of positive n_1 , n_2 , and n_3 values that satisfy $n_1^2 + n_2^2 + n_3^2 \leq n'^2$

Fig 4.22

Density of States

$g(E)$ = Density of states

$g(E) dE$ is the number of states (*i.e.*, wavefunctions) in the energy interval E to $(E + dE)$ per unit volume of the sample.

$$g(E) = \left(8\pi 2^{1/2}\right) \left(\frac{m_e}{h^2}\right)^{3/2} E^{1/2}$$

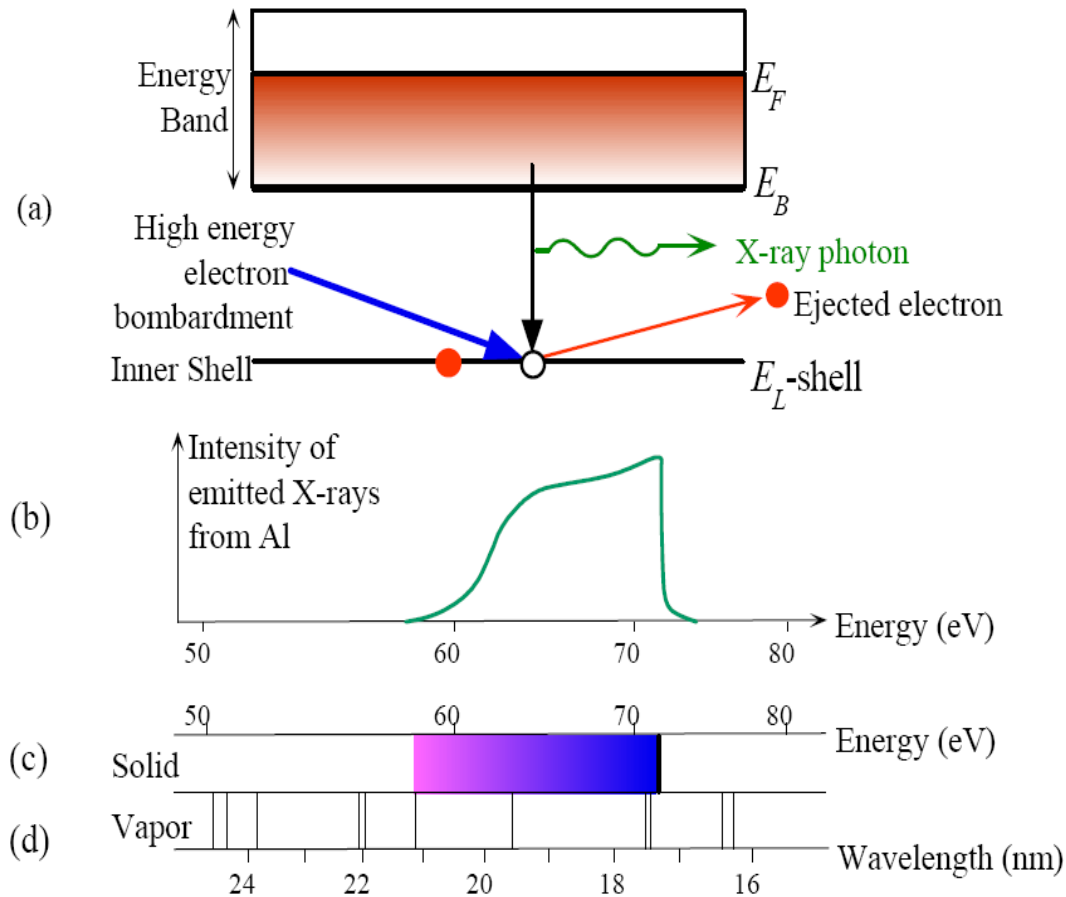
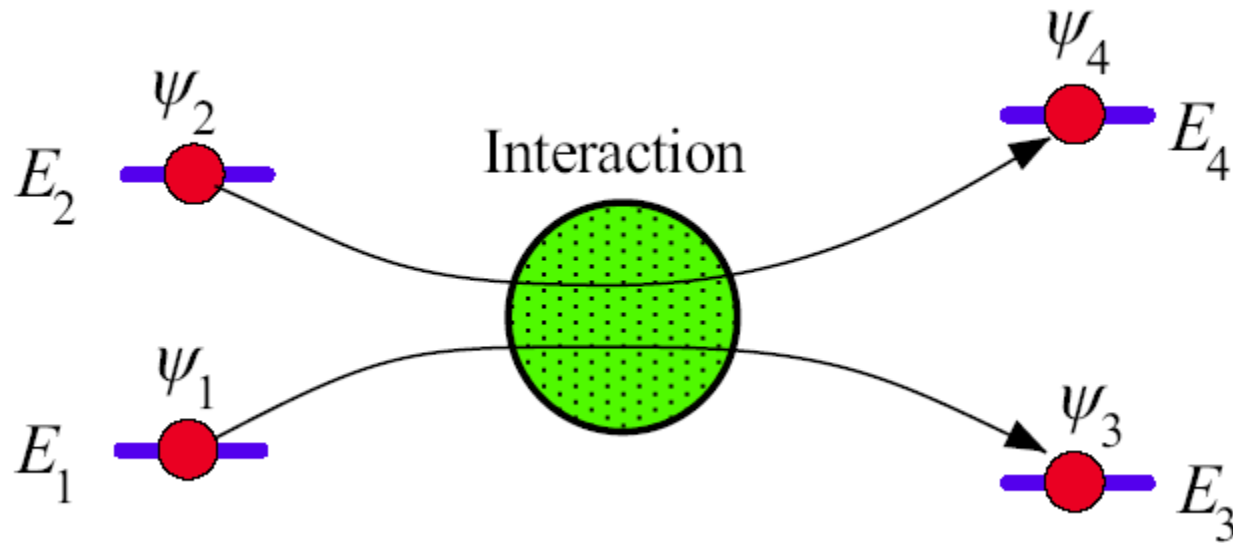
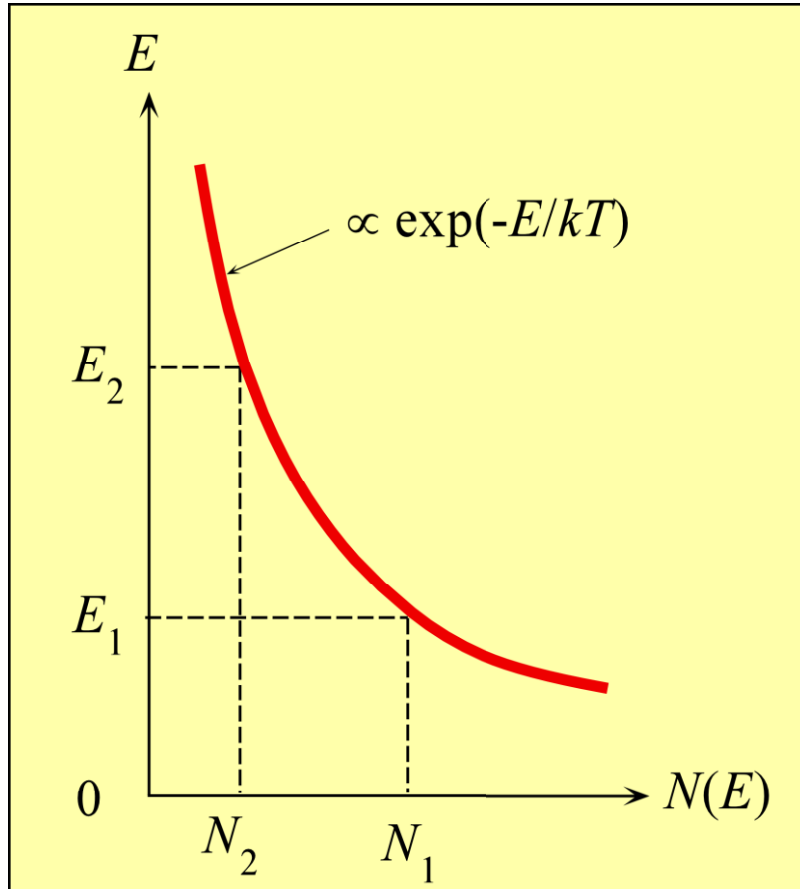


Fig 4.23



Two electrons with initial wavefunctions ψ_1 and ψ_2 at E_1 and E_2 interact and end up with different energies E_3 and E_4 . Their corresponding wavefunctions are ψ_3 and ψ_4 .

Fig 4.24



The Boltzmann energy distribution describes the statistics of particles, such as electrons, when there are many more available states than the number of particles.

Fig 4.25

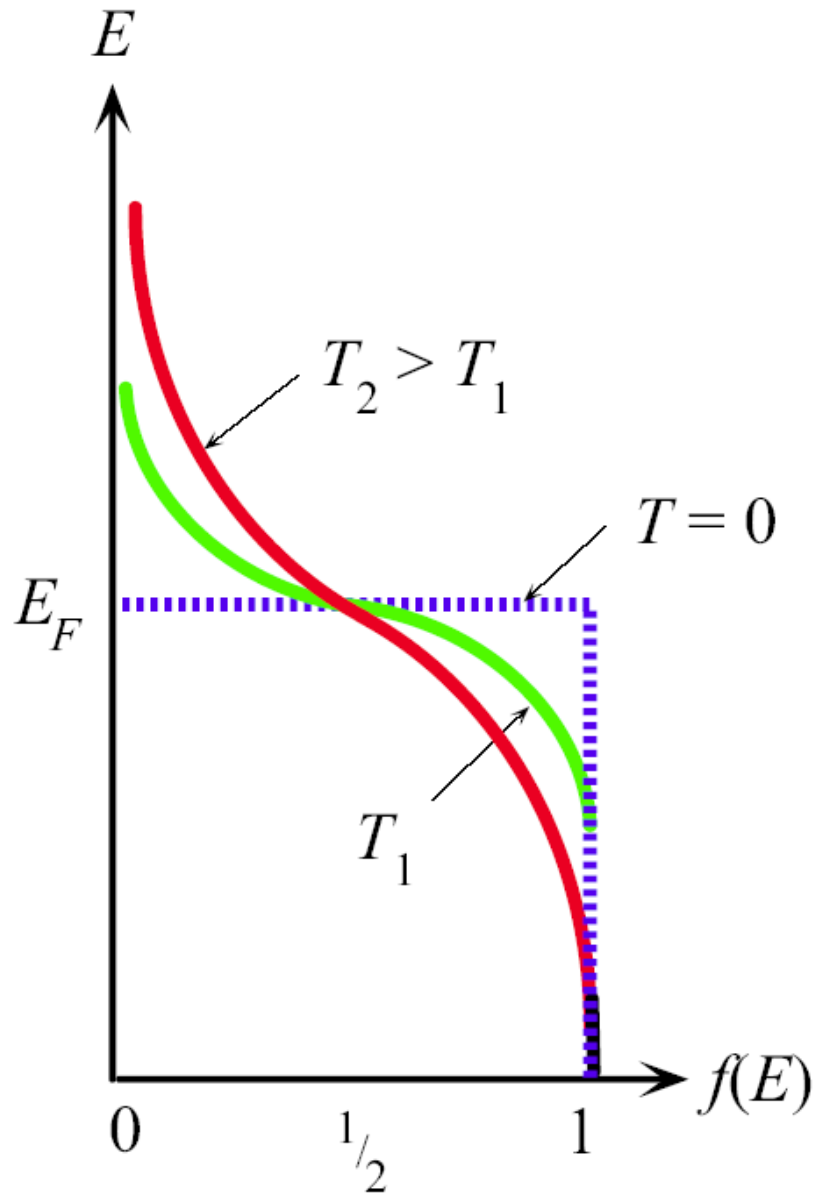
Boltzmann Classical Statistics

Boltzmann probability function

$$P(E) = A \exp\left(-\frac{E}{kT}\right)$$

Boltzmann Statistics for two energy levels

$$\frac{N_2}{N_1} = \exp\left(-\frac{E_2 - E_1}{kT}\right)$$



The fermi-Dirac $f(E)$ describes the statistics of electrons in a solid. The electrons interact with each other and the environment, obeying the Pauli exclusion principle.

Fig 4.26

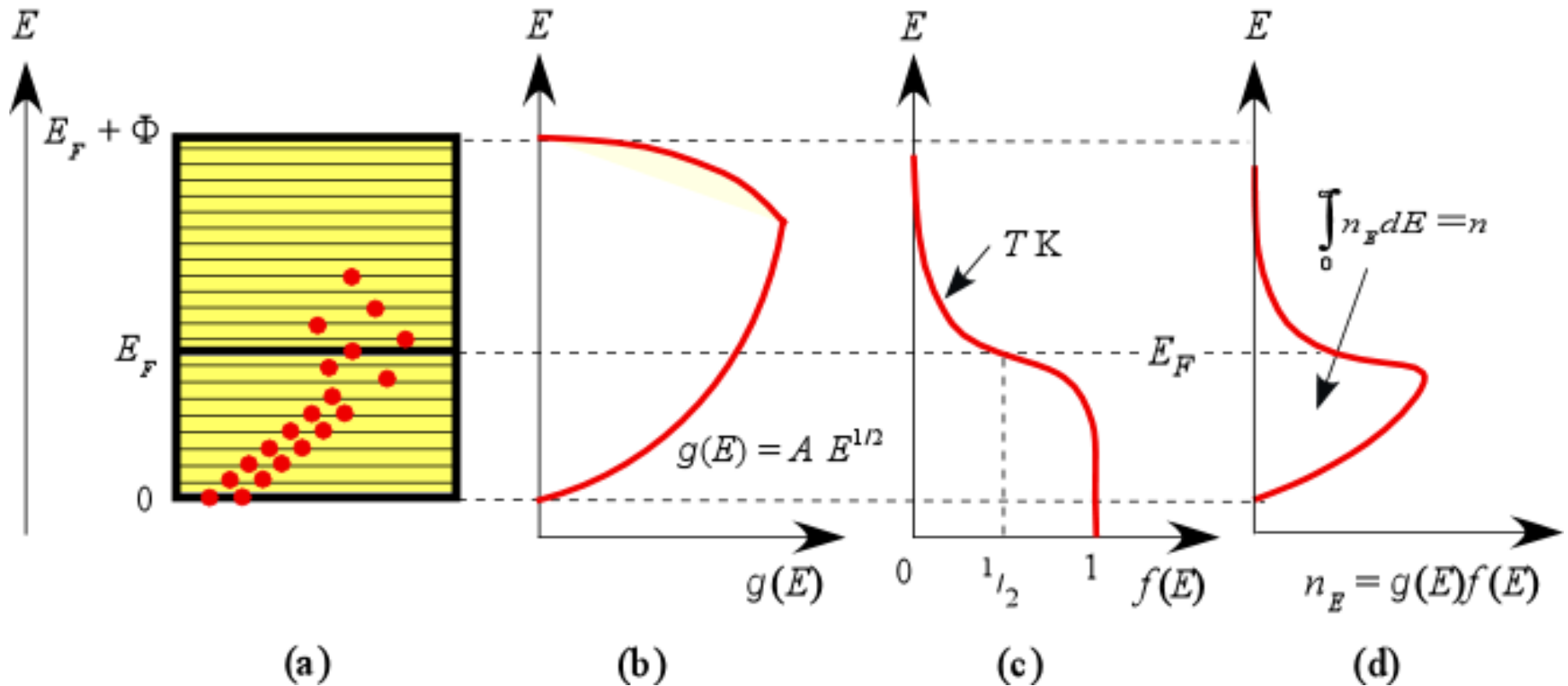
Fermi-Dirac Statistics

The Fermi-Dirac function

$$f(E) = \frac{1}{1 + \exp\left(\frac{E - E_F}{kT}\right)}$$

where E_F is a constant called the **Fermi energy**.

$f(E)$ = the probability of finding an electron in a state with energy E is given



- (a) Above 0K, due to thermal excitation, some of the electrons are at energies above E_F .
- (b) The density of states, $g(E)$ versus E in the band.
- (c) The probability of occupancy of a state at an energy E is $f(E)$.
- (d) The product of $g(E)f(E)$ is the number of electrons per unit energy per unit volume, or the electron concentration per unit energy. The area under the curve on the energy axis is the concentration of electrons in the band.

Fig 4.27

Fermi Energy

Fermi energy at $T = 0$ K

$$E_{FO} = \left(\frac{h^2}{8m_e} \right) \left(\frac{3n}{\pi} \right)^{2/3}$$

n is the concentration of conduction electrons (free carrier concentration)

Fermi energy at T (K)

$$E_F(T) = E_{FO} \left[1 - \frac{\pi^2}{12} \left(\frac{kT}{E_{FO}} \right)^2 \right]$$

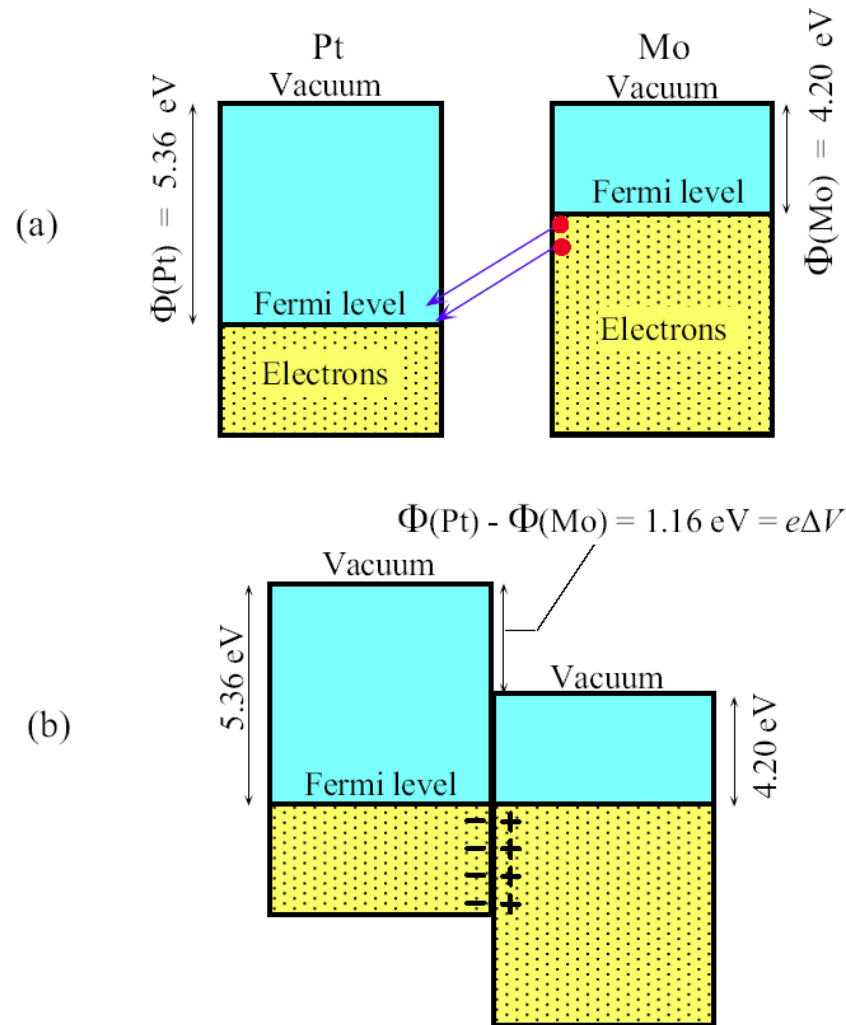
Average energy per electron

Average energy per electron at 0 K

$$E_{\text{av}}(0) = \frac{3}{5} E_{FO}$$

Average energy per electron at T (K)

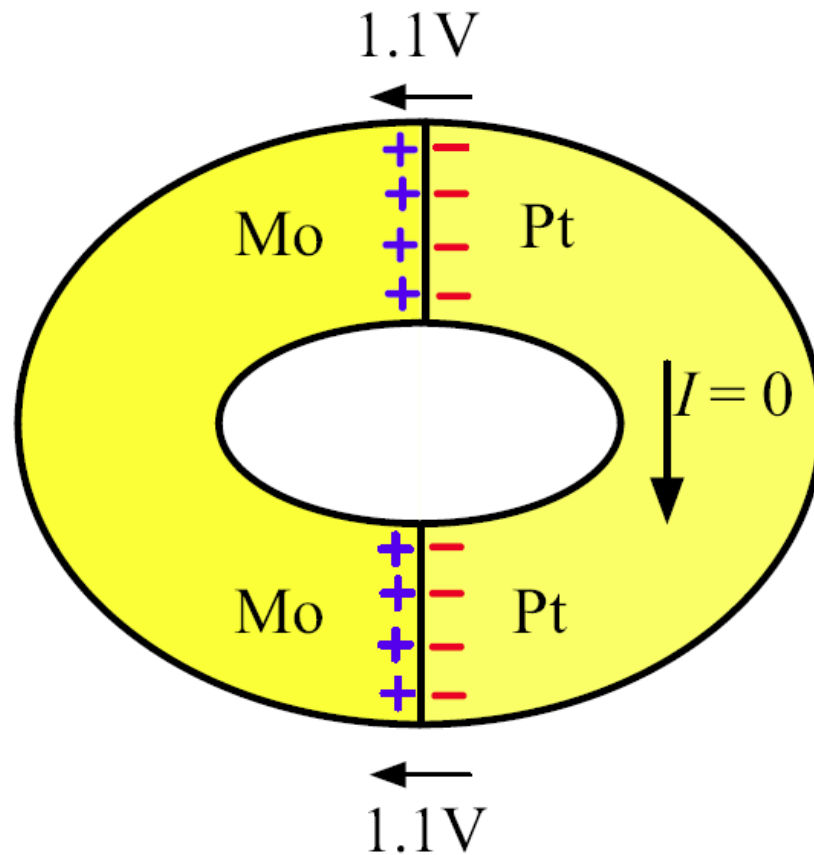
$$E_{\text{av}}(T) = \frac{3}{5} E_{FO} \left[1 + \frac{5\pi^2}{12} \left(\frac{kT}{E_{FO}} \right)^2 \right]$$



- (a) Electrons are more energetic in Mo, so they tunnel to the surface of Pt.
- (b) Equilibrium is reached when the Fermi levels are lined up.

When two metals are brought together, there is a contact potential ΔV .

Fig 4.28



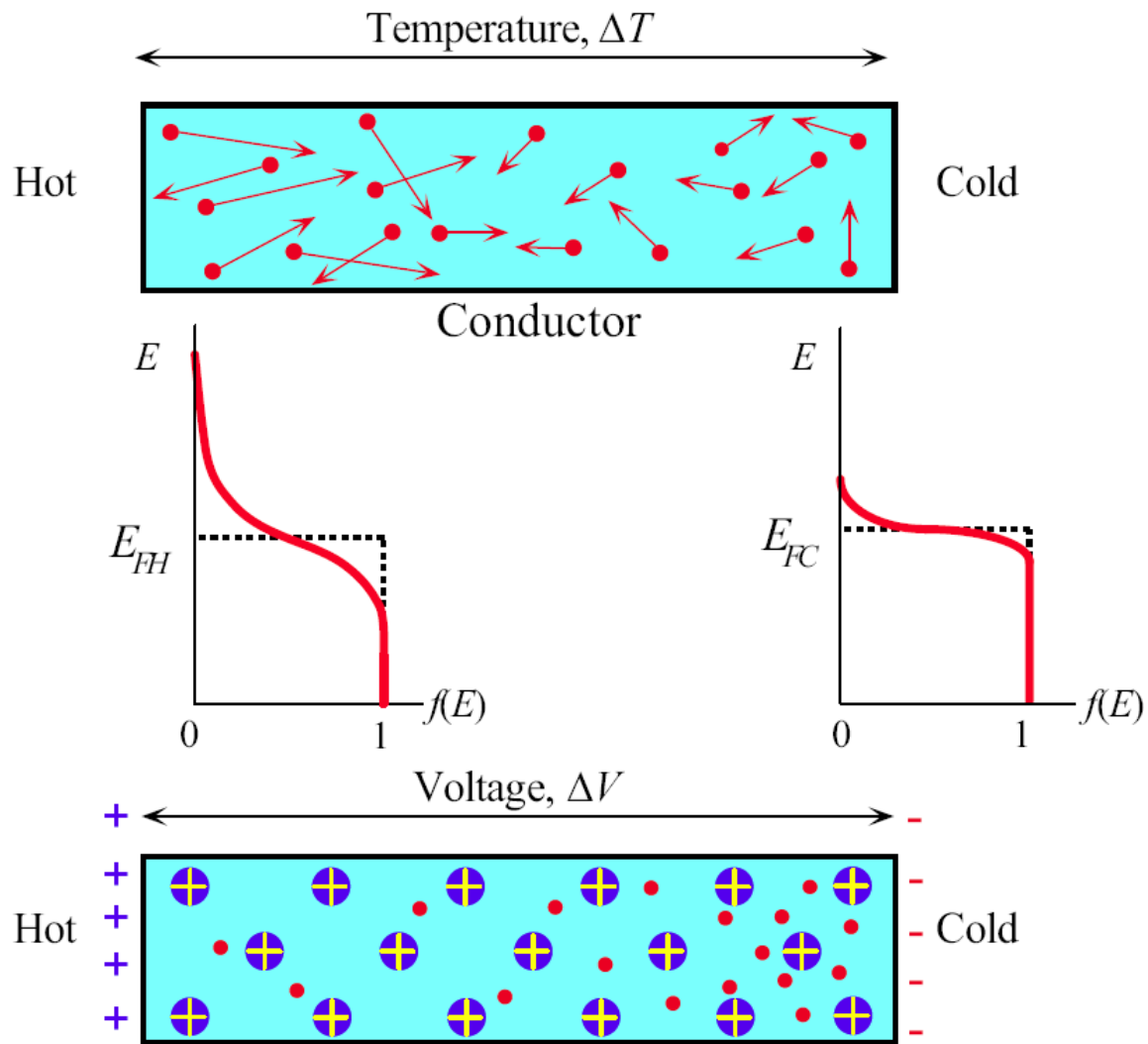
There is no current when a closed circuit is formed by two different metals, even though there is a contact potential at each contact.

The contact potentials oppose each other.

Fig 4.29

Fermi Energy Significance

For a given metal the Fermi energy represents the free energy per electron called the **electrochemical potential**. The Fermi energy is a measure of the potential of an electron to do electrical work ($e \times V$) or nonmechanical work, through chemical or physical processes.



The Seebeck effect. A temperature gradient along a conductor gives rise to a potential difference.

Fig 4.30

Seebeck Effect

Seebeck effect (thermoelectric power)

is the built-in potential difference ΔV across a material due to a temperature difference ΔT across it.

$$S = \frac{\Delta V}{\Delta T}$$

Sign of S

is the potential of the cold side with respect to the hot side; negative if electrons have accumulated in the cold side.

Seebeck coefficient for metals

$$S \approx -\frac{\pi^2 k^2 T}{3eE_{FO}} x$$

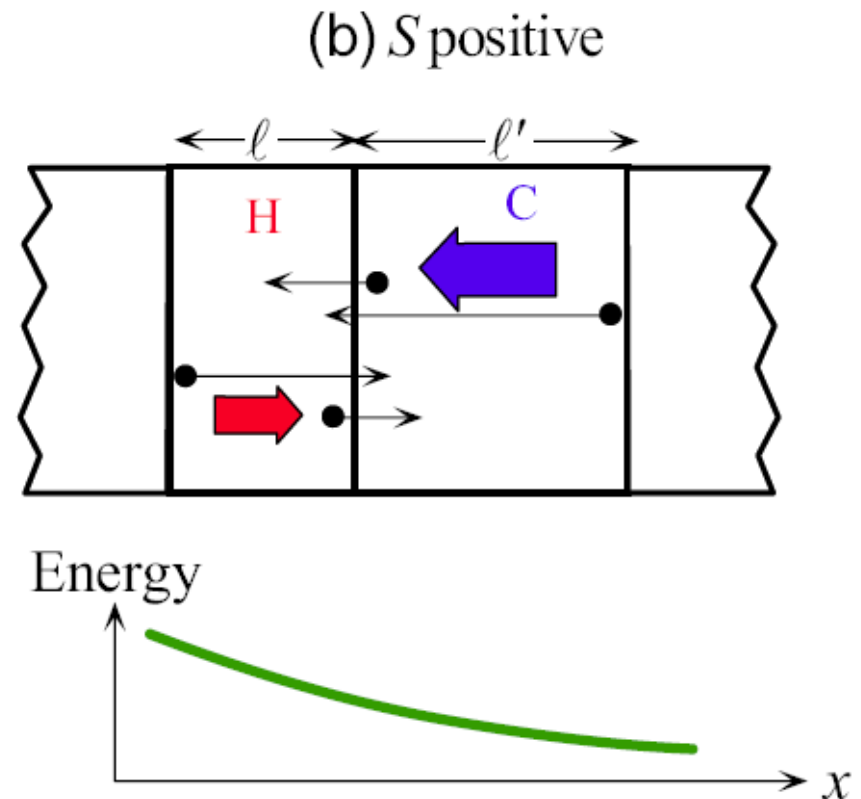
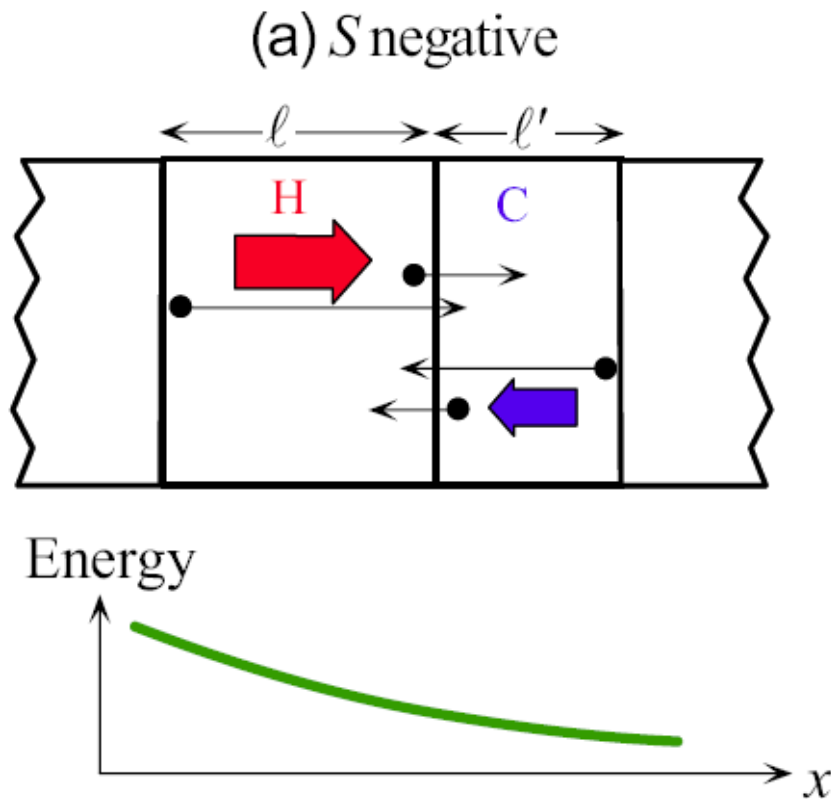
Mott and Jones thermoelectric power equation

x = a numerical constant that takes into account how various charge transport parameters, such as the mean free path ℓ , depend on the electron energy.

x values are tabulated in Table 4.3

Table 4.3 Seebeck coefficients of selected metals (from various sources)

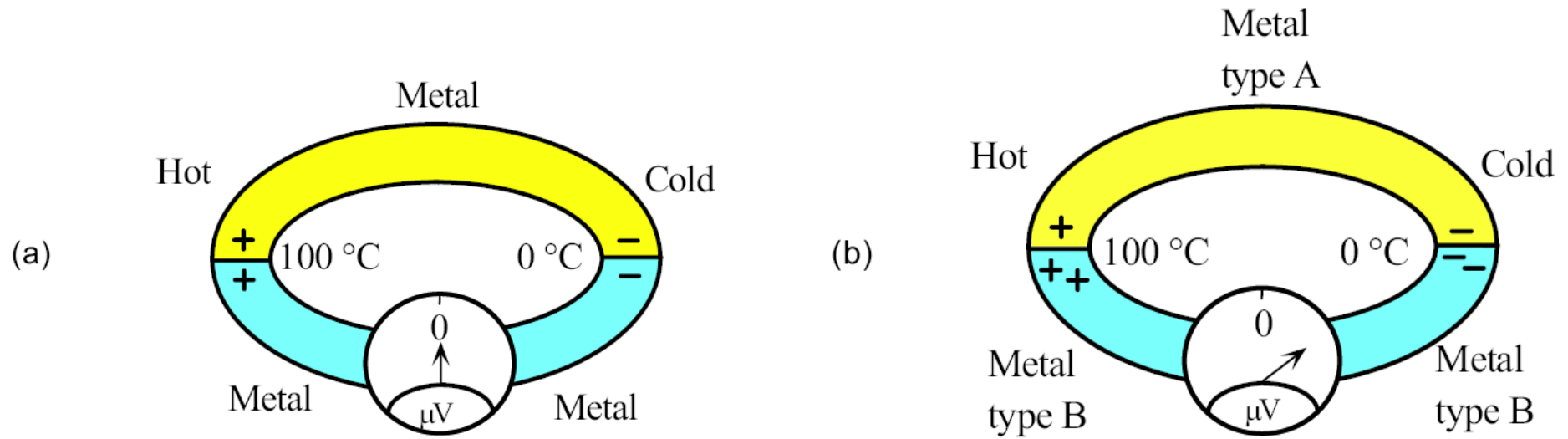
Metal	S at 0 °C ($\mu\text{V K}^{-1}$)	S at 27 °C ($\mu\text{V K}^{-1}$)	E_F (eV)	x
Al	−1.6	−1.8	11.6	2.78
Au	+1.79	+1.94	5.5	−1.48
Cu	+1.70	+1.84	7.0	−1.79
K		−12.5	2.0	3.8
Li	+14		4.7	−9.7
Mg	−1.3		7.1	1.38
Na		−5	3.1	2.2
Pd	−9.00	−9.99		
Pt	−4.45	−5.28		



Consider two neighboring regions H (hot) and C (cold) with widths corresponding to the mean Free paths ℓ and ℓ' in H and C.

Half the electrons in H would be moving in the $+x$ direction and the other half in the $-x$ direction. Half of the electrons in H therefore cross into C, and half in C cross into H.

Fig 4.31



- (a) If Al wires are used to measure the Seebeck voltage across the Al rod, then the net emf is zero.
- (b) The Al and Ni have different Seebeck coefficients. There is therefore a net emf in the Al-Ni Circuit between the hot and cold ends that can be measured.

Fig 4.32

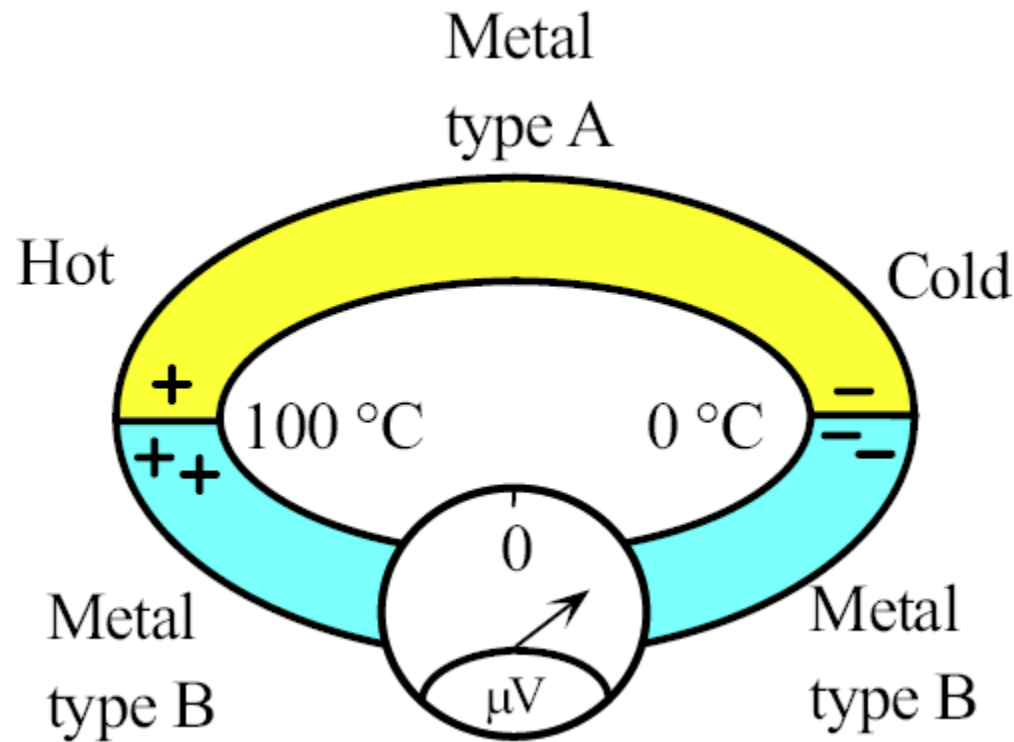
Thermocouple

We can only measure differences between thermoelectric powers of materials.

When two different metals A and B are connected to make a **thermocouple**, then the net EMF is the voltage difference between the two elements.

$$V_{AB} = \int_{T_o}^T (S_A - S_B) dT = \int_{T_o}^T S_{AB} dT$$

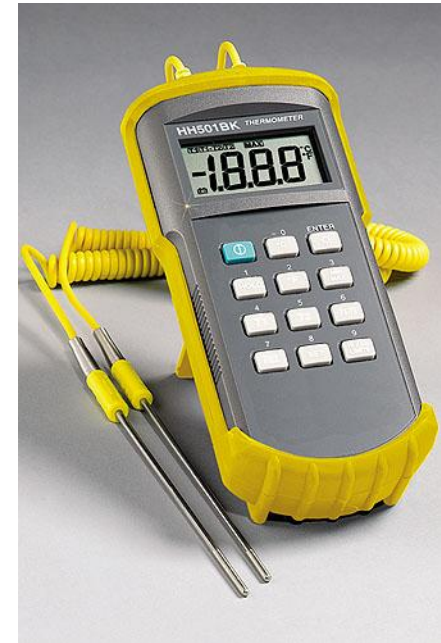
Thermocouple Equation



$$V_{AB} = a\Delta T + b(\Delta T)^2$$

Table 4.4 Thermoelectric emf for metals at 100 and 200 °C with respect to Pt and the reference junction at 0 °C

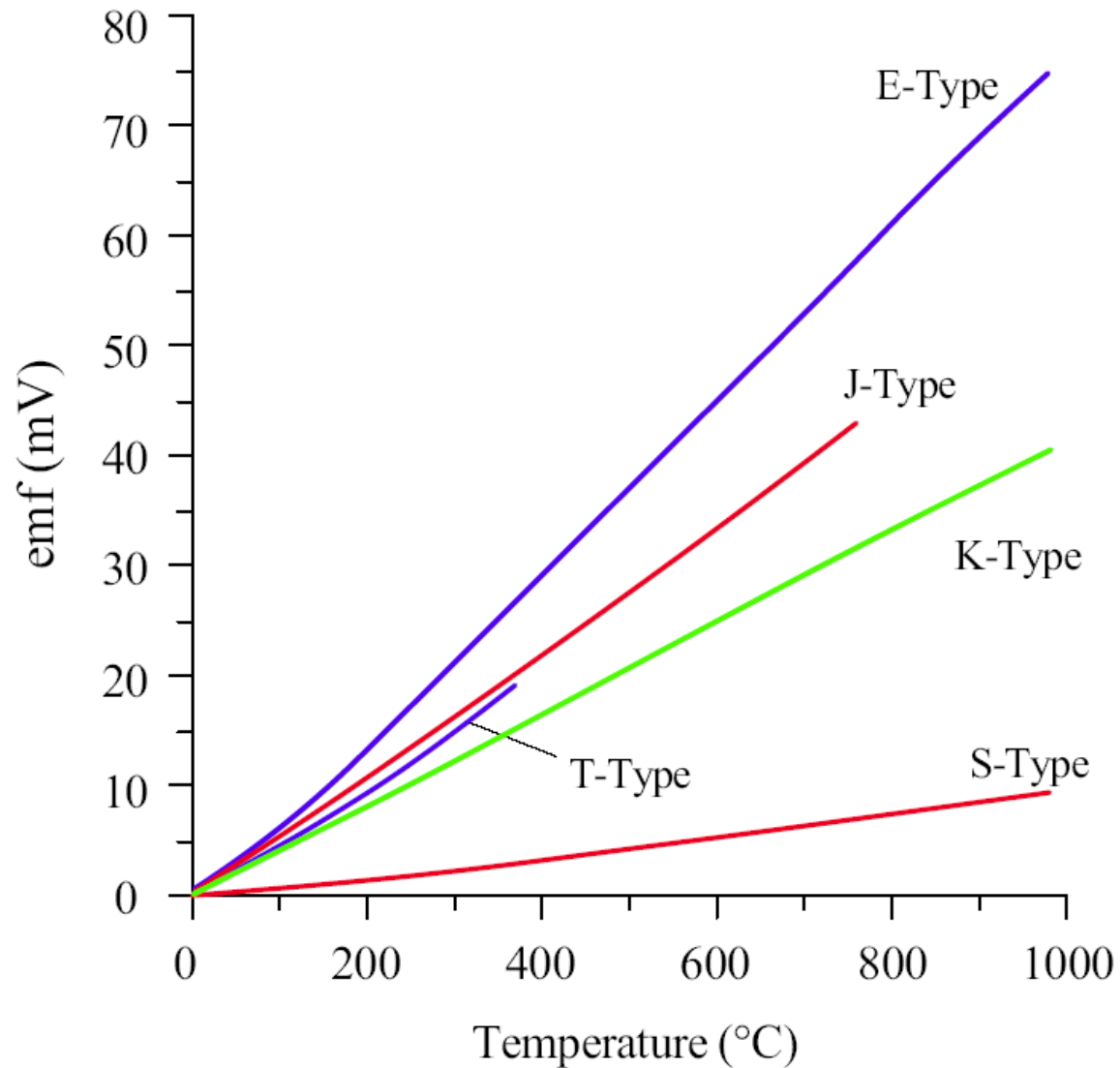
Material	emf (mV)	
	At 100 °C	At 200 °C
Copper, Cu	0.76	1.83
Aluminum, Al	0.42	1.06
Nickel, Ni	−1.48	−3.10
Palladium, Pd	−0.57	−1.23
Platinum, Pt	0	0
Silver, Ag	0.74	1.77
Alumel	−1.29	−2.17
Chromel	2.81	5.96
Constantan	−3.51	−7.45
Iron, Fe	1.89	3.54
90% Pt–10% Rh (platinum-rhodium)	0.643	1.44



Thermocouples are widely used to measure the temperature.

LEFT: A thermocouple pair embedded in a stainless steel sheath-probe. The thermocouple junction inside the probe is in thermal contact with the probe tip, and, electrically insulated from the probe metal.

|SOURCE: Courtesy of Omega



Output emf versus temperature (°C) for various thermocouple between 0 and 1000 °C

Fig 4.33

Examples of vacuum tubes using thermionic emission



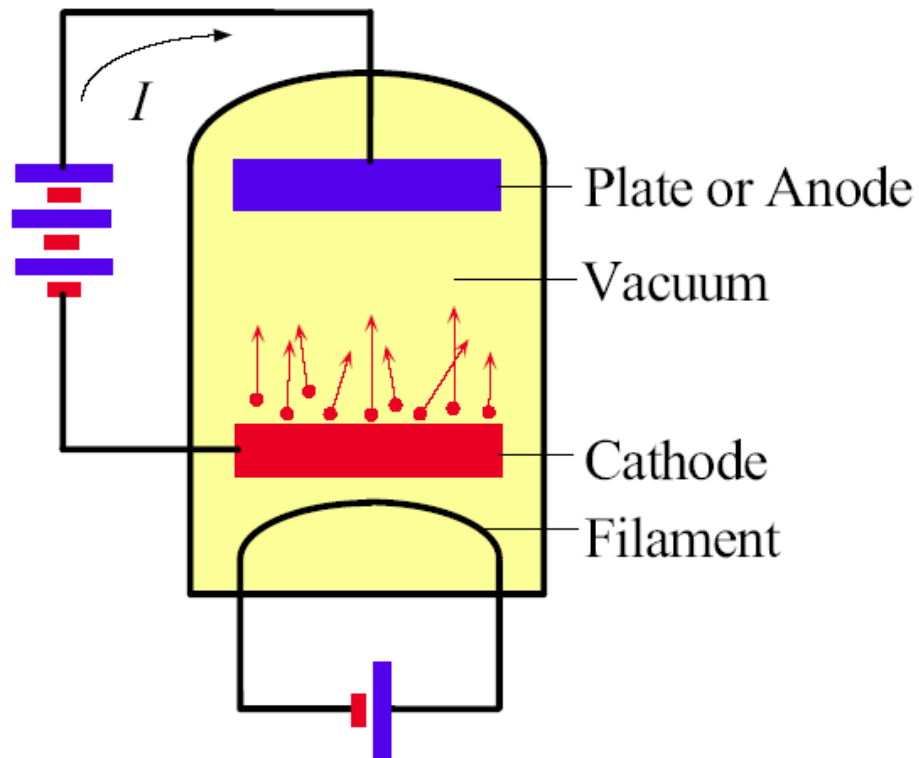
TOP: UHF Tetrode vacuum tubes that can handle up to 30 kW, and provide gains up to 17 dB

|SOURCE: Courtesy of Thales

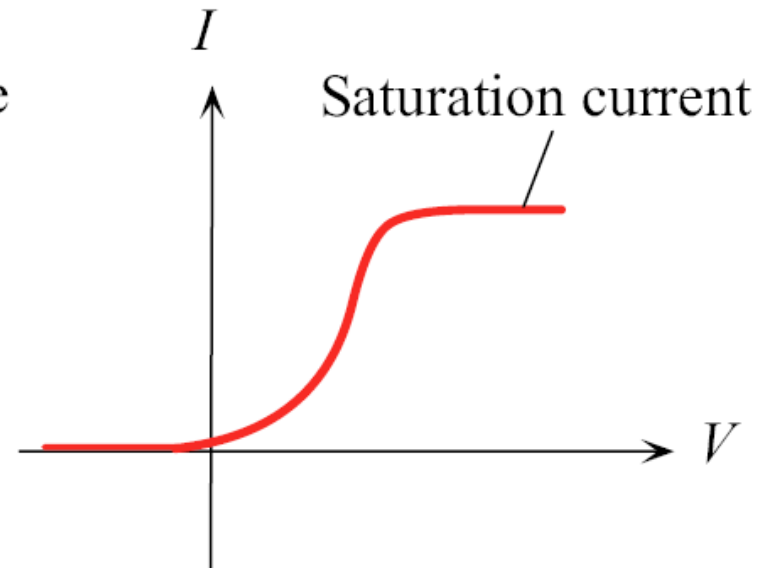


LEFT: Klystrons are used as the final amplifier stage in many UHF television transmitters.

|SOURCE: Courtesy of Thales



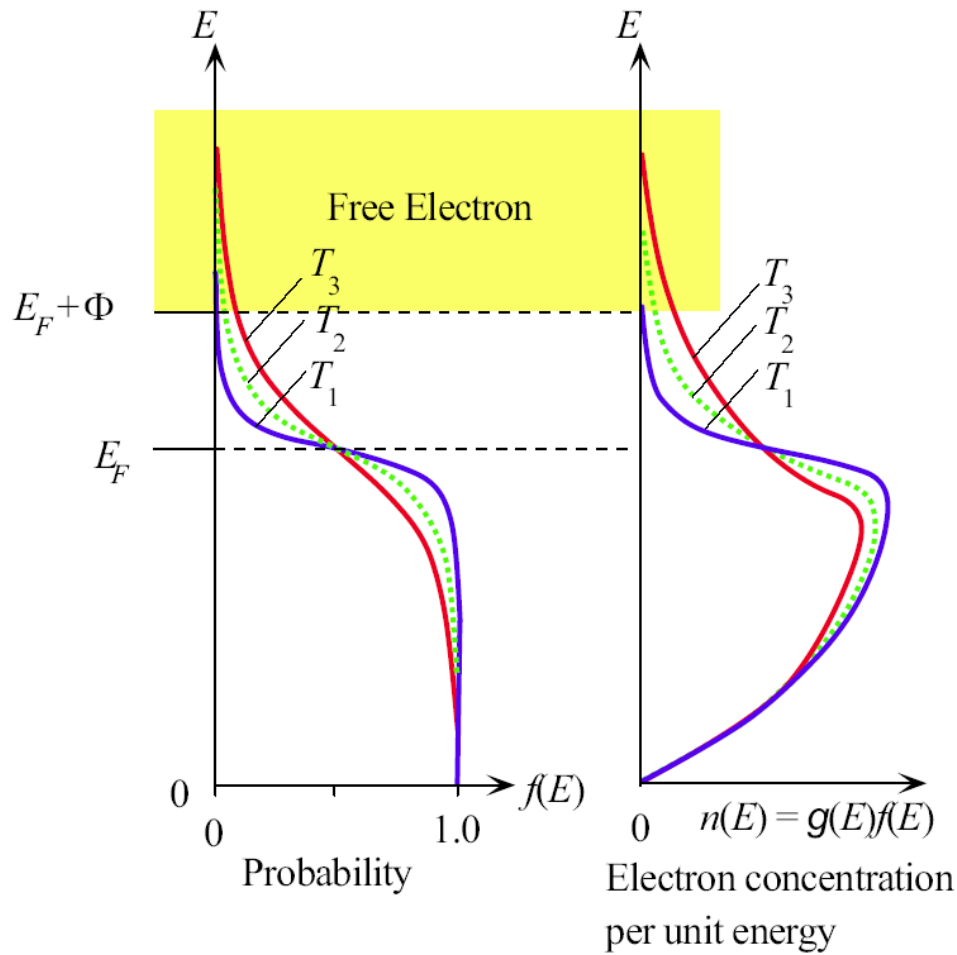
(a)



(b)

- (a) Thermionic electron emission in a vacuum tube.
 (b) Current-voltage characteristics of a vacuum diode.

Fig 4.34



Fermi-Dirac function $f(E)$ and the energy density of electrons $n(E)$ (electrons per unit energy And per unit volume) at three different temperatures. The electron concentration extends more And more to higher energies as the temperature increases. Electrons with energies in excess of $E_F + \Phi$ can leave the metal (thermionic emission)

Fig 4.35

Thermionic Emission

Richardson-Dushman thermionic emission equation

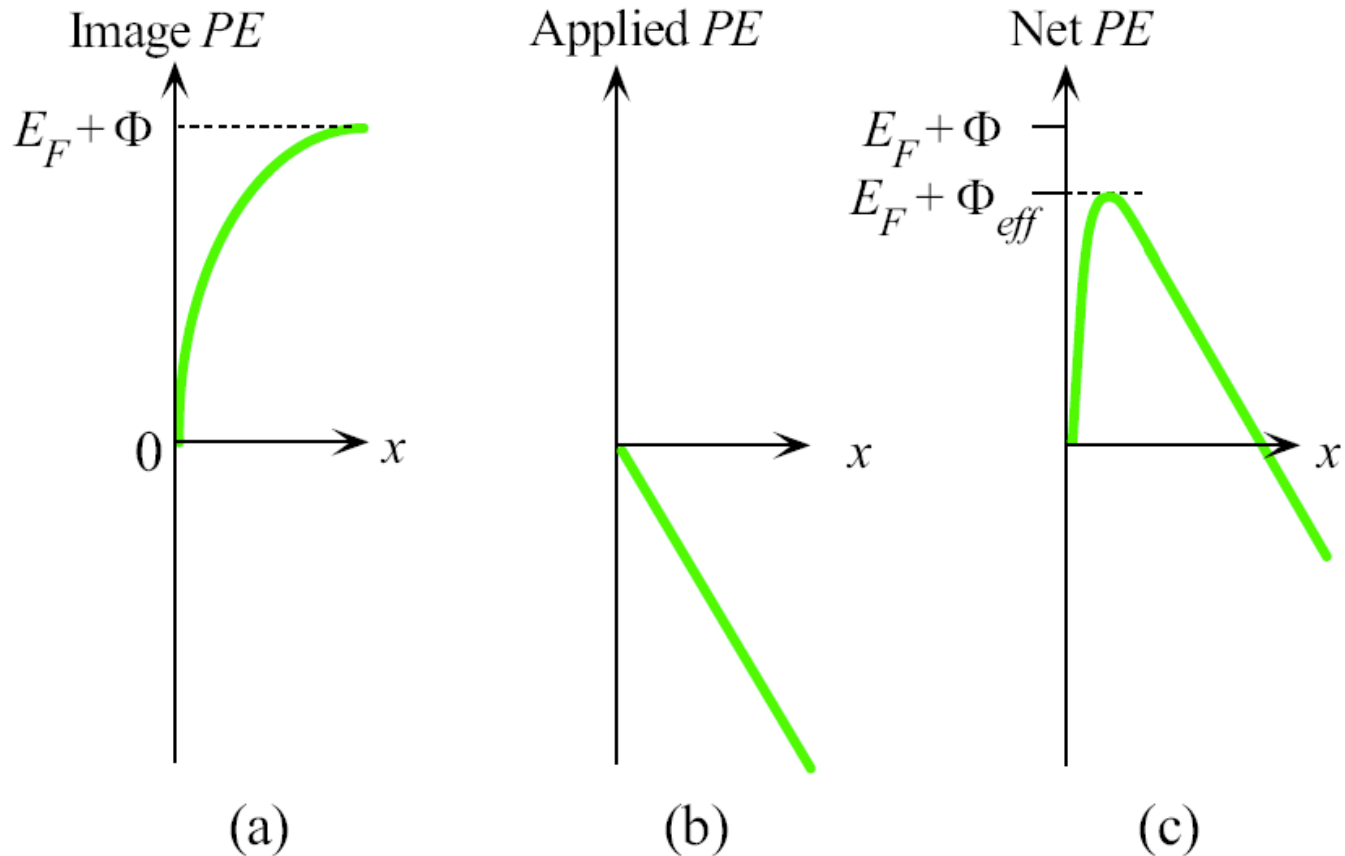
$$J = B_o T^2 \exp\left(-\frac{\Phi}{kT}\right)$$

$$B_o = 4\pi e m_e k^2 / h^3 = 120 \cdot 10^6 \text{ A m}^{-2} \text{ K}^{-2}$$

Richardson-Dushman constant

$$J = B_e T^2 \exp\left(-\frac{\Phi}{kT}\right)$$

where B_e = effective emission constant



- (a) PE of the electron near the surface of a conductor.
- (b) Electron PE due to an applied field, that is, between cathode and anode.
- (c) The overall PE is the sum.

Fig 4.36

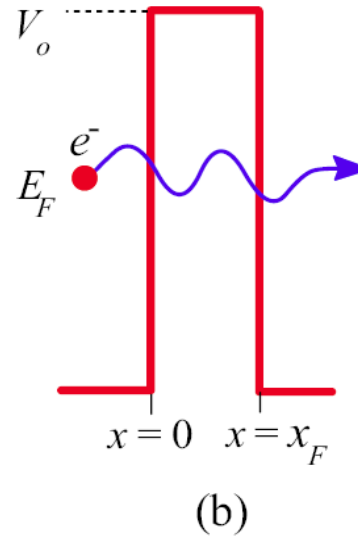
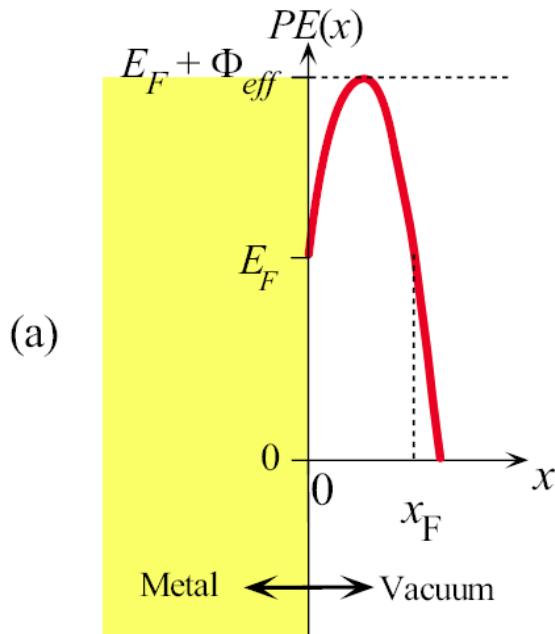
Schottky effect

When a positive voltage is applied to the anode with respect to the cathode, the electric field at the cathode helps the thermionic emission process by lowering the *PE* barrier Φ by an amount $\beta_s \mathcal{E}^{1/2}$. The current density in field assisted thermionic emission is

Metal's work function Schottky coefficient

$$J = B_e T^2 \exp \left(- \frac{\Phi - \beta_s \mathcal{E}^{1/2}}{kT} \right)$$

Field assisted emission is field assisted tunneling from the cathode



(a) Field emission is the tunneling of an electron at an energy E_F through narrow PE barrier induced by a large applied field.

(b) For simplicity, we take the barrier to be rectangular.

(c) A sharp point cathode has the maximum field at the tip where the field emission of electrons occurs.

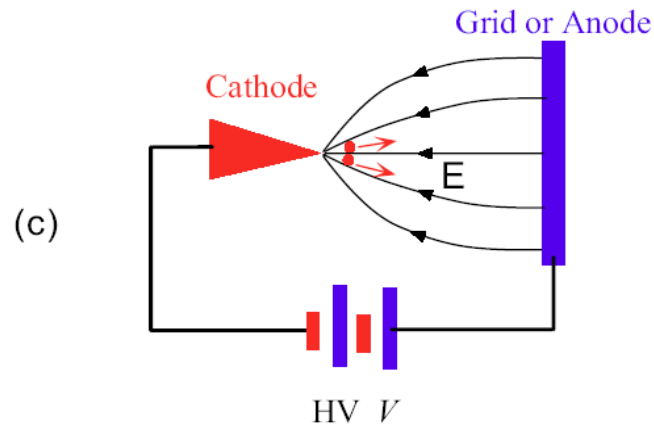


Fig 4.37

Field-assisted Tunneling

Field-assisted tunneling probability

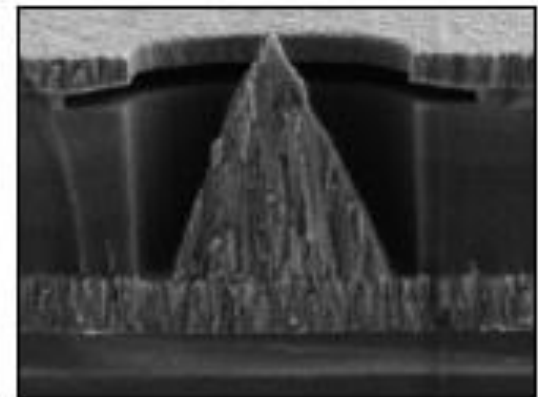
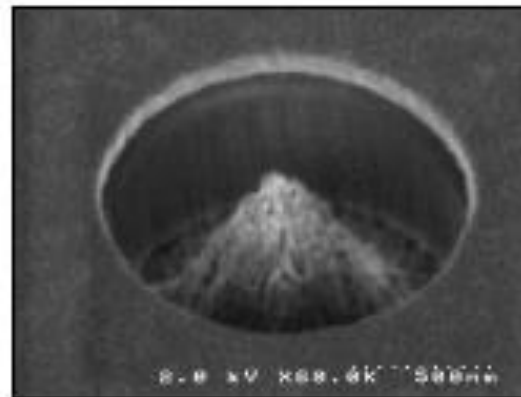
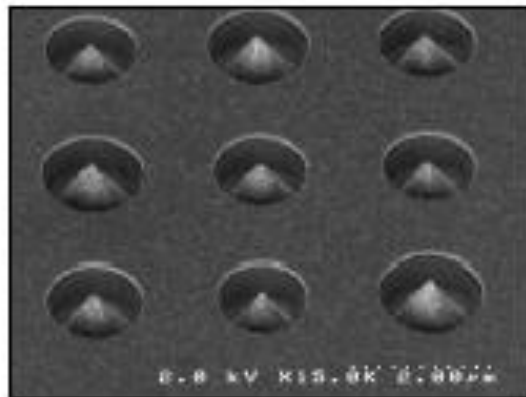
Effective work function due to the Schottky effect

$$p \approx \exp \left[- \frac{2(2m_e \Phi_{\text{eff}})^{1/2} \Phi}{e\hbar\mathcal{E}} \right]$$

Field-assisted tunneling: the Fowler-Nordheim equation

$$J_{\text{field-emission}} \approx C \mathcal{E}^2 \exp \left(- \frac{\mathcal{E}_c}{\mathcal{E}} \right)$$

Applied field at the cathode



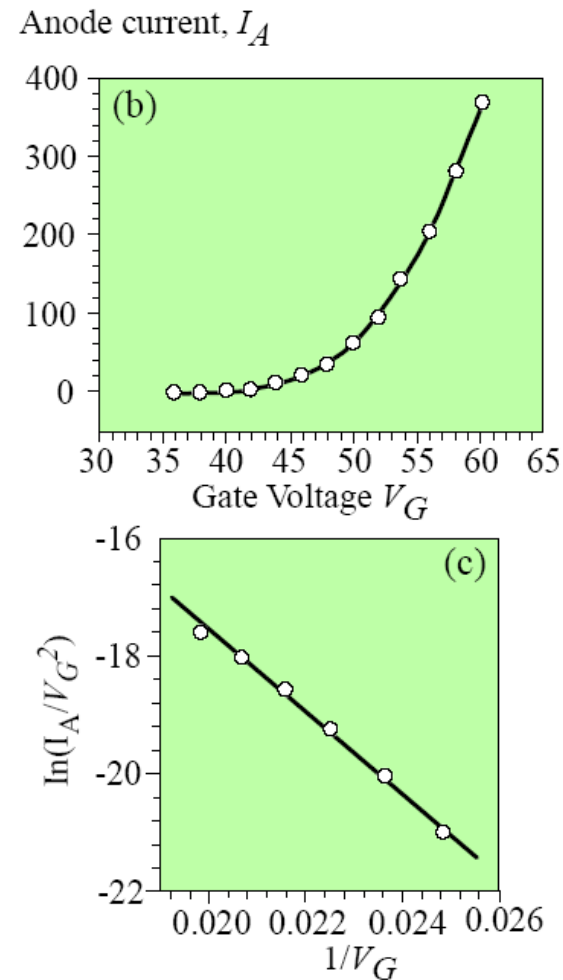
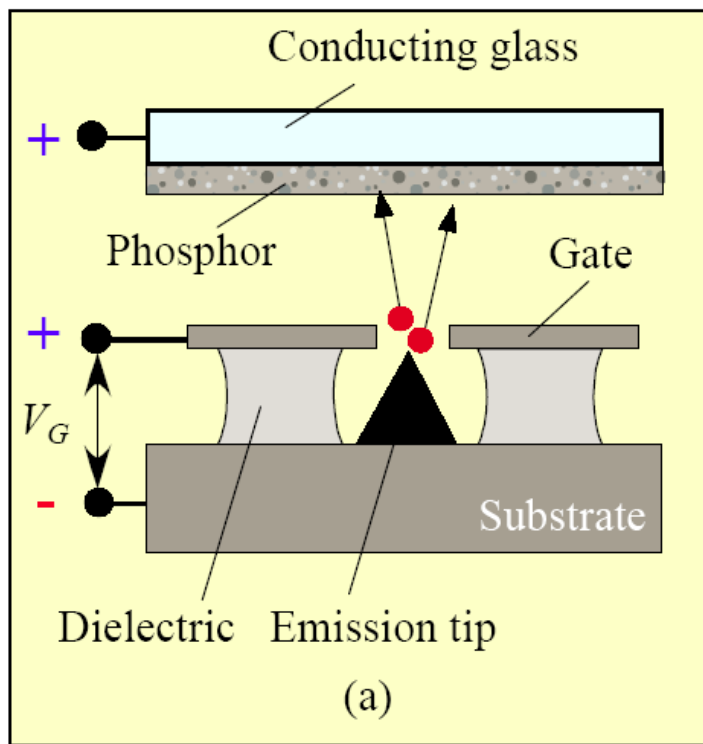
Left: A scanning electron microscope image of an array of electron field emitters (icebergs). Center: One iceberg. Right: A cross section of a field emitter. Each iceberg is a source of electron emission arising from Fowler–Nordheim field emission; for further information see B. Chalamala, et al., *IEEE Spectrum*, April 1998, pp. 42–51.

| SOURCE: Courtesy of Dr. Babu Chalamala, Flat Panel Display Division, Motorola.



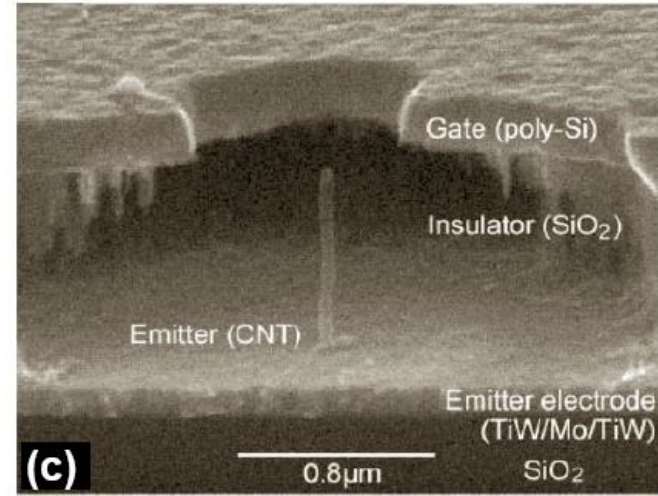
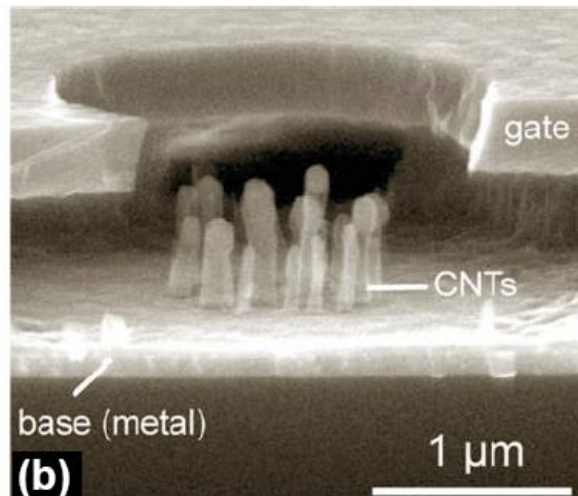
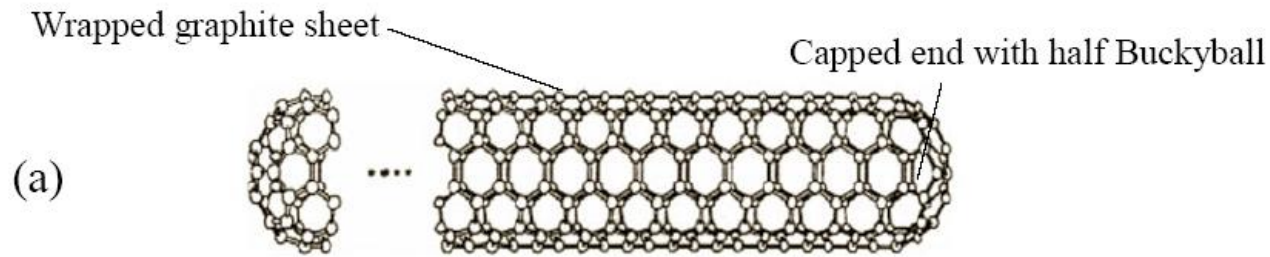
Motorola's prototype flat panel display based on the Fowler-Nordheim field emission principle. The display is 14 cm in diagonal and 3.5 mm thick with a viewing angle 160° . Each pixel ($325\text{ }\mu\text{m}$ thick) uses field emission of electrons from microscopic sharp point sources (icebergs). Emitted electrons impinge on colored phosphors on a screen and cause light emission by cathodoluminescence. There are millions of these microscopic field emitters to constitute the image.

| SOURCE: Courtesy of Dr. Babu Chalamala, Flat Panel Display Division, Motorola.



- (a) Spindt-type cathode and the basic structure of one of the pixels in the FED.
- (b) Emission (anode) current versus gate voltage.
- (c) Fowler-Nordheim plot that confirms field emission.

Fig 4.38



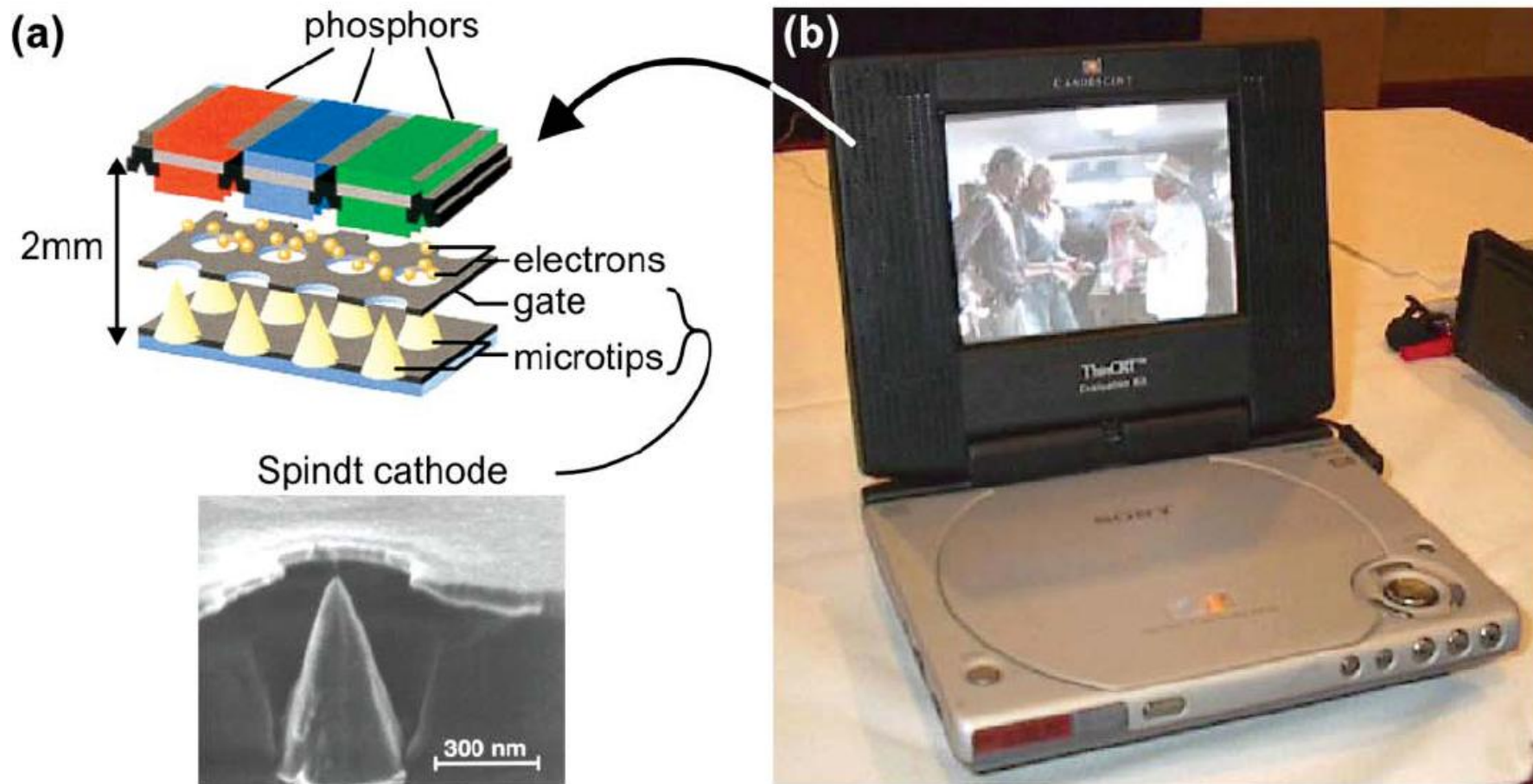
(a) A carbon nanotube (CNT) is a whisker-like very thin and long carbon molecule with rounded ends; almost a perfect shape as an electron field-emitter. **(b)** Multiple CNTs as electron emitters. **(c)** A single CNT as an emitter.

[SOURCE: Courtesy of Professor W.I. Milne, University of Cambridge; G. Pirio *et al*, *Nanotechnology*, **13**, 1, 2002.

Fig 4.39

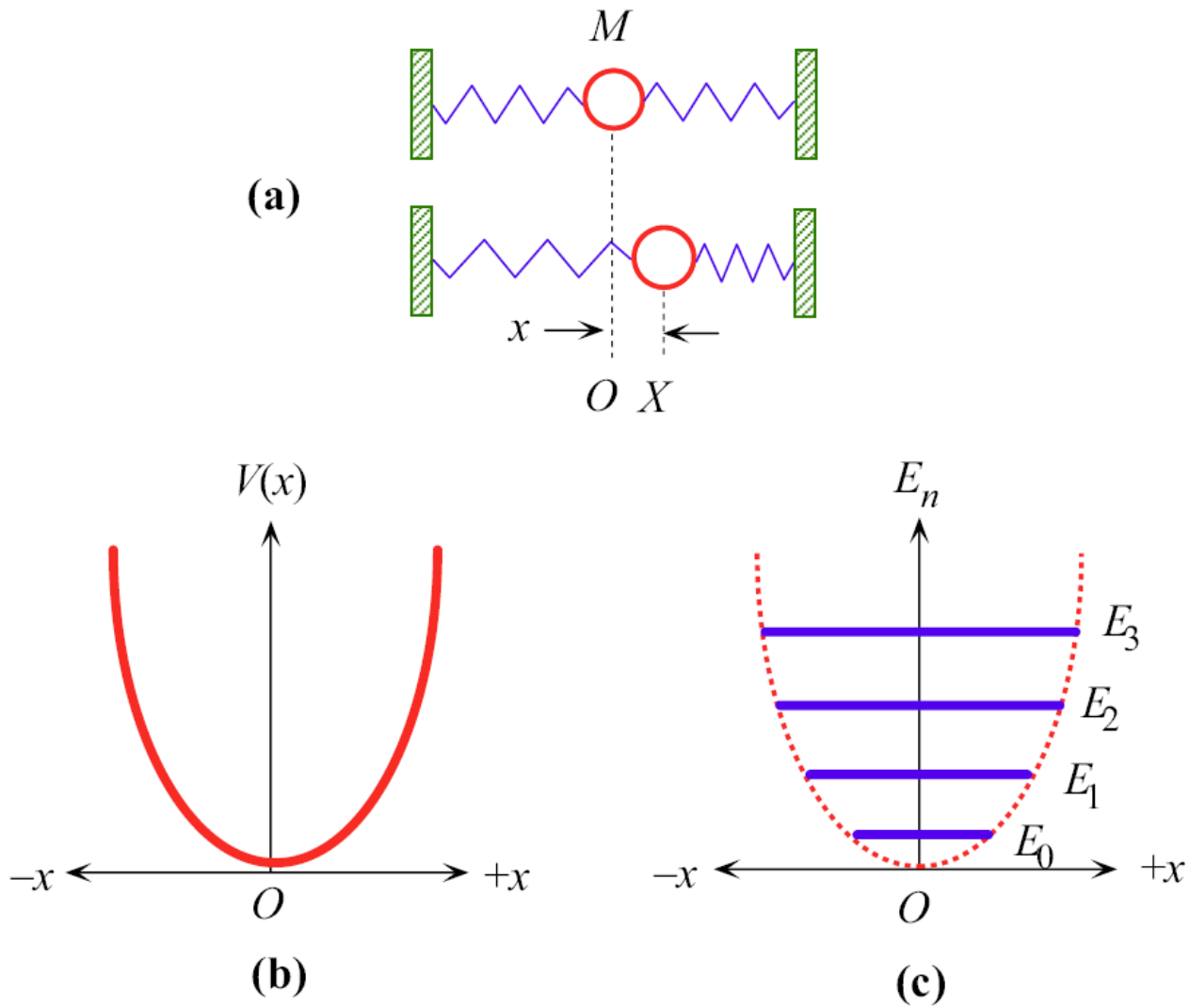
CNT (Carbon NanoTube)

A carbon nanotube (CNT) is a very thin filament-like carbon molecule whose diameter is in the nanometer range but whose length can be quite long, e.g., 10-100 microns, depending on how it is grown or prepared.



Cross-section of a field emission display showing a Spindt tip cathode, (b) Sony portable DVD player using a field emission display.

SOURCE: Courtesy of Professor W.I. Milne, University of Cambridge, England. *Carbon nanotubes as field emission sources*, W. I. Milne, K. B. K. Teo, G. A. J. Amaratunga, P. Legagneux, L. Gangloff, J.-P. Schnell, V. Semet, V. Thien Binh and O. Groening, *Journal of Materials Chemistry*, **14**, 933, 2004



(a) Harmonic vibrations of an atom about its equilibrium position assuming its neighbors are fixed.

(b) The *PE* curve $V(x)$ versus displacement from equilibrium, x .

(c) The energy is quantized.

Fig 4.40

Quantum Harmonic Oscillator

Harmonic potential energy

$$V(x) = \frac{1}{2} \overset{\text{Constant}}{\beta} x^2$$

Schrodinger equation for the harmonic oscillator

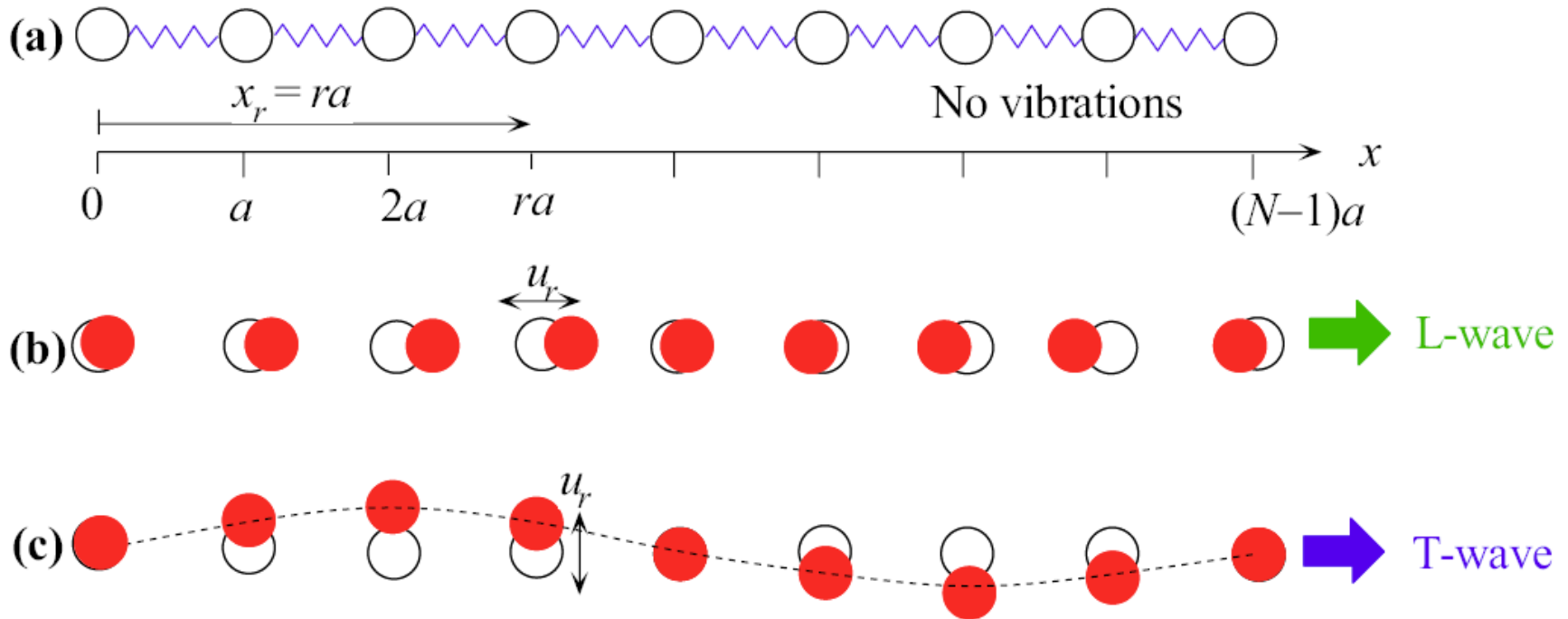
$$\frac{d^2\psi}{dx^2} + \frac{2M}{\hbar^2} \left(E - \frac{1}{2} \beta x^2 \right) \psi = 0$$

Energy of the harmonic oscillator

$$E_n = \left(n + \frac{1}{2} \right) \hbar \omega$$

Quantum number = 0, 1, 2, ...

Angular vibrational frequency of the oscillator.
 $\omega = (\beta/M)^{1/2}$.



(a) A chain of N atoms through a crystal in the absence of vibrations.


(b) Coupled atomic vibrations generate a traveling longitudinal (L) wave along x . Atomic displacements (u_r) are parallel to x .

(c) A transverse (T) wave traveling along x . Atomic displacements (u_r) are perpendicular to the x axis. (b) and (c) are snapshots at one instant.

Fig 4.41

Lattice Waves: Phonons

Traveling-wave-type lattice vibrations along x

$$u_r = A \exp[j(Kx_r - \omega t)]$$


Phonon Energy

Phonon wavevector

Phonon frequency

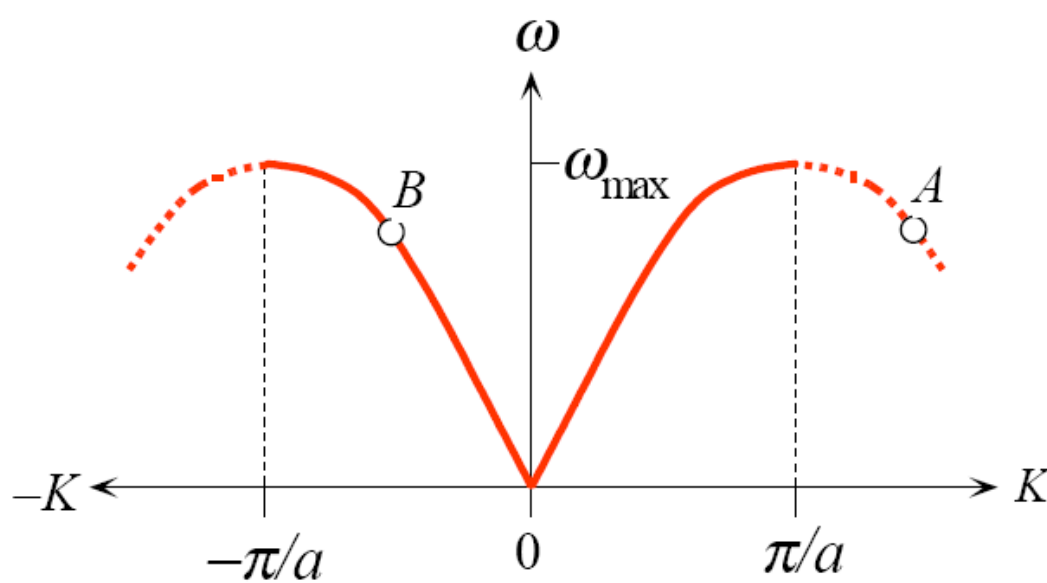
$$E_{\text{phonon}} = \hbar\omega = h\nu$$

Phonon Momentum

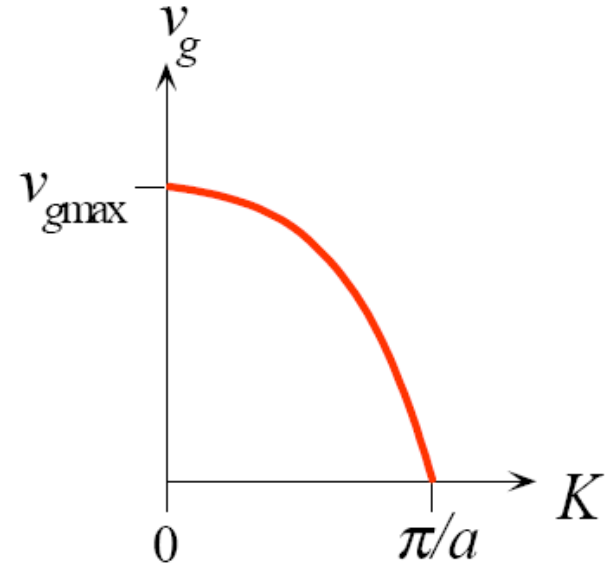
$$p_{\text{phonon}} = \hbar K$$

Dispersion Relation

$$\omega = 2\left(\frac{\beta}{M}\right)^{1/2} \left| \sin\left(\frac{1}{2} Ka\right) \right|$$



(a)



(b)

- (a) Frequency ω versus wavevector K relationship for lattice waves.
 (b) Group velocity v_g versus wavevector K .

Fig 4.42

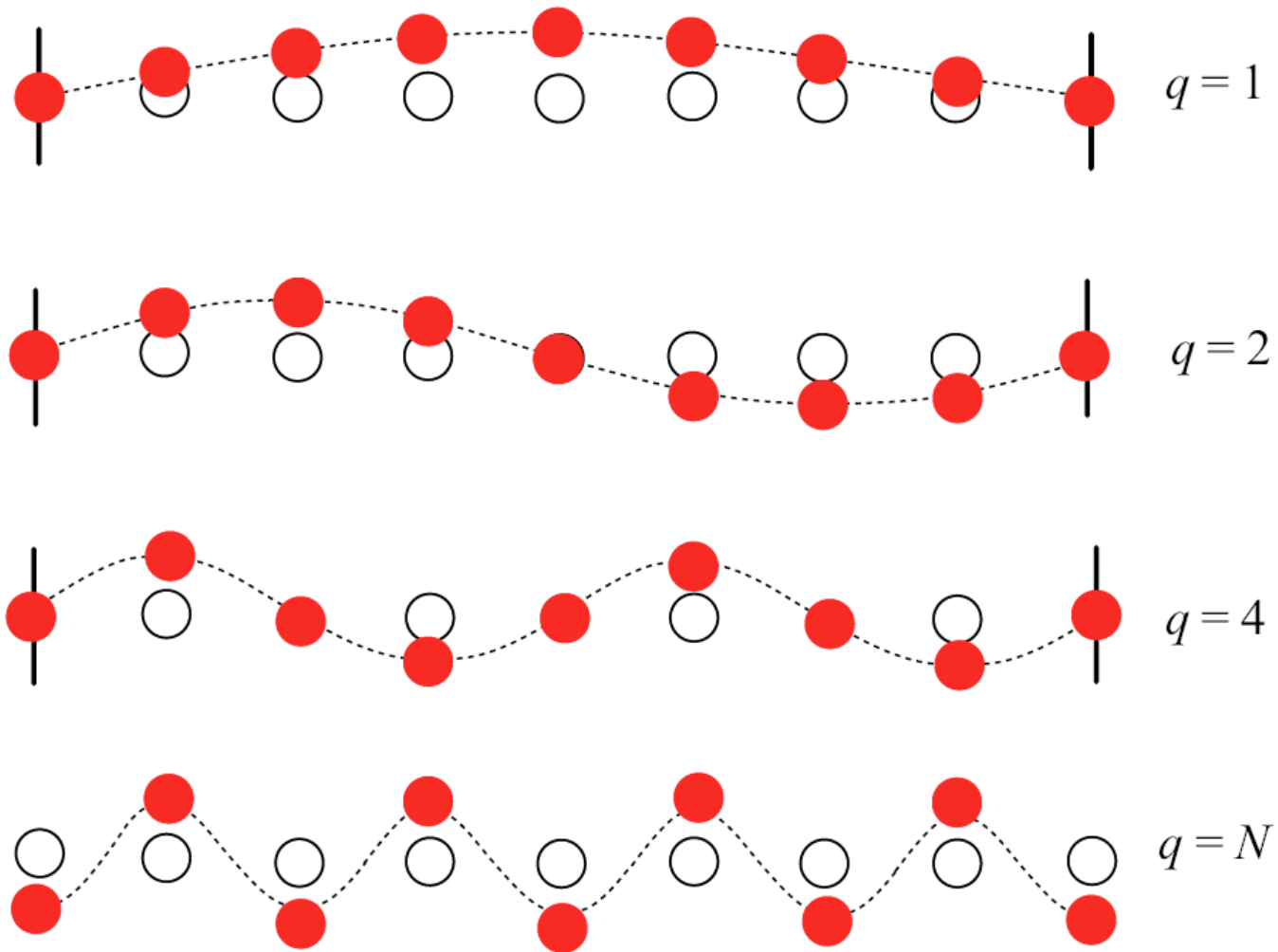
Group Velocity

The velocity at which traveling waves carry energy

$$v_g = \frac{d\omega}{dk} = \left(\frac{\beta}{M} \right)^{1/2} a \cos\left(\frac{1}{2} Ka \right)$$

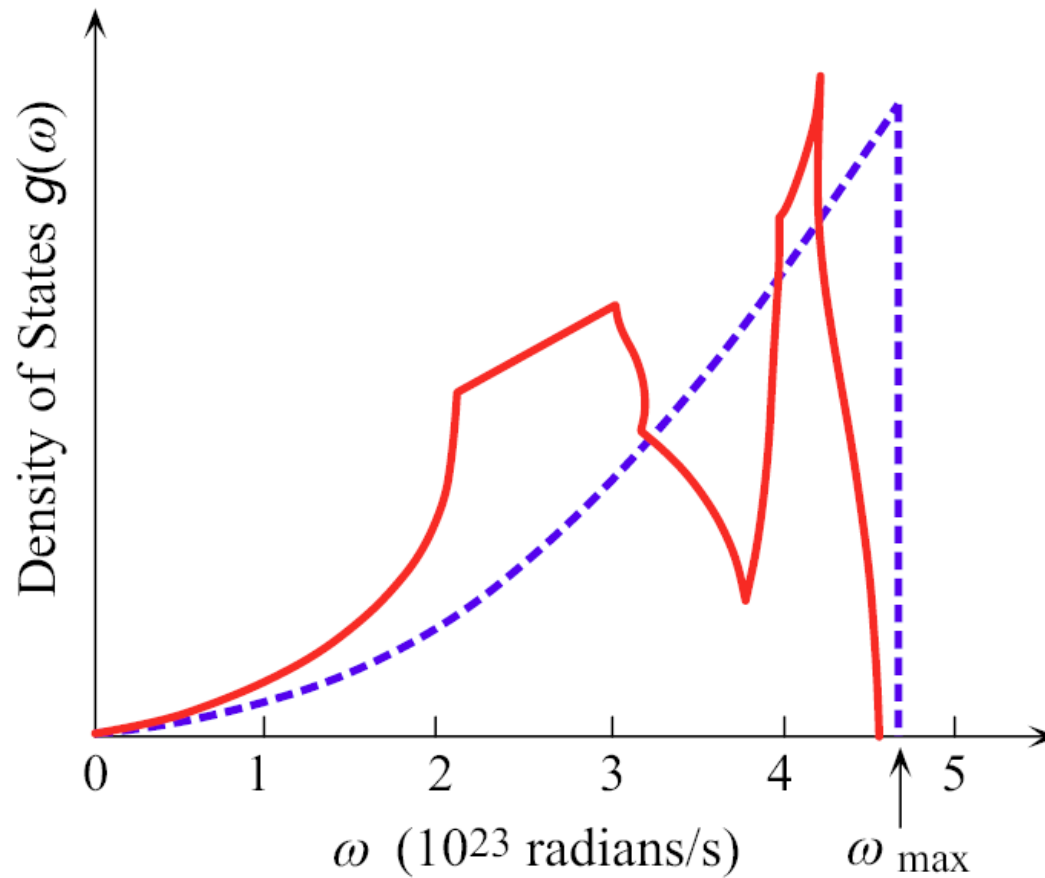
$$v_g \approx \left(\frac{Y}{\rho} \right)^{1/2}$$

Y = elastic modulus (Example 1.5), ρ = density



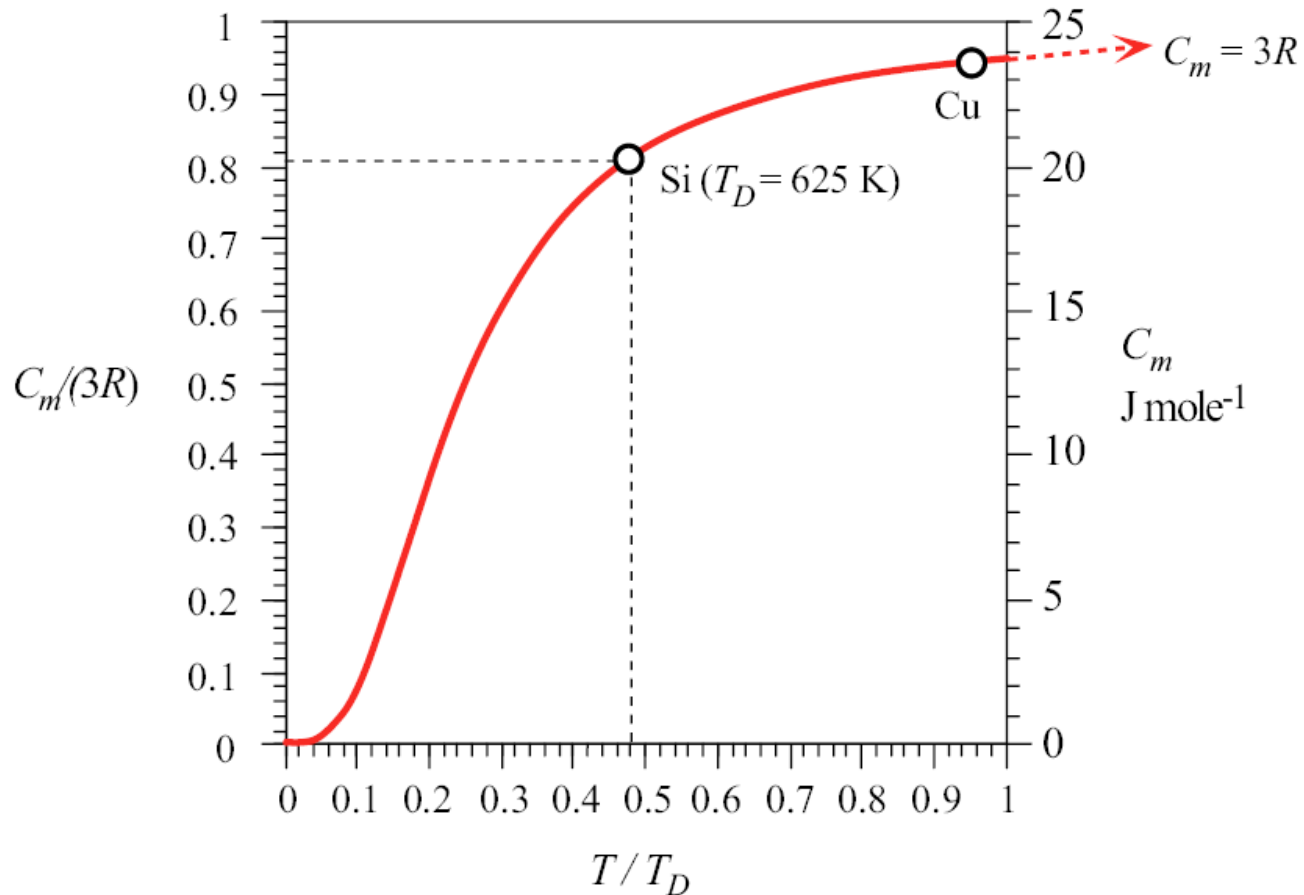
Four examples of standing waves in a linear crystal corresponding to $q = 1, 2, 4$, and N . q is maximum when alternating atoms are vibrating in opposite directions. A portion from a very long crystal is shown.

Fig 4.43



Density of states for phonons in copper. The solid curve is deduced from experiments on Neutron scattering. The broken curve is the three-dimensional Debye approximation, scaled So that the areas under the two curves are the same.
 This requires that $\omega_{\max} \approx 4.5 \times 10^{13} \text{ rad s}^{-1}$, or a Debye characteristic temperature $T_D = 344 \text{ K}$.

Fig 4.44



Debye constant-volume molar heat capacity curve. The dependence of the molar heat capacity C_m on temperature with respect to the Debye temperature: C_m vs. T/T_D . For Si, $T_D = 625 \text{ K}$ so that at room temperature (300 K), $T/T_D = 0.48$ and C_m is only $0.81(3R)$.

Fig 4.45

Debye frequency and temperature

Debye frequency: maximum vibration (angular) frequency in the crystal

$$\omega_{\max} \approx v \left(6\pi^2 N_A / V \right)^{1/3}$$

Avogadro's number

Mean velocity of lattice waves

Crystal volume

Debye temperature: all vibrations are fully excited up to ω_{\max}

$$T_D = \frac{\hbar \omega_{\max}}{k}$$

Debye heat capacity

Heat capacity per
mole ↓

$$C_m \approx 9R \left(\frac{T}{T_D} \right)^3 \int_0^{T=T_D} \frac{x^4 e^x dx}{(e^x - 1)^2}$$

High temperatures

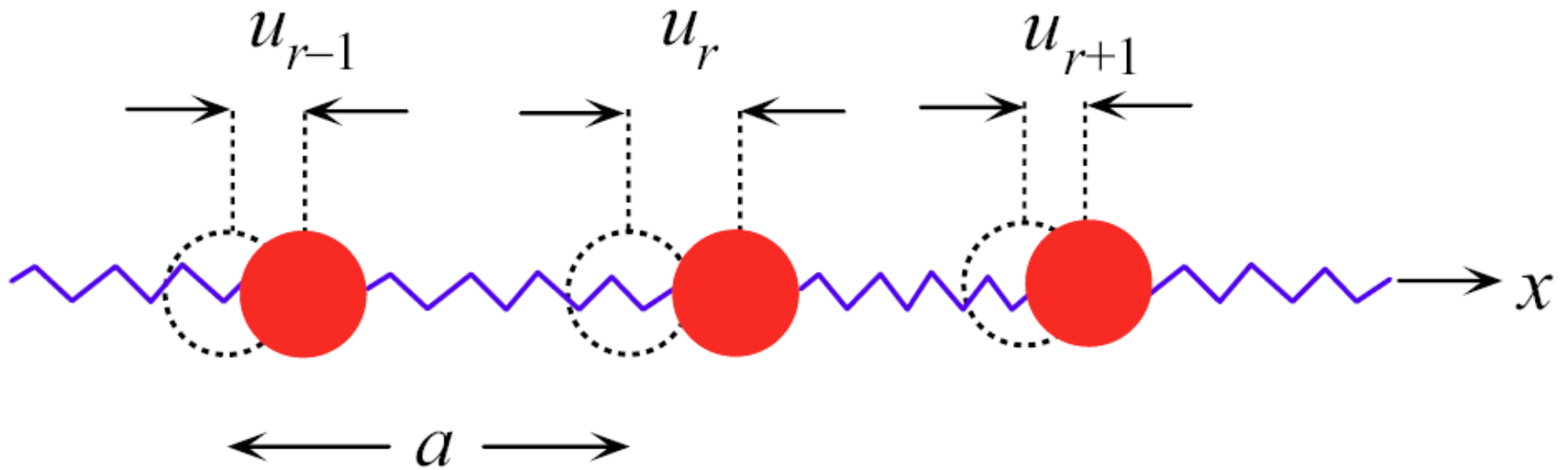
$$C_m \approx 3R$$

Low temperatures

$$C_m \propto \left(\frac{T}{T_D} \right)^3$$

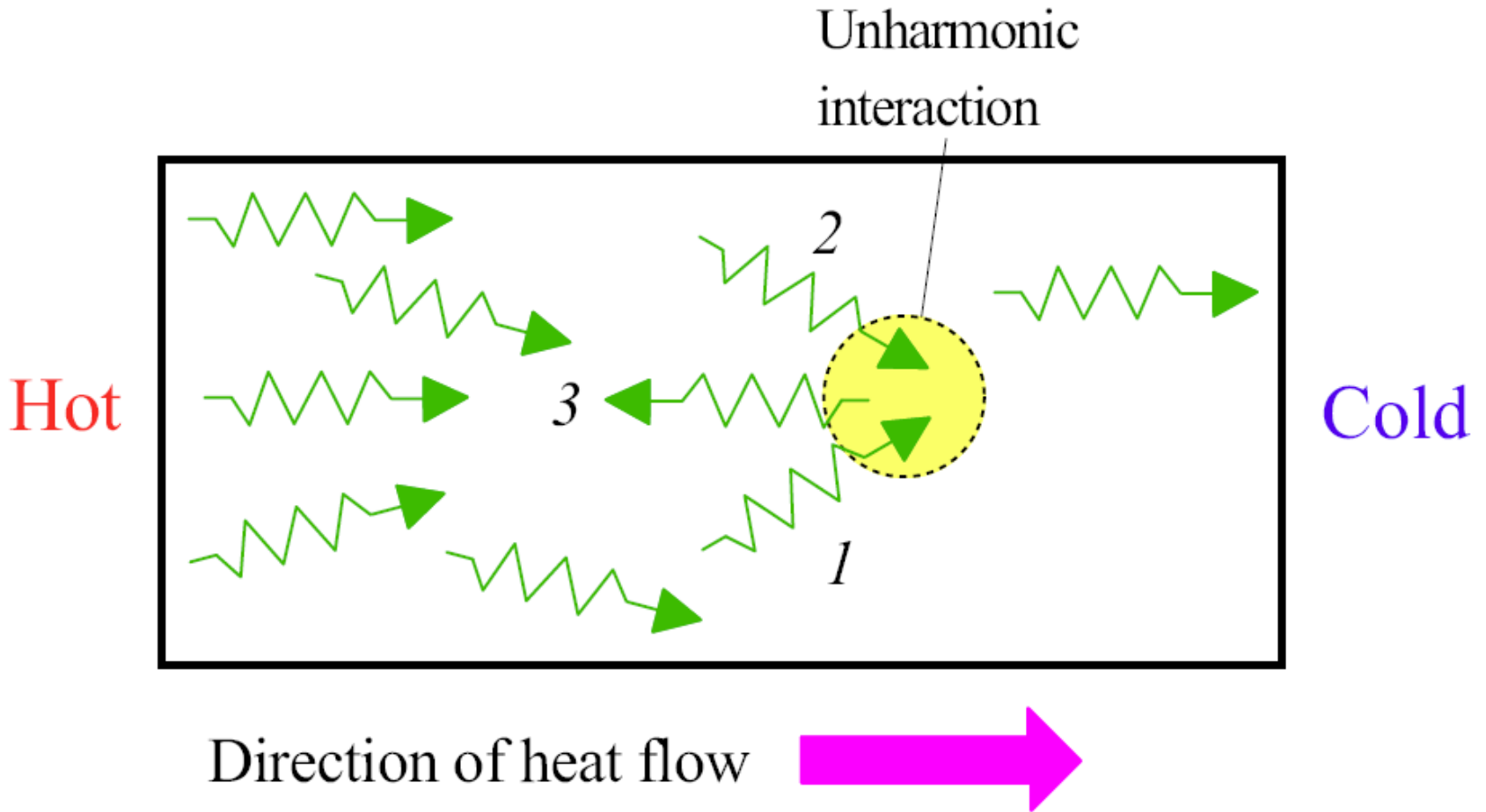
Table 4.5 Debye temperatures T_D , heat capacities, and thermal conductivities of selected elements

	Crystal							
	Ag	Be	Cu	Diamond	Ge	Hg	Si	W
T_D (K)*	215	1000	315	1860	360	100	625	310
C_m (J K ⁻¹ mol ⁻¹) [†]	25.6	16.46	24.5	6.48	23.38	27.68	19.74	24.45
c_s (J K ⁻¹ g ⁻¹) [†]	0.237	1.825	0.385	0.540	0.322	0.138	0.703	0.133
κ (W m ⁻¹ K ⁻¹) [†]	429	183	385	1000	60	8.65	148	173



Atoms executing longitudinal vibrations parallel to x .

Fig 4.46



Phonons generated in the hot region travel toward the cold region and thereby transport heat energy. Phonon-phonon unharmonic interaction generates a new phonon whose momentum is toward the hot region.

Fig 4.47

Thermal Conductivity

Thermal conductivity κ

Measures the rate at which heat can be transported through a medium per unit area per unit temperature gradient.

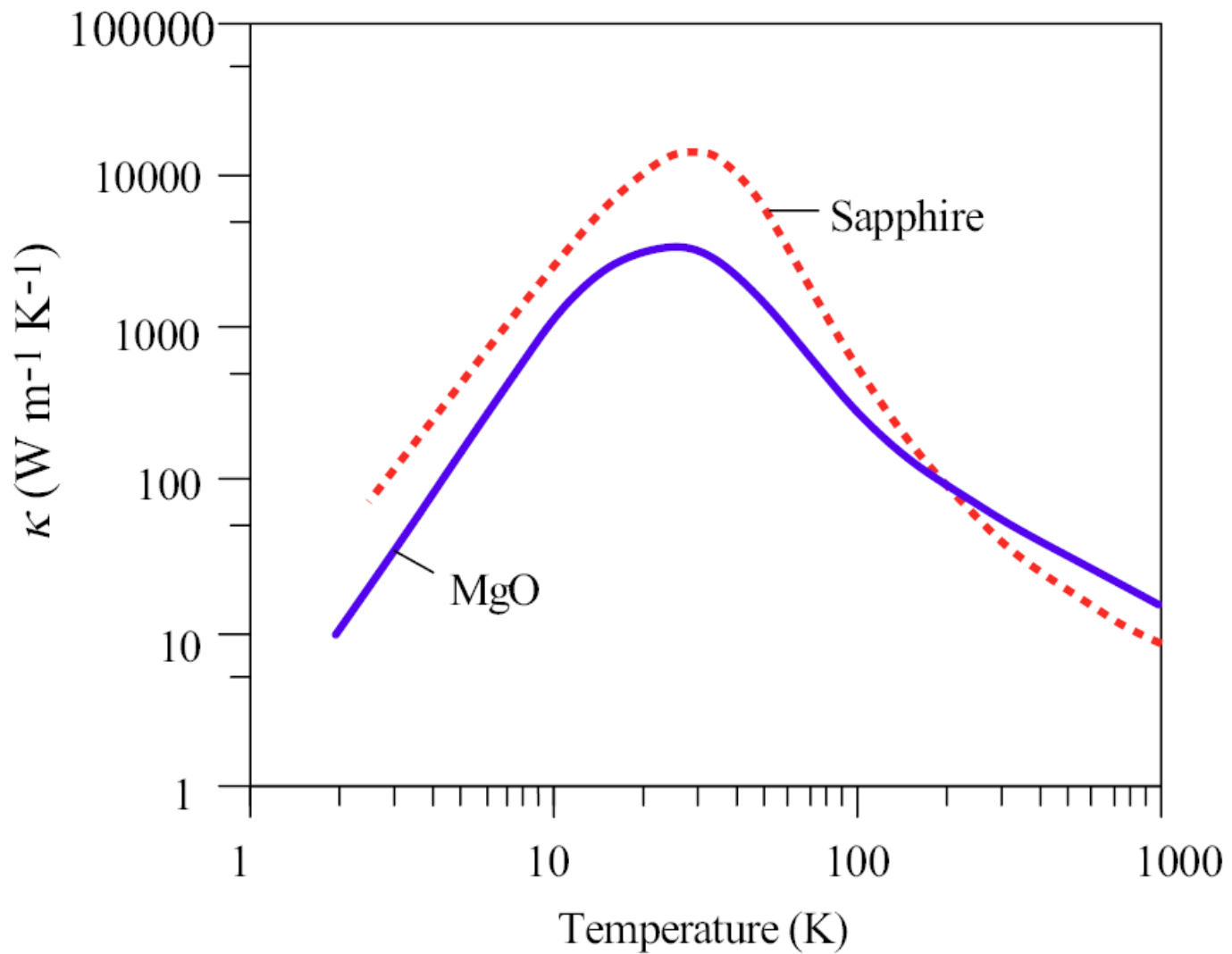
Thermal conductivity due to phonons

$$\kappa = \frac{1}{3} C_v v_{ph} \ell_{ph}$$

Heat capacity per unit volume

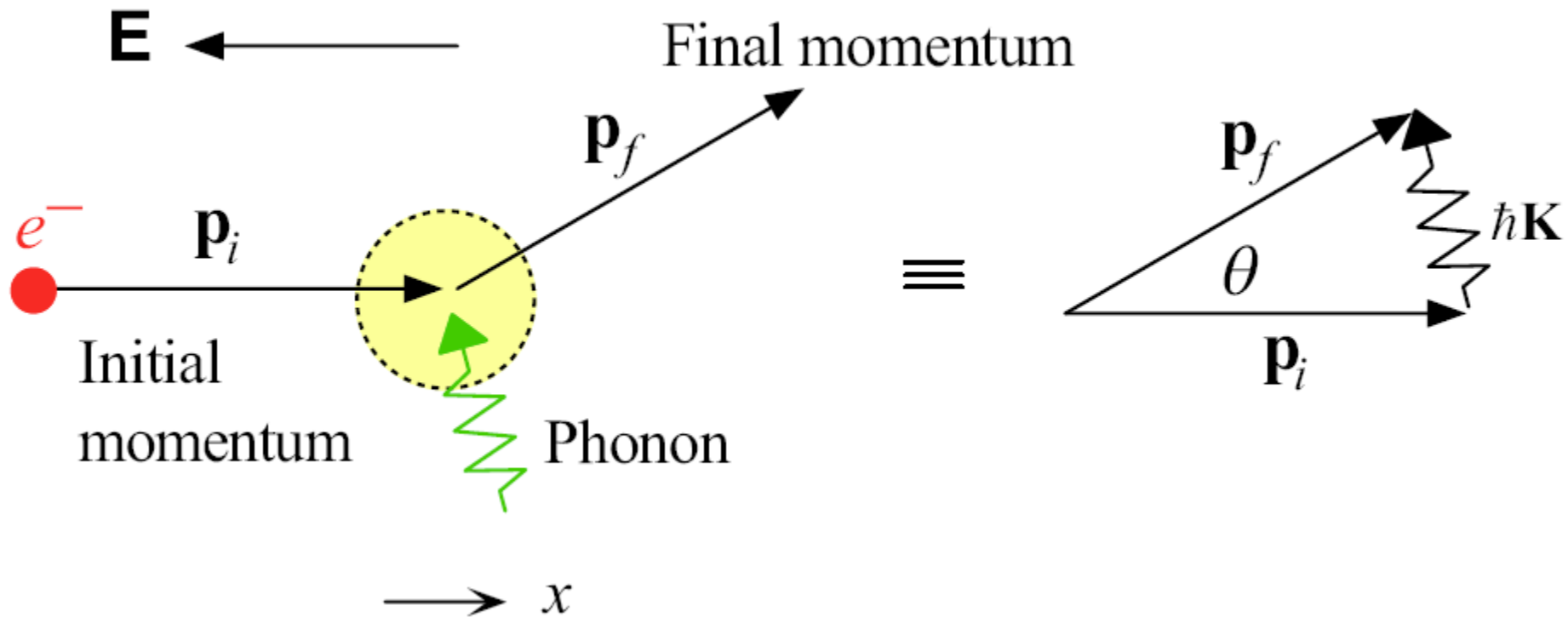
Phonon velocity

Phonon mean free path



Thermal conductivity of sapphire and MgO as a function of temperature.

Fig 4.48



Low-angle scattering of a conduction electron by a phonon.

Fig 4.49

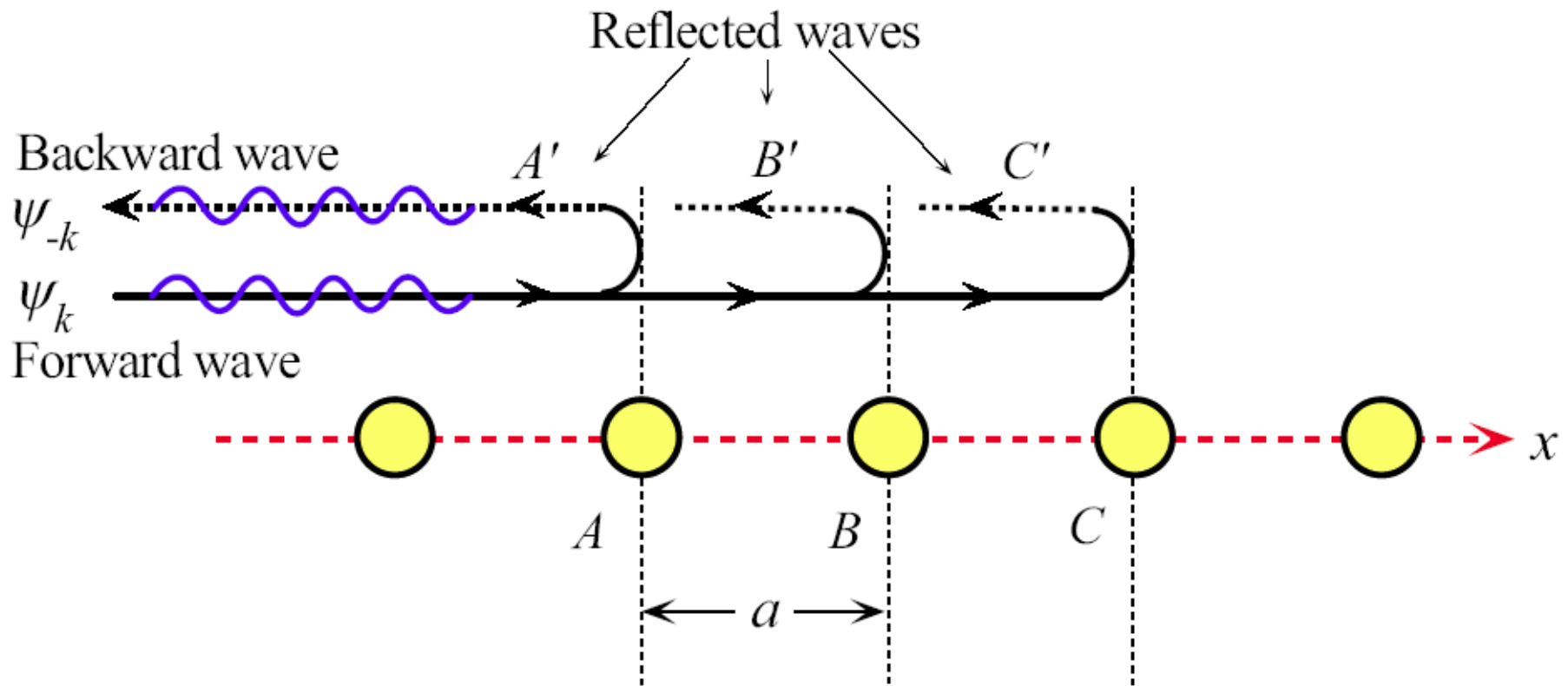
Electrical Conductivity

Electrical conductivity $T > T_D$

$$\sigma \propto \tau \propto \frac{1}{n_{\text{ph}}} \propto \frac{1}{T}$$

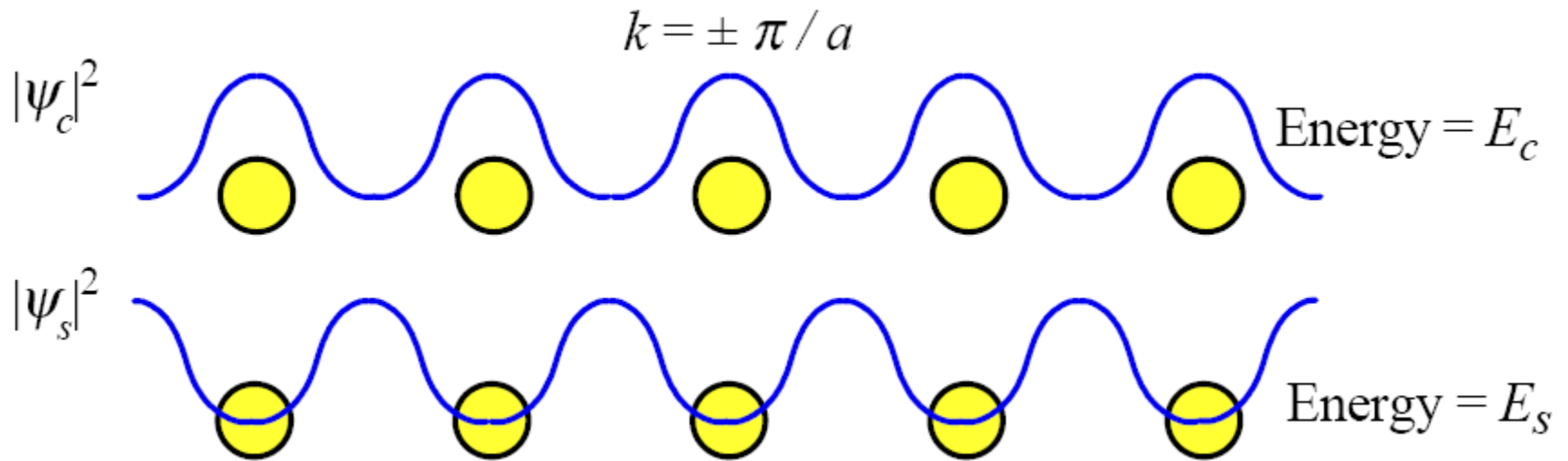
Electrical conductivity $T < T_D$

$$\sigma \propto N \tau \propto \frac{N}{n_{\text{ph}}} \propto \frac{1}{T^5}$$



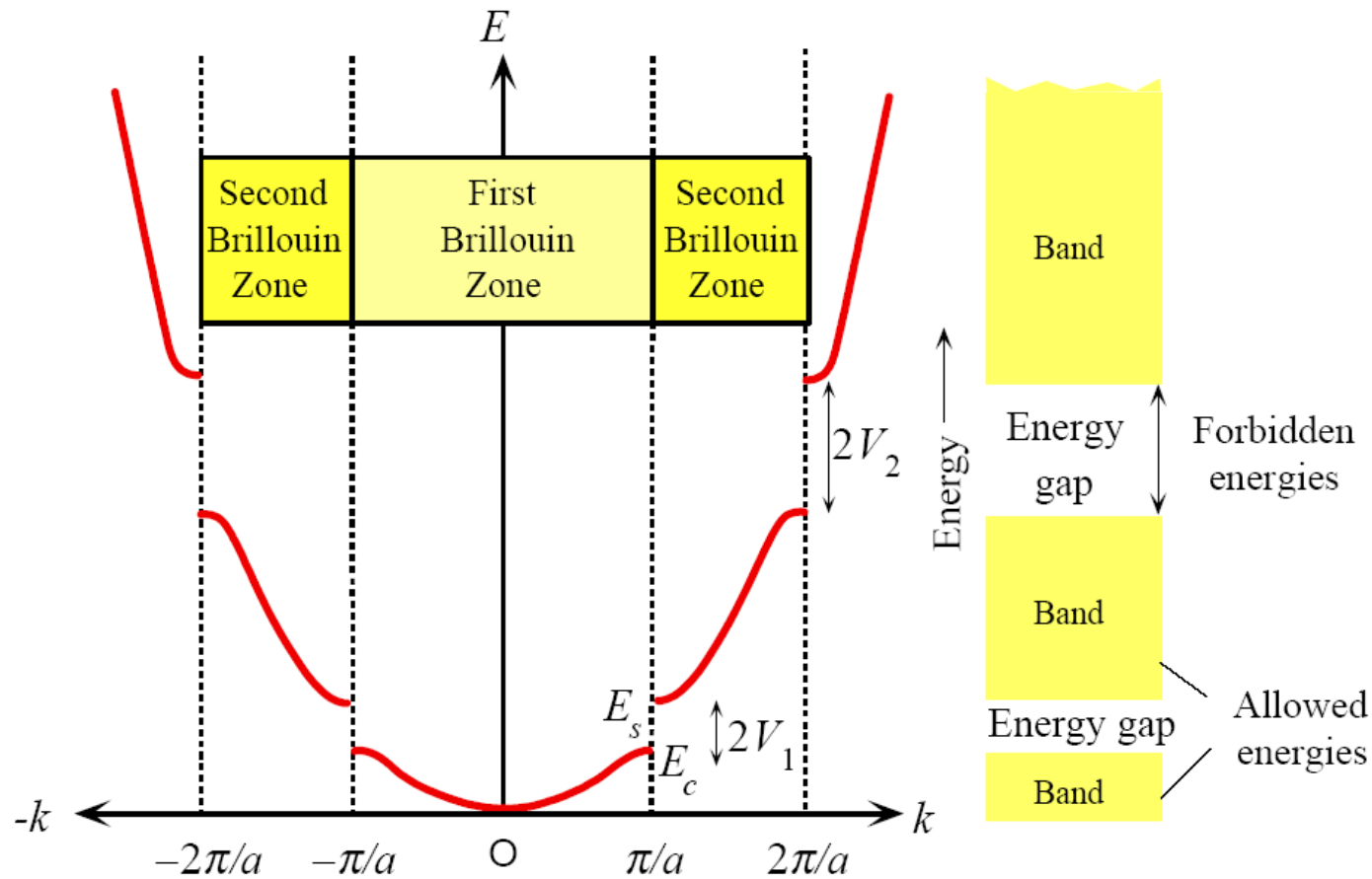
An electron wave propagation through a linear lattice. For certain k values, the reflected waves at successive atomic planes reinforce each other, giving rise to a reflected wave traveling in the backward direction. The electron cannot then propagate through the crystal.

Fig 4.50



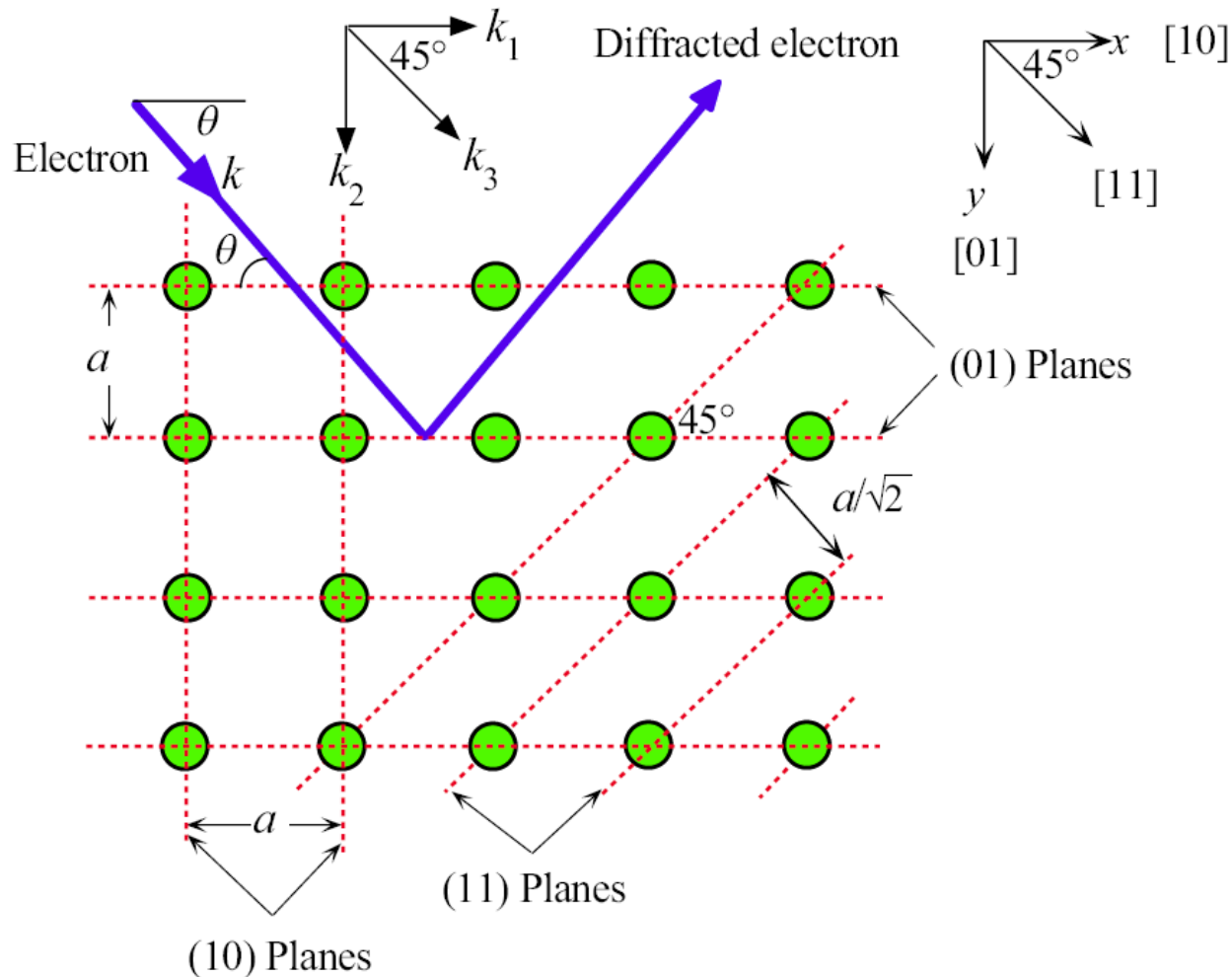
Forward and backward waves in the crystal with $k = \pm \pi/a$ give rise to two possible standing waves ψ_c and ψ_s . Their probability density distributions $|\psi_c|^2$ and $|\psi_s|^2$ have maxima either at the ions or between the ions, respectively.

Fig 4.51



The energy of the electron as a function of its wavevector k inside a one-dimensional crystal. There are discontinuities in the energy at $k = \pm n\pi/a$, where the waves suffer Bragg reflections in the crystal. For example, there can be no energy value for the electron between E_c and E_s . therefore, $E_s - E_c$ is an energy gap at $k = \pm \pi/a$. Away from the critical k values, the E - k vector is like that of a free electron, with E increasing with k as $E = \hbar^2 k^2 / 2m_e$. In a solid, these energies fall within an energy band.

Fig 4.52



Diffraction of the electron in a two dimensional cubic crystal. Diffraction occurs whenever k has a component satisfying $k_1 = \pm n\pi/a$, $k_2 = \pm n\pi/a$ or $k_3 = \pm 2^{1/2}n\pi/a$. In general terms, when $k\sin\theta = n\pi/d$.

Fig 4.53

Bragg Diffraction

The diffraction conditions can all be expressed through the **Bragg diffraction** condition $2d \sin \theta = n\lambda$, or

Bragg diffraction condition

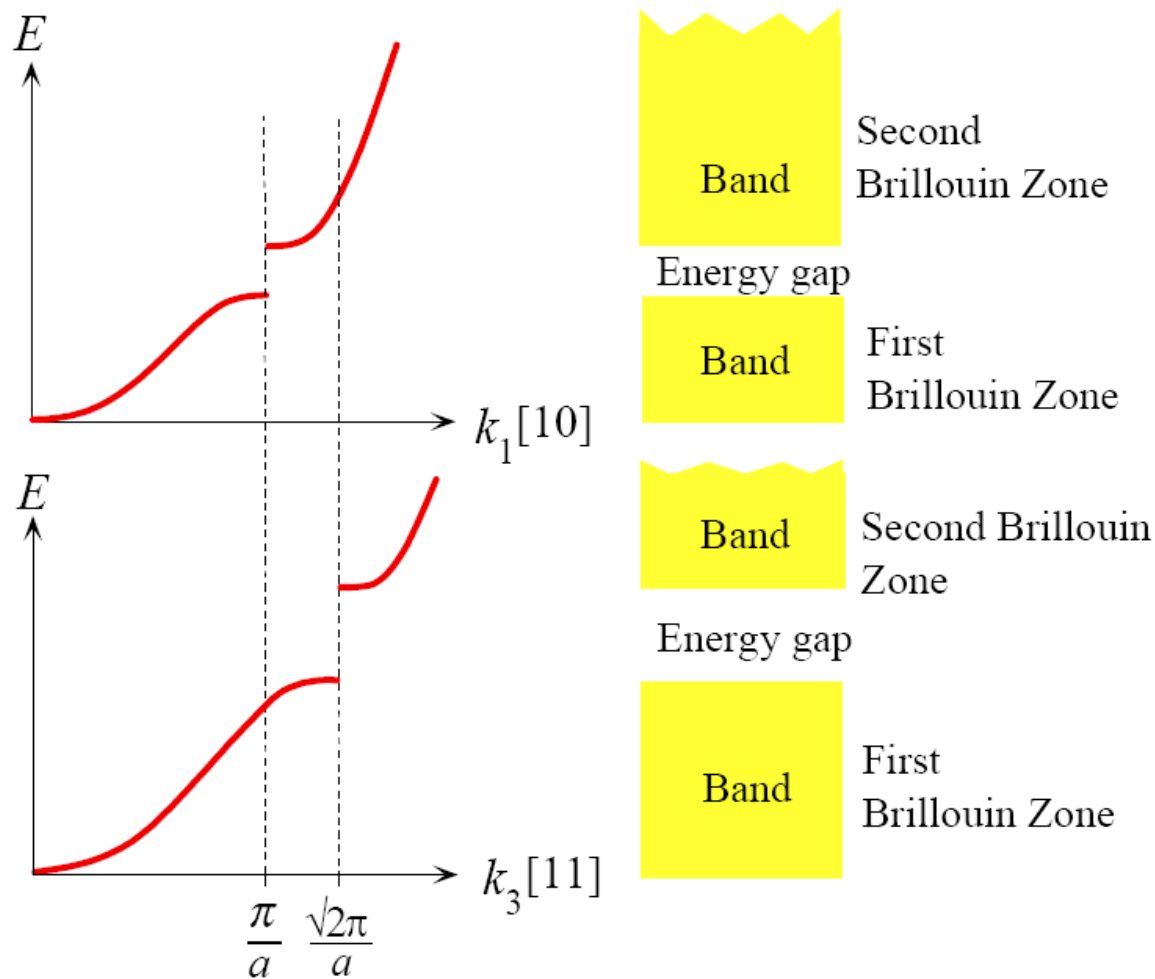
$$k \sin \theta = \frac{n\pi}{d}$$

Wavevector = $2\pi / \lambda$

Integer

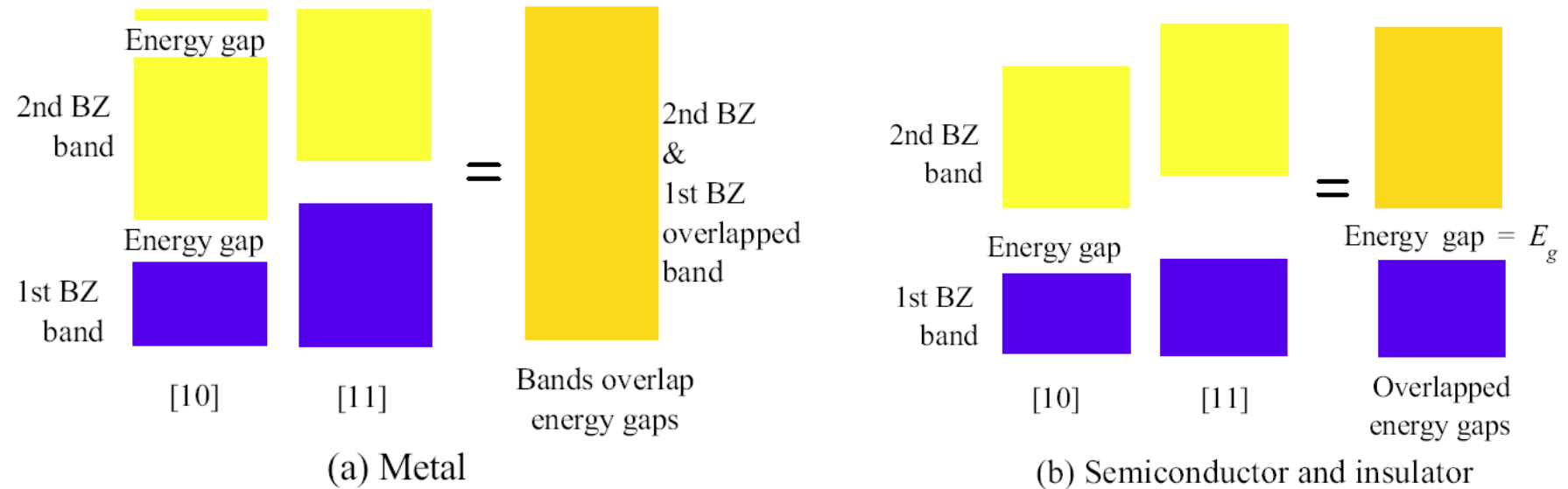
Angle between incident wave and diffracting planes

Interplanar separation of the planes involved in the diffraction



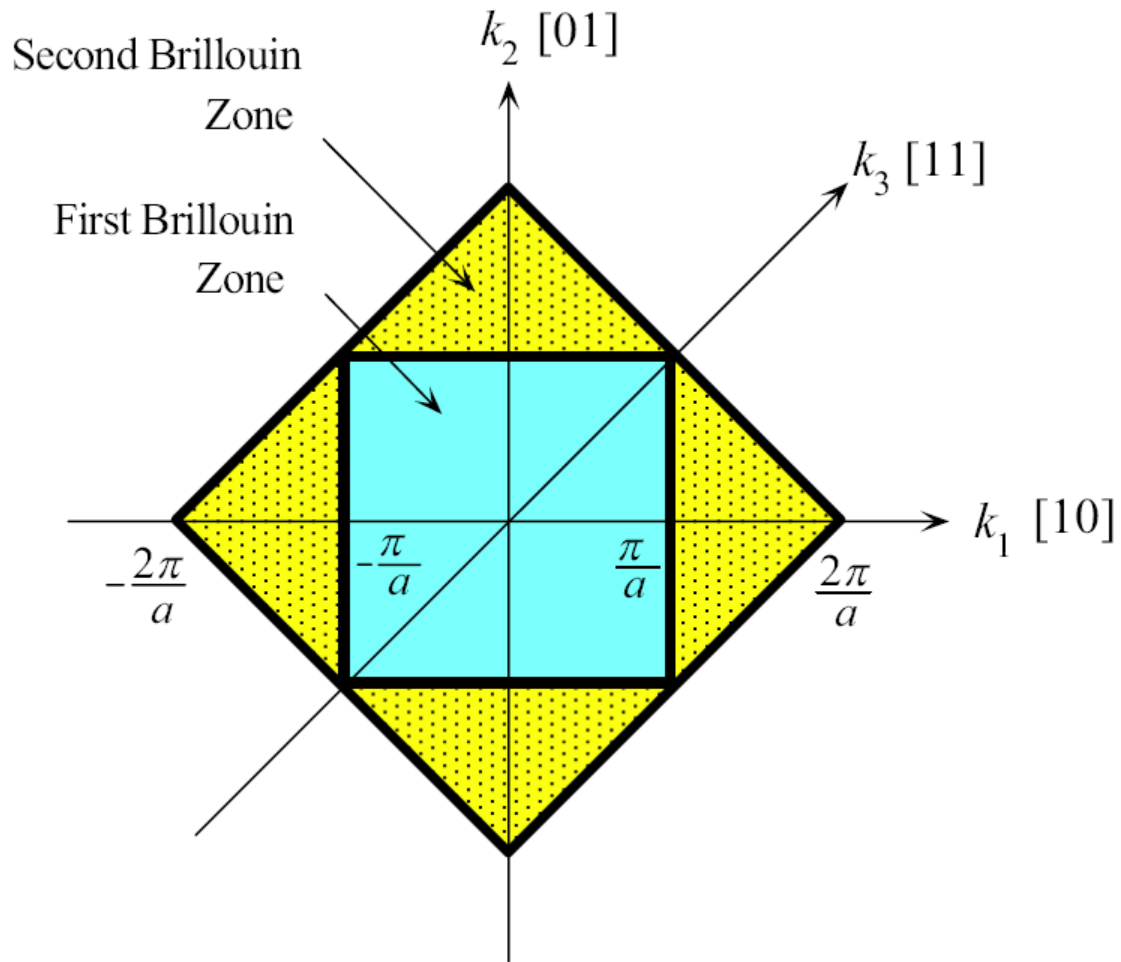
The E - k behavior for the electron along different directions in the two-dimensional crystal. The energy gap along [10] is at π/a whereas it is at $\sqrt{2}\pi/a$ along [11].

Fig 4.54



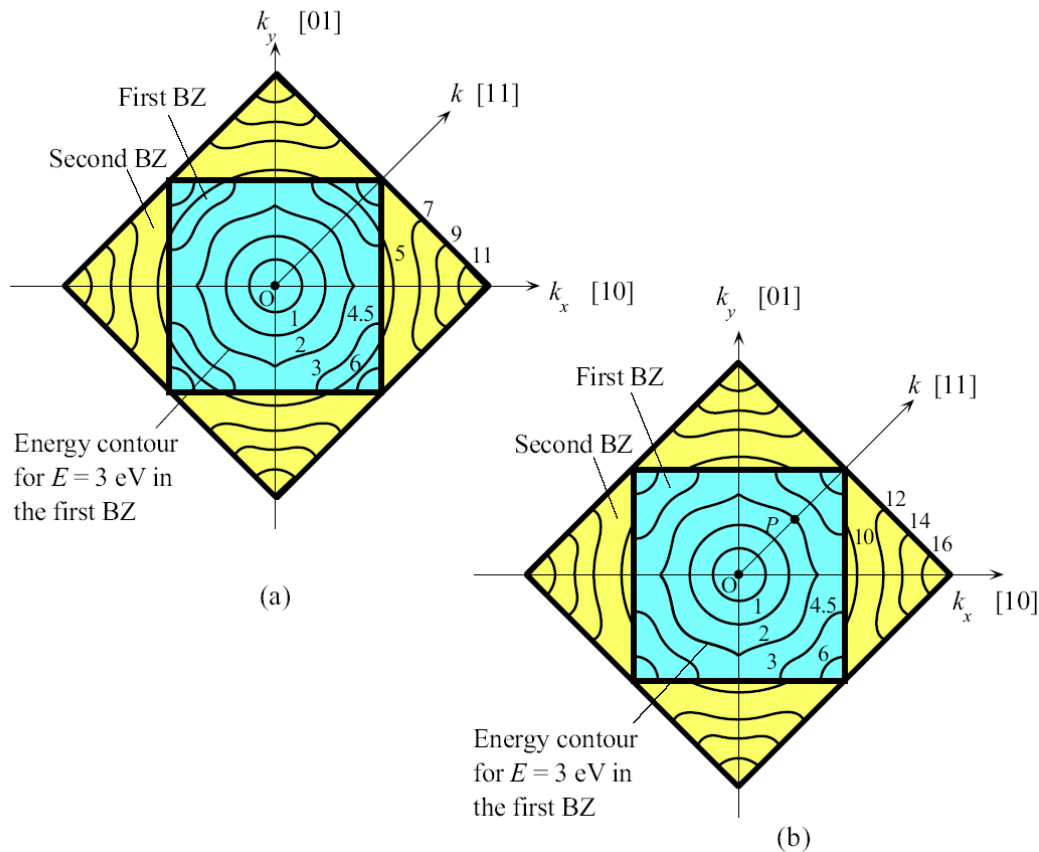
- (a) For the electron in a metal, there is no apparent energy gap because the second BZ (Brillouin zone) along [10] overlaps the first BZ along [11]. Bands overlap the energy gaps. Thus, the electron can always find any energy by changing its direction.
- (b) For the electron in a semiconductor, there is an energy gap arising from the overlap of the energy gaps along the [10] and [11] directions. The electron can never have an energy within this energy gap E_g .

Fig 4.55



The Brillouin zones in two dimensions for the cubic lattice.
 The Brillouin zones identify the boundaries where there are discontinuities in the energy (energy gaps)

Fig 4.56



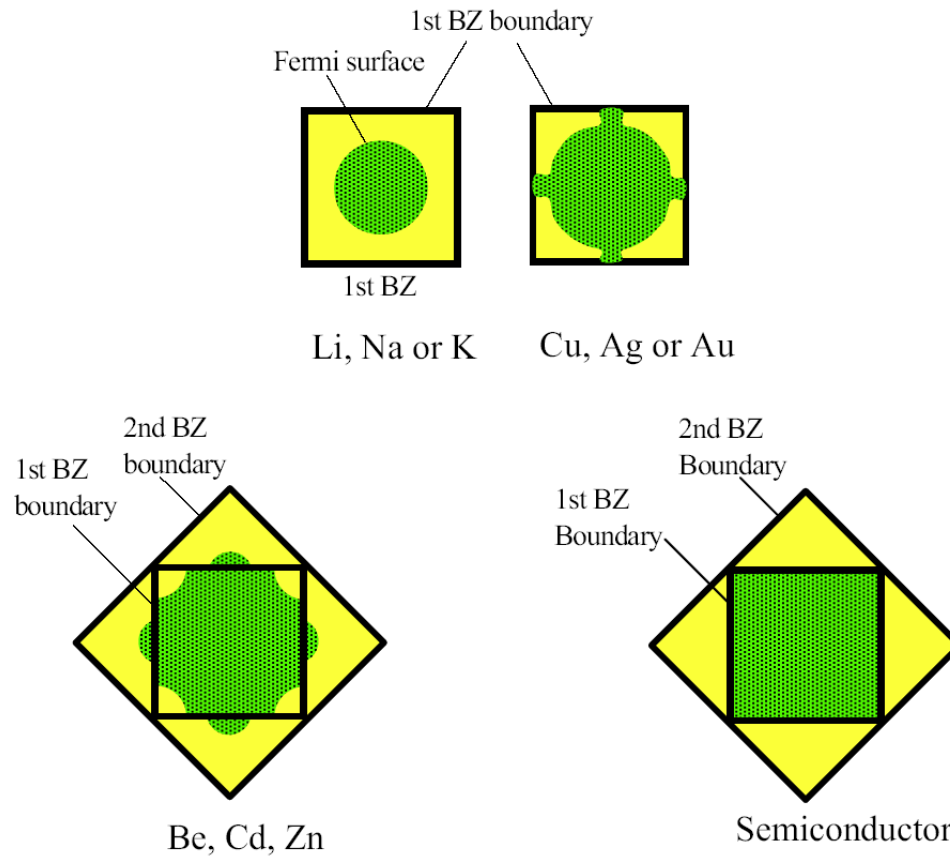
Energy contours in k space (space defined by k_x, k_y).

Each contour represents the same energy value. Any point P on the contour gives the values of k_x and k_y for that energy in that direction from O . For point P , $E = 3$ eV and OP along [11] is k .

(a) In a metal, the lowest energy in the second zone (5 eV) is lower than the highest energy (6 eV) in the first zone. There is an overlap of energies between the Brillouin zones.

(b) In a semiconductor or an insulator, there is an energy gap between the highest energy contour (6 eV) in the first zone and the lowest energy contour (10 eV) in the second zone.

Fig 4.57



Schematic sketches of Fermi surfaces in two dimensions, representing various materials qualitatively.

- (a) Monovalent group IA metals.
- (b) Group IB metals.
- (c) Be (Group IIA), Zn, and Cd (Group IIB).
- (d) A semiconductor.


Fig 4.58

Gruneisen's Model of Thermal Expansion

Asymmetric potential energy curve

$$U(r) = U_{\min} + a_2(r - r_o)^2 + a_3(r - r_o)^3 + \dots$$

Harmonic term Unharmonic term

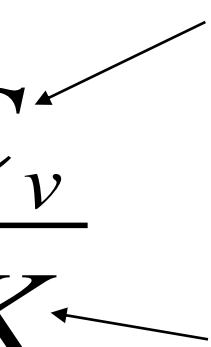


Linear expansion coefficient λ

$$\lambda \propto \frac{a_3}{a_2} \frac{C_v}{K}$$

Heat capacity per unit volume

Bulk modulus



Gruneisen's Law

Thermal expansion coefficient

$$\lambda \approx \frac{1}{3} \gamma \frac{C_v}{K}$$

The Gruneisen parameter

Specific heat capacity

Density

$$\lambda = \frac{1}{3} \gamma \frac{\rho C_m}{M_{\text{at}} K} = \frac{1}{3} \gamma \frac{\rho c_s}{K}$$

Note: Due to an error, the numerical constant “1/3” was printed as “3”. There is a derivation in the web-article *Thermal Expansion and Thermal Fatigue* under Selected Topics at <http://electronicmaterials.usask.ca>, this is “1/3”.

The Grüneisen parameter for some selected materials with different types of interatomic bonding. Only typical values are used; and for certain materials there can be significant variation in quoted data in the literature⁵. Data selectively extracted and combined from a number of different sources.

Material	ρ g cm⁻³	λ 10⁻⁶ K⁻¹	K GPa	c_s J kg⁻¹ K⁻¹	γ_G
Iron (metallic, BCC)	7.9	12	170	450	1.7
Copper (metallic, FCC)	8.96	17	140	385	2.1
NaCl (ionic)	2.17	44	25	850	1.8
CsI (ionic)	4.51	48	13	201	2.1
Germanium (covalent)	5.32	6	77	322	0.81
Silicon (covalent)	2.32	2.6	99	703	0.47
Glass (covalent-ionic)	2.45	8	50	800	0.61
ZnSe (ionic/covalent)	5.27	7.4	62	350	0.75
Tellurium (covalent/van der Waals)	6.24	17	30	200	1.23
Polystyrene (van der Waals)	1.1	80	~3	1300	0.50
Polyethylene terephthalate PET (van der Waals)	1.38	70	~3	1200	0.38

Table 4.7

Property	Diamond	Silicon	Germanium	Tin
Melting temperature, °C	3800	1417	937	232
Covalent radius, nm	0.077	0.117	0.122	0.146
Bond energy, eV	3.60	1.84	1.7	1.2
First ionization energy, eV	11.26	8.15	7.88	7.33
Bandgap, eV	?	1.12	0.67	?

Table 4.8

Metal	Group	M_{at}	Density (g cm⁻³)	E_F (eV) [Calculated]	E_F (eV) [Experiment]
Cu	I	63.55	8.96	—	6.5
Zn	II	65.38	7.14	—	11.0
Al	III	27	2.70	—	11.8

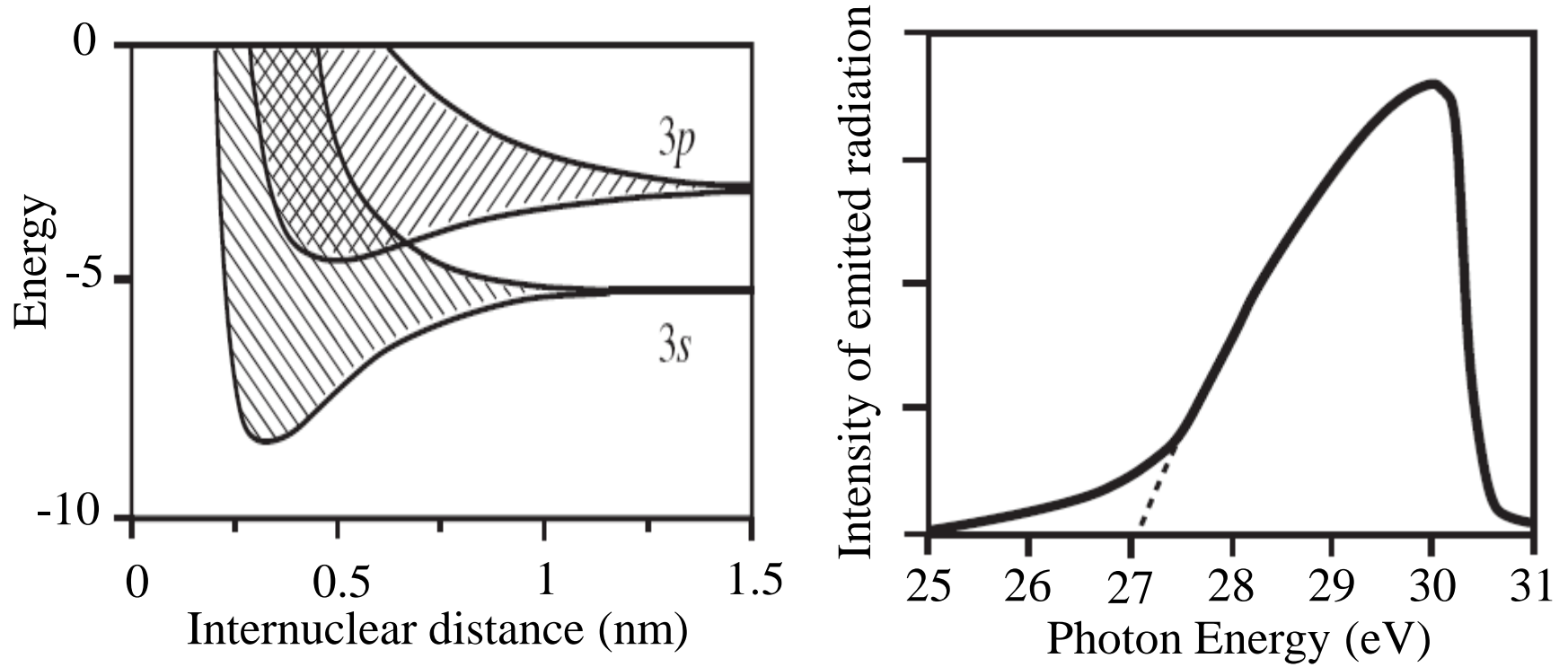
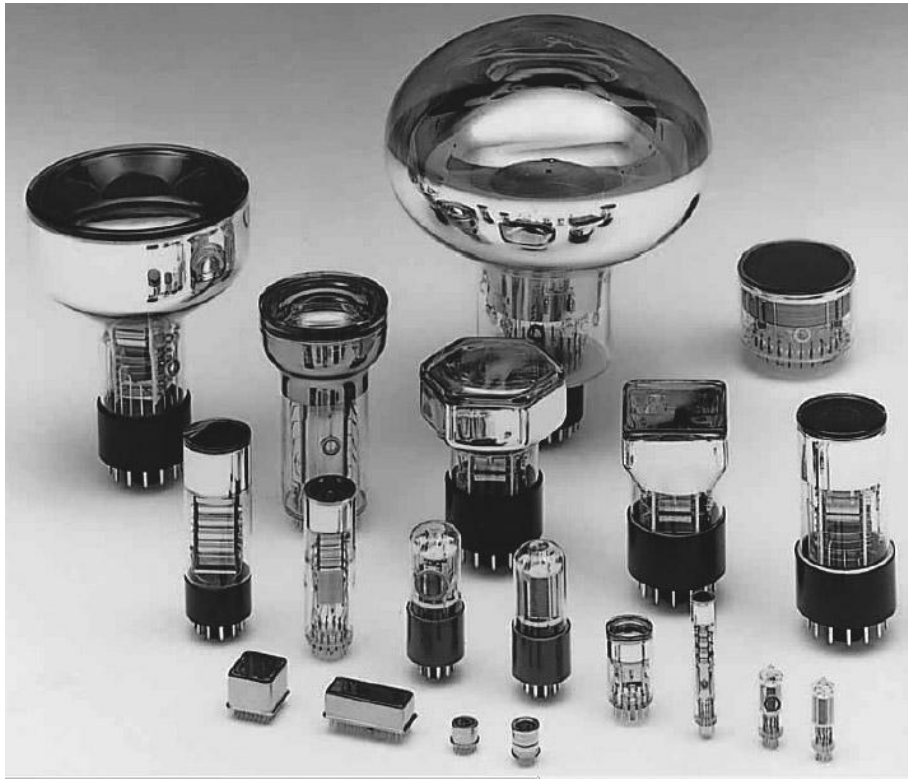
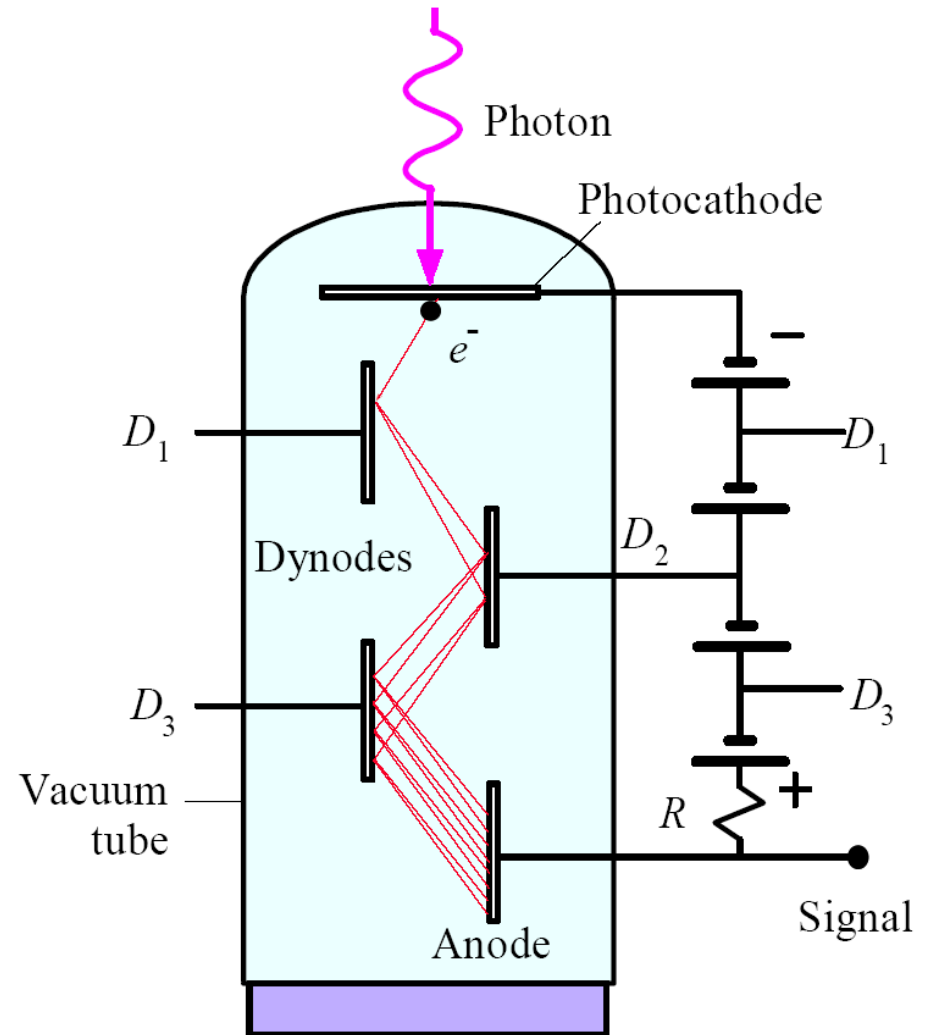


Fig 4.59



Examples of photomultiplier tubes

[SOURCE: Courtesy of Hamamatsu]



The photomultiplier tube

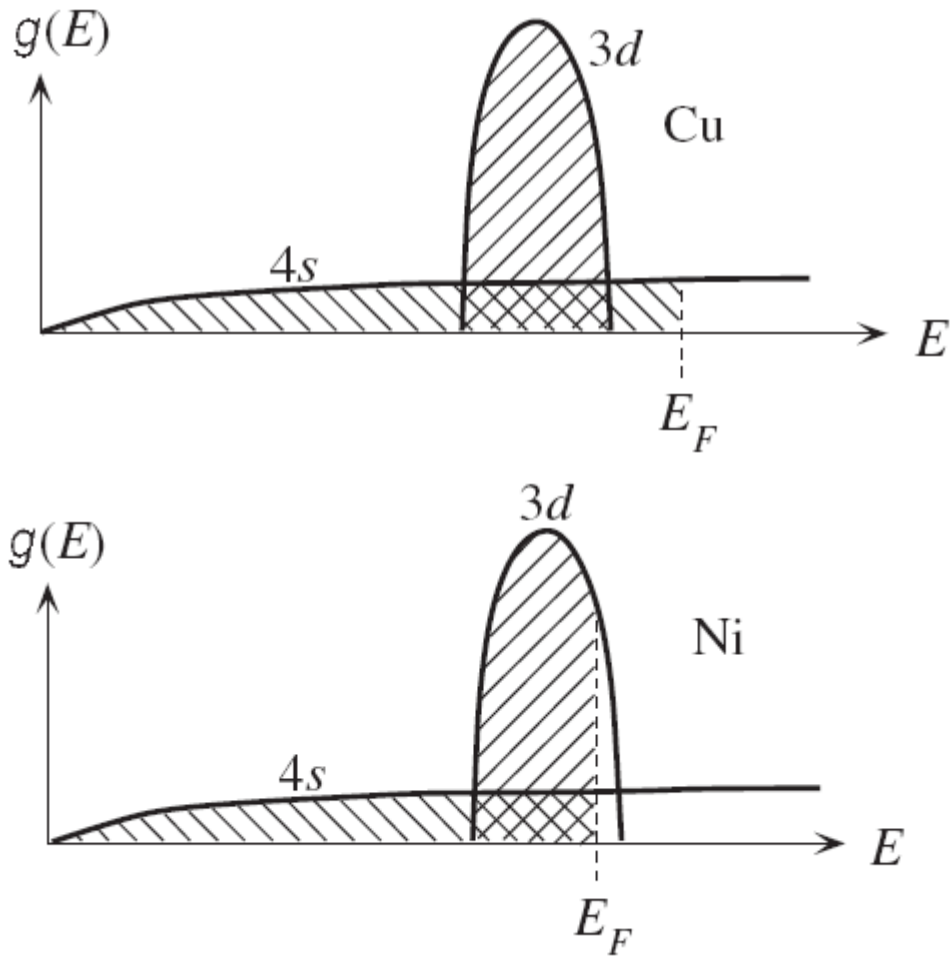
Fig 4.60

Table 4.9

	$B_e \text{ (A m}^{-2} \text{ K}^{-2}\text{)}$	$\Phi \text{ (eV)}$
Th on W	3×10^4	2.6
Oxide coating	100	1

Table 4.10 Tests on a Motorola FED micro field emitter

V_G	40.0	42	44	46	48	50	52	53.8	56.2	58.2	60.4
I_{emission}	0.40	2.14	9.40	20.4	34.1	61	93.8	142.5	202	279	367



Density of states and electron filling in Cu and Ni.

Fig 4.61